

https://dspace.org/

Development and application of passive samplers based on polymer inclusion membranes for evaluating the fate of trace metals polluted by acid mine drainage

Motsoane, Nthabiseng Marcia

2019

https://hdl.handle.net/10539/28041

Downloaded from a DSpace repository. https://dspace.org/

Development and application of passive samplers based on polymer inclusion membranes for evaluating the fate of trace metals polluted by acid mine drainage

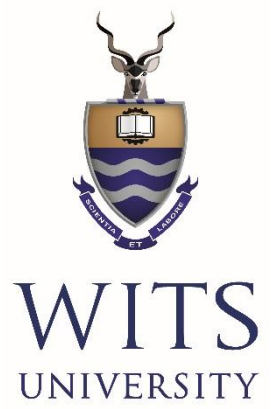

By

Nthabiseng Marcia Motsoane

A thesis submitted to the University of Witwatersrand in fulfilment of the requirement of the Doctor of Philosophy in Chemistry

Declaration

I declare that this research is my own, unaided work. It is being submitted for the Degree of Doctor of Philosophy at the University of the Witwatersrand, Johannesburg. It has not been submitted before for any degree or examination at any other University.

……..

(Signature of Candidate)

……..

(Date)

Abstract

The shortcomings of conventional sampling methods such as grab sampling have led to the development of alternative approaches especially those based on passive samplers. The challenge of passive samplers despite being cheap to use and being integrative is that there are limited commercial suppliers. Further, technical development is also still ongoing on the types of design and membrane materials. In this work, the technical development, optimization and preliminary application of a polymer inclusion membrane passive sampler is reported. Compared to commercial passive samplers, our passive sampler is reusable, rugged and able to tolerate harsh environmental conditions ensuring maximum efficiency for target compounds.

The passive sampler consisted of a chamber made of polytetrafluoroethylene (PTFE) with a lumen that holds 5.5 mL of a receiver solution. A polymer inclusion membrane (PIM) composed of polyvinyl chloride as the base polymer and diethyl hexyl phosphoric acid (D2EHPA) as the carrier was then placed as a sealer for the receiver phase and a barrier to separate the receiver from the source solution. A polytetrafluoroethylene screw cap was used to hold the membrane and the chamber together. The final assembled polymer inclusion membrane passive sampler housing has a length of 46 mm. Target compounds diffuse from the sample solution through the membrane into the receiver solution. The membrane is incorporated by a mobile carrier that transports the target metal species from the sample into the receiver solution. The driving force in this case is the proton in the acceptor solution that is back transported across to the sample solution.

The polymer inclusion membrane was characterized by atomic force microscopy and scanning electron microscopy, and results showed that the PIM's roughness increased after the sampler had been deployed for 12 days. Fourier transform infra-red revealed the presence of carrier molecules. The contact angle temperature (~78.80^{o}C) showed that the polymer had hydrophilic surfaces due to the carrier functional groups. The effect of variables such as the carrier composition, pH, membrane thickness, receiver phase concentration and the stability of PIM were optimised to calculate the time-weighted average concentration of first and second

row transition metal elements which are Ni (II), Co (II), Cu (II), and Cd (II). The PIM optimum conditions were composed of 40% D2EHPA as a carrier and 60% PVC as a base polymer, sample pH of 3-7, 1 mol L^{-1} HNO_3 as acceptor solution and membrane thickness of 150 µm. The stability of PIM as passive was tested up to three cycles and showed remarkable stability. The stability was further followed using thermal gravimetric analysis and Phosphorus-31 NMR spectroscopy. The developed passive sampler showed a large time lag up to five days for all the metals and then uptake became linear up to 13 days. Thus slow release of the metals from the PIM into the bulk acceptor solution was the rate limiting factor. The passive sampler is best suited to be deployed for two weeks instead of a short period of time.

The passive samplers were deployment in dam water and acid mine drainage (AMD) in the laboratory and in the field to study the transport and fate of these metals. The PIM-based passive sampler was able to extract the metals as it seemed to tolerate high metal content in AMD. The release of H^+ on the source phase from the acceptor solution also prevented any fouling. Linear uptake of the metals was observed in PIM sampler but laboratory-based uptake in AMD failed because of precipitation that reduced the amount of the bioavailable fraction. Metals like Fe and Al were found to control these reactions along with redox potential. The PIM based sampler showed high versatility as it could tolerate AMD matrix.

Dedication

This dissertation and all my academic achievements are dedicated to my mother Garatwe Salome Motsoane, and my late father Daniel Tabampe Motsoane who pushed for me to have a good education. My brothers, Sello Motsoane, Lehlohonolono Motsoane and Toko Motsoane, thank you for your love, support and for believing in me. Lastly, to my daughter Kamohelo Motsoane, your love letters kept me alive throughout this journey.

Acknowledgments

Firstly, I would like to thank heavenly my father for giving me the strength and wisdom to pursue my PhD studies.

I would also like to convey in so many ways my sincere gratitude to Prof. Luke Chimuka for his academic and life supervision, mentorship and efforts to avail financial support for my studies. Thank you for the extra help you gave me during your office hours on the few concepts I struggled with. I really appreciate your dedication.

My co-supervisor Dr Heidi Richards for believing in me and your constant reminders like "Nthabi you can do this". The trip to Spain (Euromembrane conference) was one of the biggest highlights of my PhD studies. Prof Luke and Dr Heidi, thank you for making me a better person and for shaping my career. I am truly humbled to have worked with you. I will also like to thank Dr Izak Kotze for his guidance and assistance with NMR analysis. Prof Hlanganani Tutu and Prof Ewa Cukrowska, I appreciate all the contributions and ideas towards this project.

Many thanks go to the Environmental Analytical Chemistry group members at the University of Witwatersrand. However, I would like to pay special thanks to Dr. Somandla Ncube, for his time in bringing my mind back to the academic life; advices that made this research work a journey joyfully travelled. To Yannick Nuapia, Pfano Nekhunguni, Xolisiwe Sebutsoe, Kitondo Mwelwa (Mr K), Maletsatsi Kgatitsoe and Alseno Mosai my appreciation for your inputs to my work remain second to none and the jokes shared in Lab 411. To Kgomotso Maiphetlho and Divya Latcheman, I am truly grateful and honoured to have worked and co-supervised inspirational students like you as my first ever honours students under the supervision of Dr Heidi Richards.

My extended gratitude goes to Dineo Nhlane for assistance with AFM data acquisition, Mr Chuene Mogehle and Mokgaetji Monyai for ICP-OES analysis,

Brayner Nelwalani for SEM data acquisition and Ms Ignatia Khumalo for access and use of analytical balance. The physics department for designing the passive samplers and special thanks goes to Lundersteady Mafemba. The school of chemistry stuff Khwezi Ndawonde, Mary-Ann Xaba, thank you for the warm atmosphere that provided an excellent learning environment.

I will also like to thank the Motsoane's family and Lebakeng's family for being part of my life. Special thanks to my aunt Lizzy Lebakeng for encouraging me to continue with my studies.

To Eric Moshani, thank you for your love and never-ending support during the last year of this journey.

Lastly, I would like to thank the Water Research Commission (WRC) and National Research Funding (NRF) of South Africa for their financial support towards this project.

Table of contents

Declaration i

Abstract ii

Dedication iv

Acknowledgments v

Table of contents vii

List of figures xii

List of tables xix

List of abbreviations xx

CHAPTER 1 1

1 Introduction 2

CHAPTER 2 5

2 Literature review 6

2.1 Acid mine drainage 6

2.1.1 Trace metals: sources and effects 9

2.1.2 The elements under study 10

2.1.3 Technologies for the removal of trace metals 15

2.1.4 Liquid membranes 15

2.2 Polymer inclusion membranes 20

2.2.1 Classification of carriers used in PIM 24

2.2.2 Transport mechanism across the PIM 28

2.2.3 Extraction and transport of target ions by PIMs 30

2.2.4 Morphological structure and properties of PIM 32

2.2.5 Advantage of PIM 34

2.2.6 Stability of PIM 34

2.2.7 Application of PIM 35
2.3 Sampling strategies to monitor metal ion in water 35
2.3.1 Grab sampling 35
2.4 Passive sampling 36
2.4.1 Passive sampling background 36
2.4.2 Theory of the passive sampler 39
2.4.3 Types of passive samplers 42
2.4.4 Technical developments and optimisation in passive samplers 46
2.4.5 Sampling/application area 49
CHAPTER 3 50
3 Aims and Objectives 51
3.1 Aim 51
3.2 Novelty 51
3.3 Motivation 52
CHAPTER 4 53
4 Research methodology 54
4.1 Chemicals and calibration standards 54
4.2 Instrumentation 54
4.3 Experimental 55
4.3.1 Preparation of membrane 55
4.3.2 Passive sampler design 56
4.3.3 Assembling PIM-based passive sampler components 58
4.3.4 Experimental set up of PIM pasive sampler 59
4.3.5 Optimization of the PIM composition 60
4.4 Field application of the developed passive sampler 62

4.4.1 Sampling sites for PIM deployment 62
4.4.2 Construction of sampling cages 63
4.4.3 Deployment of passive samplers in the dam and AMD 64
4.4.4 Collection of passive samplers and analysis of metal ions 65
CHAPTER 5 66
5 Results and discussion 67
5.1 Polymer inclusion membrane-based passive sampler optimisation 67
5.1.1 Effect of D2EHPA composition 67
5.1.2 Effect of receiver solution 68
5.1.3 Effect of receiver phase concentration 69
5.1.4 Effect of pH in the source solution 70
5.1.5 Effect of membrane thickness 71
5.1.6 Effect of stirring rate 73
5.1.7 Effect of passive sampler exposure area 74
5.1.8 Deployment time 75
5.2 PIM stability, re-use and characterisation 76
5.2.1 PIM stability and re-use 76
5.2.2 Scanning electron microscopy (SEM) 78
5.2.3 Thermogravimetric analysis (TGA) 78
5.2.4 Nuclear magnetic resonance (^{31}P NMR) 79
5.2.5 Contact angle 80
5.3 Studying the effects of sample matrix in laboratory experiment from field samples 81
5.3.1 Physical-chemical properties of dam water during lab PIM sampler deployment 81

5.3.2 Effect of contact time in laboratory-based experiments from field samples ……83

5.3.3 Effect of stirring rate in laboratory-based experiments..... 87

5.3.4 Comparison receiver solution pH during sampler deployment in different sample matrix 89

5.4 Application in dam water 91

5.4.1 Total metal ion concentrations in Fleurhof Dam 91

5.4.2 Metal uptake during PIM sampler field deployment in dam water 92

5.4.3 Uptake of other metals by PIM-base sampler..... 94

5.4.4 pH changes in the acceptor phase of the PIM-based passive sampler deployed at Fleurhof Dam for different days..... 95

5.4.5 Fouling on the passive samplers deployed at Fleurhof dam 96

5.4.6 Comparison of the bioavailable fraction of the metals in PIM sampler deployed in the field and in laboratory from Fleurhof dam water 97

5.4.7 Passive sampling vs grab sampling in dam water..... 98

5.5 Field deployment of the developed passive sampler in acid mine drainage 99

5.5.1 Physical-chemical properties of AMD..... 99

5.5.2 Total metal ion concentrations found AMD 99

5.5.3 pH changes in the acceptor phase at AMD site..... 103

5.5.4 Fouling on the passive samplers deployed in AMD 103

5.5.5 Comparison of the bioavailable fraction of the metals in PIM sampler deployed in the field and in laboratory from AMD water 104

5.5.6 Other metal ion uptake by PIM-based passive sampler in AMD for nine days exposure..... 105

5.5.7 Passive sampling vs grab sampling in AMD 106

5.5.8 Literature comparison of deployment time with other PIMs..... 107

5.6 Characterisation of PIM before and after field deployment 109
5.6.1 FTIR 109
5.6.2 AFM 110
CHAPTER 6 113
6 Conclusions and recommendations 114
6.1 Conclusions 114
6.2 Future studies and recommendations 114
References 116

List of figures

Figure 1: Acid mine drainage through a stream in Roodepoort, Johannesburg West. The sampling site was near a mine tailing, with active AMD production 6

Figure 2: Speciation diagram for the iron, (Sanchez España et al., 2014) 8

Figure 3: Speciation diagram for the cadmium, (Li et al., 2006) 11

Figure 4: Speciation diagram for the nickel, (Boubatra et al., 2011) 12

Figure 5: Speciation diagram for the copper, (Cuppett et al., 2006) 13

Figure 6: Speciation diagram for the cobalt, (Collins et al., 2010) 14

Figure 7: Types of liquid membrane a) bulk liquid membrane b) emulsion liquid membrane and c) supported liquid membrane, (Zawierucha et al, 2016) 18

Figure 8: Evolution of PIM and number of papers produced, (Almeida et al., 2017) 20

Figure 9: Structures of a) PVC and b) CTA 21

Figure 10: PIM, the idea of carrier transport, (Rajewski et al., 2016) 22

Figure 11: Simplified scheme of PIM matrix, (Rajewski., 2016) 22

Figure 12: Structure of D2EHPA. 25

Figure 13: Octahedral coordination of nickel with D2EHPA, (Van de Voorde et al.,2007) 27

Figure 14: Cobalt-D2EHPA tetrahedral complex, (Van de Voorde et al., 2007) 27

Figure 15: Square-planar complex of copper with D2EHPA, (Van de Voorde et al., 2007) 27

Figure 16: Square-planar complex of cadmium with D2EHPA 28

Figure 17: Transport mechanism through PIM 30

Figure 18: Polymer inclusion membrane passive samplers, (Almeida et al., 2017) 31

Figure 19: The number of publications on passive samplers for water monitoring 37

Figure 20: The number of citations per year of passive samplers for water monitoring 38

Figure 21: An Illustration of the uptake of the passive sampler in the water body where the concentration changes all the time. Passive sampler measures the integrative average concentration since sampling is performed continuously..... 38

Figure 22: Representation of the different accumulation regimes during exposure of a passive sampler, copied from (Vrana et al., 2005)..... 40

Figure 23: Views of the prototype Chemcatcher device, used during sampler development. The PTFE body parts (1st generation) support the receiving phase and the diffusion membrane and sealed them in place. The sampler is sealed by means of a screw cap for storage and transport (Nyoni et al., 2010). 43

Figure 24: A representation of the free ionic species in a gel assembly that's in contact with natural water. The DBL is the diffusive boundary layer (Davison and Zhang, 2012). 44

Figure 25: A simple representation of the DGT device with the functional components as indicated (Mengistu et al., 2012). 45

Figure 26: Dimensions of the a) small exposure area and b) large exposure area 48

Figure 27: Elcometer motorised film applicator with casted membrane 56

Figure 28: Polytetrafluoroethylene rod 57

Figure 29: Components of the PIM a) receiver solution chamber, b) screw cap and (c) screw cap with a widow opening 57

Figure 30: Fully assembled passive sampler housing 58

Figure 31: Unassembled PIM-based passive sampler..... 58

Figure 32: Assembled PIM-based passive sampler with exposure area 58

Figure 33: PIM-based passive sampler holder 60

Figure 34: PIM-based passive sampler deployed..... 60

Figure 35: Sampling sites used for the deployment of PIM-based passive samplers, a) is the acid mine drainage impacted sampling site b) Fleurhof dam which is in close proximity to a mine tailing. 63

Figure 36: a) threaded steel rods and b) plastic mesh was wrapped around the steel rod structure in order to seal the Cages used for housing the passive samplers during field deployments, c) and d) deployment of the passive samplers, (e) picture of passive samplers submerged in the field. 64

Figure 37: Effect of extractant (D2EHPA) concentration (%w/w) in the membrane (n = 3, SD) Feed phase: 1 mg L^{-1} of the metal ion concentration, pH = 6.0, Stripping phase: 1mol $L^{-1}HNO_3$, Carrier: 40%, Operation temperature: 25°C, Time: 1 days, stirring speed of 200 rpm, Thickness of PIM: 150 μm. 68

Figure 38: Effect of various acids on the receiver solution set at pH 6 (n = 3, SD) Feed phase: 1 mg L^{-1} of the metal ion concentration, pH: 6.0, Carrier: 40%, Operation temperature: 25°C, Time: 1 day, Stirring speed: 200 rpm, Thickness of PIM: 150 μm. 69

Figure 39: Effect of stripping phase concentration on the extraction of metal ions (n = 3, SD) Feed phase: 1 mg L^{-1} of the metal ion concentration, pH: 6.0, Carrier: 40%, Operation temperature: 25°C, Time: 1 day, stirring speed: 200 rpm, Thickness of PIM: 150 μm. 70

Figure 40: The effect of pH on the membrane extraction capacity (n = 3, SD) Feed phase: 1 mg L^{-1} of the metal ion concentration, Stripping phase: 1 mol L^{-1} HNO_3, Carrier: 40%, Operation temperature: 25°C, time: 1 day, Stirring speed: 200 rpm Thickness of PIM: 150 μm. 71

Figure 41: Effect of the thickness of PIM on the transport (n = 3, SD) Feed phase: 1 mg L^{-1} of the metal ion concentration, pH = 6.0, Stripping phase: 1mol $L^{-1}HNO_3$, Carrier: 40%, Operation temperature: 25°C, Time: 1 day, stirring speed: 200 rpm 72

Figure 42: The effect of different stirring speed on concentration in the receiver solution of the passive sampler was investigated at 0, 200 and 400 rpm (n = 3, SD) Feed phase: 1 mg L^{-1} of the metal ion concentration, pH: 6.0, Stripping phase: 1mol

$L^{-1}HNO_3$, Time: 5 days, Carrier: 40%, Operation temperature: 25ºC, Thickness of PIM: 150 μm. 73

Figure 43: pH 6 PIM-based passive sampler window opening results after day 2 (n = 3, SD) Feed phase: 1 mg L^{-1} of the metal ion concentration, pH: 6.0, Stripping phase: 1mol $L^{-1}HNO_3$, Carrier: 40%, Operation temperature: 25ºC, Time: 1 day, stirring speed: 200 rpm, Thickness of PIM: 150 μm. 74

Figure 44: Transport of metal ion across PIM (n = 3, SD) Feed phase: 1 mg L^{-1} of the metal ion concentration, pH: 6.0, Stripping phase: 1mol $L^{-1}HNO_3$, Carrier: 40%, Operation temperature: 25ºC, stirring speed: 200 rpm, Thickness of PIM: 150 μm. 76

Figure 45: Stability of PIM for three consecutive experiments (n = 3, SD) Feed phase: 1 mg L^{-1} of the metal ion concentration, pH: 6.0, Stripping phase: 1mol $L^{-1}HNO_3$, Carrier: 40%, Operation temperature: 25ºC, Time: day 3, stirring speed: 200 rpm, Thickness of PIM: 150 μm. 77

Figure 46: Membrane before a) and after b) extraction. 77

Figure 47: SEM image surface of the a) before extraction and b) after extraction of PIM..... 78

Figure 48: Thermogram a) PVC, b) before, and c) after extraction of PIM 79

Figure 49: ^{31}P NMR spectrum of PIM Composition 80

Figure 50: Uptake of metal ion in the laboratory using Fleurhof dam spiked with 1 mgL^{-1} metal ion (n = 3, SD) Feed phase: 1 mg L^{-1} of the metal ion concentration, pH: 6.0, Stripping phase: 1mol $L^{-1}HNO_3$, Carrier: 40%, Operation temperature: 25ºC, stirring speed: 200 rpm, Thickness of PIM: 150 μm. 83

Figure 51: Uptake of Cu (II) and Fe (II) in in the laboratory using dam unspiked (n = 3, SD) Feed phase: 1 mg L^{-1} of the metal ion concentration, pH: 6.0, Stripping phase: 1mol $L^{-1}HNO_3$, Carrier: 40%, Operation temperature: 25ºC, stirring speed: 200 rpm, Thickness of PIM: 150 μm. 84

Figure 52: Uptake of Co (II), Ni (II) and Cd (II) in in the laboratory using Fleurhof dam unspiked (n = 3, SD) Feed phase: 1 mg L^{-1} of the metal ion concentration, pH:

6.0, Stripping phase: 1mol $L^{-1}HNO_3$, Carrier: 40%, Operation temperature: 25ºC, stirring speed: 200 rpm, Thickness of PIM: 150 μm 85

Figure 53: Metal ion deployed in AMD water in the laboratory (n = 3, SD) Feed phase: 1 mg L^{-1} of the metal ion concentration, pH: 2.83, Stripping phase: 1mol $L^{-1}HNO_3$, Carrier: 40%, Operation temperature: 25ºC, stirring speed: 200 rpm, Thickness of PIM: 150 μm. 86

Figure 54: Fe precipitation after day 5 in the laboratory set up 86

Figure 55: Effect of stirring rate using Fleurhof dam water spiked with 1 mgL^{-1} of each metal ion (n = 3, SD) Feed phase: 1 mg L^{-1} of the metal ion concentration, pH: 6.0, Stripping phase: 1mol $L^{-1}HNO_3$, Carrier: 40%, Operation temperature: 25ºC, stirring speed: 200 rpm, Thickness of PIM: 150 μm. 88

Figure 56: Effect of stirring rate on uptake of PIM-based passive sampler in AMD in the laboratory (n = 3, SD) Feed phase: 1 mg L^{-1} of the metal ion concentration, pH: 2.83, Stripping phase: 1mol $L^{-1}HNO_3$, Carrier: 40%, Operation temperature: 25ºC, stirring speed: 200 rpm, Thickness of PIM: 150 μm. 88

Figure 57: Un-spiked dam water receiver solution pH 89

Figure 58: Spiked dam water receiver solution pH..... 90

Figure 59: AMD receiver solution pH 90

Figure 60: Uptake of Cu (II) and Fe (II) in PIM sampler deployed at Fleurhof dam (n = 3, SD) Feed phase: 1 mg L^{-1} of the metal ion concentration, pH: 6.0, Stripping phase: 1mol $L^{-1}HNO_3$, Carrier: 40%, Operation temperature: 25ºC, stirring speed: 200 rpm, Thickness of PIM: 150 μm. 93

Figure 61: Uptake of Cd (II), Co (II) and Ni (II) in PIM sampler deployed at Fleurhof dam (n = 3, SD) Feed phase: 1 mg L^{-1} of the metal ion concentration, pH: 6.0, Stripping phase: 1mol $L^{-1}HNO_3$, Carrier: 40%, Operation temperature: 25ºC, stirring speed: 200 rpm, Thickness of PIM: 150 μm. 93

Figure 62: Other metal ion up take by PIM-based passive sampler after day 9 at Fleurhof dam (n = 3, SD) Feed phase: 1 mg L^{-1} of the metal ion concentration, pH:

6.0, Stripping phase: 1mol $L^{-1}HNO_3$, Carrier: 40%, Operation temperature: 25°C, stirring speed: 200 rpm, Thickness of PIM: 150 μm. 94

Figure 63: Comparison of the receiver solution pH in PIM sampler deployed at diferent days at Fleurhof dam (n = 3, SD) 95

Figure 64: Picture of PIM-based passive sampler cages a) on day of deployment and b) day 12 at Fleurhof dam 96

Figure 65: PIM pictures deployed different days at Fleurhof Dam 97

Figure 66: Comparison of the metal ion bioavailable fraction in PIM sampler deployed over 5 days in laboratory and field (n = 3, SD) Feed phase: 1 mg L^{-1} of the metal ion concentration, pH: 6.0, Stripping phase: 1mol $L^{-1}HNO_3$, Carrier: 40%, Operation temperature: 25°C, stirring speed: 200 rpm, Thickness of PIM: 150 μm. 98

Figure 67: Uptake of iron at AMD site (n = 3, SD) Feed phase: 1 mg L^{-1} of the metal ion concentration, pH: 2.83, Stripping phase: 1mol $L^{-1}HNO_3$, Carrier: 40%, Operation temperature: 25°C, stirring speed: 200 rpm, Thickness of PIM: 150 μm. 100

Figure 68: Uptake of copper at AMD site days (n = 3, SD) Feed phase: 1 mg L^{-1} of the metal ion concentration, pH: 2.83, Stripping phase: 1mol $L^{-1}HNO_3$, Carrier: 40%, Operation temperature: 25°C, stirring speed: 200 rpm, Thickness of PIM: 150 μm. 101

Figure 69: Uptake of nickel at AMD site (n = 3, SD) Feed phase: 1 mg L^{-1} of the metal ion concentration, pH: 2.83, Stripping phase: 1mol $L^{-1}HNO_3$, Carrier: 40%, Operation temperature: 25°C, stirring speed: 200 rpm, Thickness of PIM: 150 μm. 101

Figure 70: Uptake of cobalt at AMD site (n = 3, SD) Feed phase: 1 mg L^{-1} of the metal ion concentration, pH: 2.83, Stripping phase: 1mol $L^{-1}HNO_3$, Carrier: 40%, Operation temperature: 25°C, stirring speed: 200 rpm, Thickness of PIM: 150 μm. 102

Figure 71: Uptake of cadmium at AMD site (n = 3, SD) Feed phase: 1 mg L^{-1} of the metal ion concentration, pH: 2.83, Stripping phase: 1mol $L^{-1}HNO_3$, Carrier: 40%,

Operation temperature: 25ºC, stirring speed: 200 rpm, Thickness of PIM: 150 μm. 102

Figure 72: pH of the receiver solution in PIM sampler deployed at diferent days at AMD 103

Figure 73: Rusting on cage surface after deployment of a) day 2 and b) day 12 at AMD 104

Figure 74: Fouling of polymer inclusion membrane after deployment at AMD site 104

Figure 75: Comparison of uptake of metals in PIM-based passive sampler deployed in AMD water in the laboratory and in the field (n = 3, SD) Feed phase: 1 mg L^{-1} of the metal ion concentration, pH: 2.83, Stripping phase: 1mol $L^{-1}HNO_3$, Carrier: 40%, Operation temperature: 25ºC, stirring speed: 200 rpm, Thickness of PIM: 150 μm. 105

Figure 76: Other metal ions up take by PIM-based passive sampler after day 9 at AMD (n = 3, SD) Feed phase: 1 mg L^{-1} of the metal ion concentration, pH: 2.83, Stripping phase: 1mol $L^{-1}HNO_3$, Carrier: 40%, Operation temperature: 25ºC, stirring speed: 200 rpm, Thickness of PIM: 150 μm. 106

Figure 77: FTIR spectrum of PIM a) before extraction, b) after extraction at Fleurhof dam and c) AMD..... 110

Figure 78: 2D and 3D-AFM images of PIM before extraction..... 111

Figure 79: 2D and 3D-AFM images of PIM after 12 days extraction at Fleurhof dam..... 112

Figure 80: 2D and 3D-AFM images of PIM after 12 days extraction at AMD site 112

List of tables

Table 1: PIM composition (total mass = 1g)..... 56

Table 2: Physical-chemical properties of dam water during sampler deployment in the laboratory 82

Table 3: Metal ion concentration in the AMD sampled in one batch but analysed different days and kept at room temperature..... 87

Table 4: Total concentrations of target metals in the dam water and their comparison to various drinking water allowed limits..... 92

Table 5: Concentrations of metals ions collected from dam water and in the receiving solution after a 12 day sampling period 99

Table 6: Concentrations of metals ions collected from AMD and in the receiving solution after a 12 day sampling period .....**Error! Bookmark not defined.**

Table 7: Recent examples of PVC/D2EHPA membrane and the maximum number of days the PIM-based passive samplers were deployed 108

Table 8: Mean square roughness values after 12 days of sampling at Fleurhof dam and AMD..... 111

List of abbreviations

AMD	Acid mine drainage
D2EHPA	Diethylhexyl phosphoric acid
PVC	Polyvinyl chloride
PIM	Polymer inclusion membranes
SLM	Supported liquid membrane
As	Arsenic
Pb	lead
Cu	Copper
Cd	Cadmium
Co	Cobalt
Ni	Nickel
Fe	Iron
Zn	Zink
Ag	Silver
Au	Gold
Mn	Manganese
Al	Aluminium
BLM	Bulk liquid membrane
ELM	Emulsion liquid membranes
IL	Ionic liquid
TWA	Time weight average concentration
LM	Liquid membranes
non-SLM	Non-supported liquid membranes
CTA	Cellulose triacetate

THF	Tetrahydrofuran
HNO_3	Nitric acid
H_2SO_4	Sulphuric acid
HCl	Hydrochloric acid
(Ni $(NO_3)_2$)	Nickel (II) nitrate
(Co $(NO_3)_2 \cdot 6H_2O$)	Cobalt (II) nitrate hexahydrate
(Cu $(NO_3)_2$)	Copper (II) nitrate
(Cd $(NO_3)_2 \cdot 4H_2O$)	Cadmium (II) nitrate
SEM	Scanning electron microscopy
FT-IR	Fourier transformed infrared spectrometry
TGA	Thermal gravimetric analysis
AFM	Atomic force microscope
NMR	Nuclear magnetic resonance
PTFE	Polytetrafluoroethylene
ACAC	Acetylacetone
DOP	Dioctyl phthalate
DGT	Diffusion gradient in thin-film
SPMD	Semipermeable membrane devices
Rs	Sampling rate
Eh	Redox potential
R_a	Mean roughness
R_q	Mean square roughness

CHAPTER 1

This chapter gives the outline on the applications of polymer inclusion membrane based passive samplers in analysis of pollutants in the environment.

1 Introduction

High metal ion concentrations are frequently encountered in natural aquatic environments especially those receiving mine tailings runoff like rivers and dams. Metal ions like cobalt, nickel, cadmium and copper act as micronutrients and are essential trace elements in plants and animals but may result in acute and chronic poisoning if taken above certain threshold levels (Grande et al., 2018; Prashanth et al., 2015). Research has indicated that long-term exposure of these trace metals can have adverse effects on aquatic species such as fish and daphnia (Cho et al., 2018). Thus, it is very important that they are monitored in the environment in order to see if their concentrations are not above levels that are detrimental to life (Duruibe et al., 2007; Javed and Usmani, 2013).

The most common approach in collecting samples for analysis is grab sampling (Garcia-Rodríguez et al., 2015; Namieśnik et al., 2005)**.** However, this approach has several drawbacks that include high cost, the introduction of artefacts from transport and storage of the sample. The grab sampling technique gives only a snapshot of the water status at a particular period and place in the investigated water (Zabiegała et al., 2010). It does not cater for variations in pollutant levels over a period and does not account for bioavailable fraction. Results from grab sampling report episodic levels and may therefore result in misinterpretation of the pollution levels of the water body under study. As such, passive sampling has been introduced to circumvent these drawbacks by deploying devices at the sampling site that can continuously collect the pollutants from water (Miege et al., 2015; Vrana et al., 2005; Zabiegała et al., 2010). This approach also combines analyte collection and pre-concentration into a one-step procedure thus reducing possibilities of sample loss, contamination or degradation as is common with grab samples (Miege et al., 2015). Passive sampling allows for determination of a time-weighted average concentration of pollutants over extended periods from hours to days and weeks. Therefore, episodic pollution events are accounted for unlike in grab sampling(Garcia-Rodríguez et al., 2016; Zabiegała et al., 2010).

Passive samplers are monitoring techniques which are composed of a semi-permeable barrier, which separates the source phase (aquatic environment), from the receiver phase, where the analyte is collected (Almeida et al., 2017; Eljaddi et al., 2017; Vera et al., 2018a)**.** The receiving phase can be a liquid as in membrane based passive sampler or resin as in diffusive gradient in thin film (DGT) passive sampler. In membrane based passive sampler, the membrane composition is selected based on the type of species being monitored. Moreover, the membrane selected determines how fast a single or multiple species are collected in the receiving phase (Nyoni et al., 2010; Vrana et al., 2005). In diffusive gradient in thin films passive sampler, the membrane separates the source and the resin embedded in a diffusive gel (Turull et al., 2016). One of the main disadvantages associated with the DGT sampler is that desorption step after extraction involving elution of the analytes from the solid sorbent is needed. The commercial DGT passive sampler is also used once and thrown away and there are limited suppliers of it. In addition, most of these passive samplers are commercialized and hence expensive and not reusable

As such, researchers continue to search for alternative passive sampler designs that are cheap, easy to use and reusable. In this regard, some passive samplers employing membranes as transporting media have been introduced (Garcia-Rodríguez et al., 2016; Gega et al, 2014; O'Rourke et al., 2009; Vera et al., 2018). Such passive samplers use an aqueous receiver phase that can be injected directly into quantitation instruments without the need for further treatment. Furthermore, high analyte pre-concentration is achieved in the receiver phase due to the driving force created by a counter ion such as H^+ ion gradient provided by the small amount of acid (<10 mL) used as the receiver phase. In this regard, polymer inclusion membrane (PIM) passive samplers have been reported in literature (Garcia-Rodríguez et al., 2016; Vera et al., 2018). Almeida et al. (2014) have used the PIM-based passive sampler for determining the time weighted average of Zn ions in urban waters (Almeida et al., 2014). The passive sampler is composed of a Teflon chamber attached to a stainless-steel base with polyvinyl chloride (PVC) as a membrane embedded with diethylhexyl phosphoric acid (D2EHPA) as cationic

carrier. The same research group has used a glass-based chamber for analysis of total ammonia concentration in freshwater and used dinonylnaphthalene sulfonic acid as a carrier, PVC as a base polymer and 1- tetradecanol as a modifier. Teflon tape was used to seal the glass threads to prevent leakage (Almeida et al., 2016).

In this study, PIM based sampler with an entirely polytetrafluoroethylene (PTFE) holders were developed, optimised and applied in the field. These have an advantage of robustness and being stable under adverse environmental conditions indicating that it can be deployed in any environmental samples, whether very acidic or basic. The combination of a PVC membrane and D2EHPA resulted in no need of using a plasticizer and a modifier during synthesis. The presence of the acidic D2EHPA in the membrane gives the membrane bactericidal properties and therefore avoids fouling of the membrane when deployed in the environment. The developed passive sampler was then used to study the transport and fate of nickel (Ni), cadmium (Cd), copper (Cu), Iron (Fe) and cobalt (Co) in AMD and dam water affected by mining activities.

CHAPTER 2

This chapter discusses the pollution of the environment due to acid mine drainage. Various sampling techniques are discussed with an emphasis on passive sampling. The benefits of membrane based passive samplers are outlined.

2 Literature review

2.1 Acid mine drainage

South African economy relies heavily on mining. Mining has been identified as a two-edged sword with both beneficial effects such as job creation, but also with negative effects related to pollution. Pollution is due to waste by-products that contain toxic metal ions. The impact of mining on the environment include soil erosion, water pollution, air pollution and loss of bio-diversity resources to the accumulation of pollutants in different media of the environment (Shokri et al., 2016; Johnson et al., 2005). In Gauteng, there are a number of tailing dumps from mostly gold mining activities (Camden-Smith et al., 2015). During rains, sulphide minerals, mostly pyrite, in the tailing dumps react with oxygen and water to form acid mine drainage (AMD) that in turn leach out toxic trace metal ions in the surrounding wetlands (Camden-Smith et al., 2015). The sulphide minerals can become unstable and oxidization occurs when exposed to atmospheric oxygen or oxygenated waters due to mining (Mocq et al, 2018; Simate et al, 2014). AMD is produced when sulphide-bearing material is exposed to oxygen and water. The acid produced dissolves salts and mobilizes heavy metals from mine workings. A considerable amount of acidic-water continues to be released from abandoned underground workings into the surface environment. Dark, reddish-brown water and pH values as low as 2.5 persist at the site as in (Figure 1).



Figure 1: Acid mine drainage through a stream in Roodepoort, Johannesburg West. The sampling site was near a mine tailing, with active AMD production

The AMD is formed when one of the most common sulphide minerals known as pyrite (FeS_2) is oxidized (Akcil, 2006; Shokri et al., 2016; Luptakova et al., 2010). The formation of AMD takes place in three major steps: (a) oxidation of pyrite into or to form ferrous ion (Eqn1), (b) oxidation of ferrous ion resulting into ferric ion (Eqn 2) and (c) hydrolysis and precipitation of ferric ion and other minerals (Eqn 3). The overall reaction is summarised in (Eqn 4).

$$2FeS_2 + 7O_2 + 2H_2O \rightarrow 2Fe^{2+} + 4SO_4^{2-} + 4H^+ \quad (1)$$

$$4Fe^{2+} + O_2 + 4H^+ \leftrightarrow 4Fe^{3+} + 2H_2O \quad (2)$$

$$Fe^{3+} + 3H_2O \leftrightarrow Fe(OH)_3 \downarrow + 3H^+ \quad (3)$$

$$FeS_2 + 14Fe^{3+} + 8H_2O \rightarrow 15Fe^{2+} + 2SO_4^{2-} + 16H^+ \quad (4)$$

Thus, the oxidation of sulphide minerals in mine waste drainage is indicated by the presence of sulphate ions which affect pH. In a highly oxidative environment due to oxygen concentration and bacterial activity, the ferrous iron released in (Eqn 1) may be oxidized to ferric iron according to (Eqn 2). If oxygen is low, (Eqn 2) will not occur until the pH reaches 8.5. In general, under many conditions, (Eqn 2) is the rate-limiting step in pyrite oxidation because the conversion of ferrous to ferric is slow at pH values below 5 under abiotic conditions. At pH values between 2.3 and 3.5, ferric iron formed in (Eqn 2) may precipitate as $Fe(OH)_3$ (Eqn 3) and to a lesser degree as $H_3OFe_3(SO_4)_2(OH)_6$ (jarosite), leaving a small amount of Fe^{3+} in solution while lowering the pH at the same time. If pH is less than 2, $Fe(OH)_3$ is not stable and Fe^{3+} remains in solution (Edwards et al., 2000).

The overall equation (Eqn 4) results in formation of the $Fe(OH)_3$ precipitate and sulphuric acid. The $Fe(OH)_3$ precipitate is responsible for the brown colour of

AMD. The presence of sulphuric acid which lowers the pH, increases the solubility of metal ions which can flow into water systems such as rivers, lakes and groundwater where they can cause serious environmental challenges (Simate et at., 2014). Thus, at typical conditions of pH and sulphate concentration in AMD solutions (e.g., pH 2.5 – 3.5 and 0.1 mol L^{-1} SO_4^{2-}), Fe(III) is chiefly present as sulphate complex (e.g $FeSO_4^-$) with a minor presence of the free aqueous ions Fe (III), and the hydroxyl containing ionic complex ($Fe(OH)_3$ etc.) having negligible presence. However, this ionic speciation strongly varies with pH and the activity of the sulphate anion, as shown in (Figure 2,) which plots the ionic species of Fe (III) as a function of pH. This figure shows that the free aqueous cations Fe (III) are only dominant at extremely acidic conditions (pH 1), while the metal sulphate complexes are dominant in the pH ranges 1 – 4.5 for Fe (III). As pH increases, the sulphate ionic complexes are progressively replaced by hydroxide forms (e.g. $Fe(OH)_3$), which become dominant at near-neutral conditions (pH 5 for Fe(III)) (España et al, 2014)

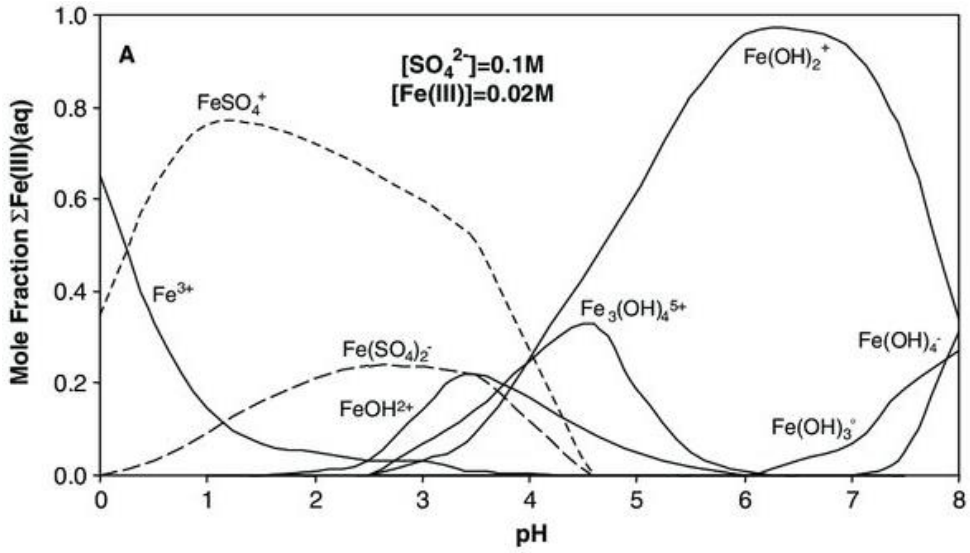

Figure 2: Speciation diagram for the iron, (Sanchez España et al., 2014)

The mining sites cause serious environmental challenges that negatively affect the surrounding ecosystems and human health (Miege et al., 2015; Brown.,et al 1984). However, it does not mean that wetlands have infinite capacity and depending on the environmental conditions, re-desorption can occur. Moreover, mining can have

negative impact on the most important elements (water, atmosphere and soil). Since Gauteng has a number of gold tailing dumps that leach out acid mine drainage, the acid mine drainage contains toxic trace metals that are deposited in the surrounding wetlands (Tutu et al., 2005). Wetlands are recognized as sinks for pollutants. In recognition of the role wetlands play, some constructed wetlands have also been made to confine the toxic metals. In some of these new constructed wetlands, plants are being grown to increases the capacity of the wetlands to retain the pollutants. The mining sites are often contaminated with several kinds of trace metals that come primarily from ore processing, and the disposal of tailings and can be released into the environment either directly or indirectly (Abdul-wahab et al, 2012). Once in the environment, these elements can be accumulated in plants and animals, and then reach human beings through the food chain (Roebbert et al., 2018). Some of these elements (As, Hg and U) are very toxic even in trace concentrations and will cause damage to the surrounding ecosystem once they exceed the threshold limits (Abdul-wahab et al., 2012). Therefore, contamination of soils, sediments, water and biota by trace metals is a primary concern in the mining sites because of their toxicity, persistence, and accumulation in food chains (Donkor et al., 2005). The trace metals from mining sites are very crucial to consider since they are not biodegradable and thus, persist in the environment until they are physically removed. They are also abundant in sediments and soils especially because they are due to mining processes (anthropogenic) and natural (Aslibekian et al., 2003).

2.1.1 Trace metals: sources and effects

The transition metals such as Fe (II), Co (II), Ni (II) and Cu (II) which have atomic numbers 26, 27, 28 and 29 respectively, belong to the same period in the periodic table and have high melting and boiling points and relatively high densities. These metals also have similar physical and chemical properties which, leads to difficulty on their extraction and separation when they are in one system. Trace metals can occur naturally in some rocks and thus they can be found at trace level concentration in soil and the aquatic environment, particularly after man made disturbances such as mining and other industrial activities as mentioned. The waste from gold mining

always contains large volumes of chemical substances such as zinc (Zn), nickel (Ni), lead (Pb), arsenic (As), Cupper (Cu) and sulphate ions which are released into the environment and thus, leads to AMD (Fashola et al., 2016). The formation of AMD become prevalent when the sulphide-rich metals accumulate and are abandoned (Concas et al., 2006). The tailings and rock dumps can easily affect the quality of ground water. Thus, there is a significant interest in monitoring of trace metals through mining and waste (Elumalai et al., 2017).

2.1.2 The elements under study

Copper (Cu), cobalt (Co), nickel (Ni), cadmium (Cd) and iron (Fe) are available in the environment and are essential for normal metabolism in living organisms. However, they become toxic when they exceed the maximum allowable limits (Roebbert et al., 2018). Thus, when the quantities of Cu (II), Co (II), Ni (II), Cd (II) and Fe (II) increase in the body they become harmful to living organisms such as humans where they can cause serious problems such as malfunctioning human organs. Other trace metals such as As, Pb, and Cd are carcinogenic (Getaneh et al, 2002). Trace metals cause oxidative stress in plants (Fayiga et al, 2005). Metal stress was reported to affect photosynthesis, chlorophyll fluorescence and stomatal resistance (Viers et al., 2018). For instance, copper inhibits photosynthesis and reproductive processes. Consequently, plant growth is reduced or impossible (Franco-Hernandez et al., 2010). Concentration of trace metals were documented and reported from different parts of the world (Fayiga et al., 2005; Hernandez et al., 2010; Javed et al., 2013). Hence there is a need for extensive monitoring of these trace metals in the environment.

2.1.2.1 Cadmium

Cadmium is one of the most toxic trace metals to most organisms. Its concentration in gold mine tailings range between 6.4 and 11.7 mg kg^{-1} have been reported by Fashola et al., (2016). It occurs in gold bearing orebodies as an isometric trace element in sphalerite and its concentration depends on the concentration of the

sphalerite in the ore body. Cadmium is of serious concern due to its accumulation in the food chain, drinking water and soil. It has an exceptionally long biological half-life (>20 years), highly mobile in soil-plant systems and can also exert a great effect on the proper functioning of the ecosystems. The bioavailability of Cd (II) and associated toxicity to soil bacteria depends on the bacterial species, concentration, environmental factors, time, speciation, soil properties and ageing (Vig et al., 2003). When cadmium is present in soils it has the potential to enter the food chain. Soils that are acidified enhance the cadmium uptake by plants. The adsorption of Cd (II) in soil is influenced by pH, exchangeable cations and ionic strength. As pH increases, the adsorption of Cd (II) increases. At lower pH cadmium speciation exist as Cd (II) and at higher pH cadmium speciation exist as hydroxide (Figure 3). Thus, adsorption of Cd (II) onto soils is a function of pH. Precipitation is another mechanism that controls the adsorption of Cd (II) on the soils. This is a potential danger to the animals that are dependent upon the plants for survival. Cadmium can accumulate in their bodies especially vital organs like kidneys (Bertin et al., 2006).

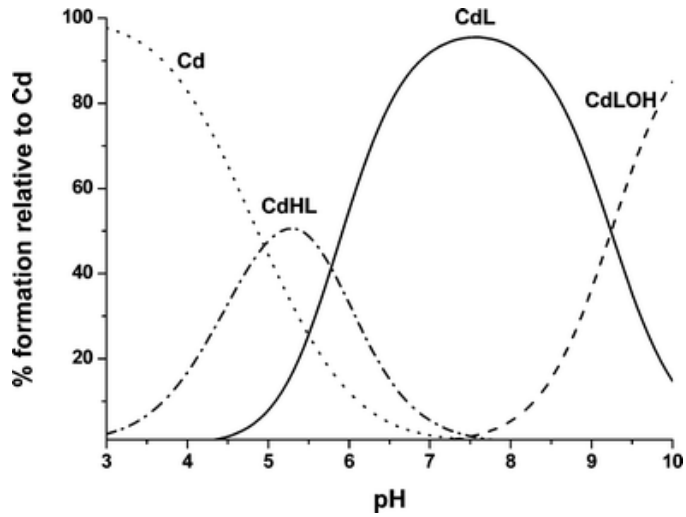

Figure 3: Speciation diagram for the cadmium, (Li et al., 2006)

2.1.2.2 Nickel

A nickel level in gold mine tailings has higher concentration of 583 mg kg^{-1}, which was reported by Matshusa et al., (2012) in South Africa (Matshusa et al., 2012). Nickel exists in gold bearing ore as pyrrhotite, which can contain up to 5% nickel

and pentlandite. Other mineral sources are chalcopyrite and gersdorffite (Cempel et al., 2006). It exists in the 0 and +2 oxidation states and less often in the -1, +1, +3 and +4 oxidation states. Among its species, the +4 oxidation state is known to be more toxic and carcinogenic compared to +2 (Iyaka et al., 2011). This shift of the oxidation state can affect the pH values since it is influenced by protons in the case of low pH values and by hydroxide ions in the case of higher pH values. This is in good agreement with the Pourbaix pH diagram for nickel in water shown in (Figure 4). Nickel toxicity arises due to its tendency to substitute other metal ions in proteins, maybe due to its high affinity for the amine groups contained in enzymes and protein or attach to cellular compounds (Cempel et al., 2006). It also intermingles with not less than 13 essential elements in living organisms. The major toxicity of Ni (II) to bacterial cells include, replacement of essential metal of metalloproteins, attachment to catalytic residues of non-metalloenzymes, allosteric inhibition of enzyme and oxidative stress that enhanced DNA damage protein impairment (Macomber et al., 2011).

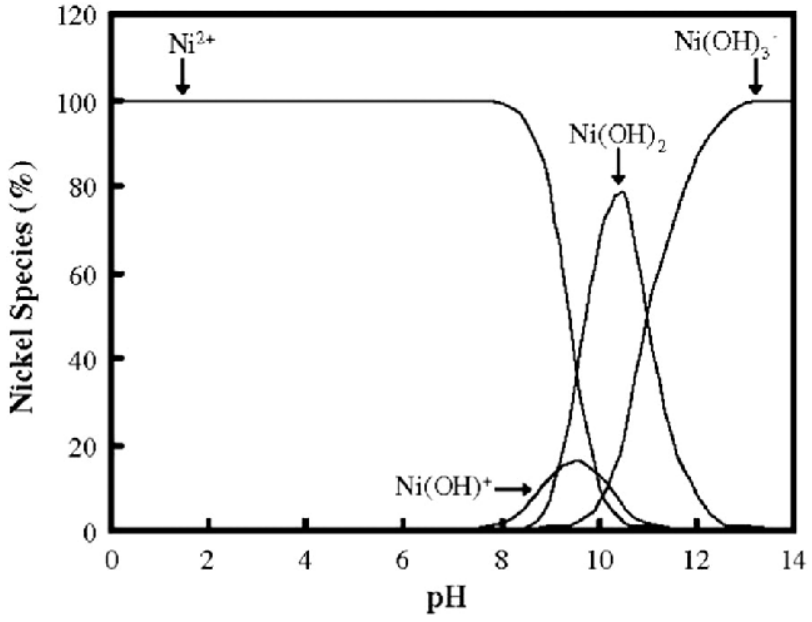

Figure 4: Speciation diagram for the nickel, (Boubatra et al., 2011)

2.1.2.3 Copper

Copper is widely distributed in sulphides, arsenites, chlorides and carbonates in gold ores. The mean concentration of 5 to 70 mg kg^{-1} exists in unpolluted soil while

higher concentrations are found in contaminated environments like mining sites, found a concentration of 92.17 mg kg^{-1} in gold mine tailings in Ghana (Stern et al., 2010). Gold mining has greatly increased Cu (II) concentration in the environment which upon release binds to particles of organic matter, clay minerals and sesquioxides leading to great accumulation in the soil (Ranjard et al., 2006). Copper, like many metals, interacts in water to form free metal cations, a variety of soluble complexes, and insoluble particles or precipitates, depending on the mineral content of the water. Free copper, which is the cupric ion (Cu), is soluble and the preferential form at low pH levels (typically below pH 6) and when there is a lack of anionic ligands. In pure water, soluble copper hydroxo complexes form at low and high pH values (Figure 5). Copper exists in two states, oxidized state Cu (II), and reduced state, Cu (I). The ability to exist in these two states makes this metal potentially toxic because the conversion between Cu (II) to Cu (I) could lead to a generation of superoxide and hydroxyl radicals (Stern et al., 2010). Excessive Cu concentration has deleterious effects on soil microbes (Amico et al., 2008). Copper toxicity is as a result of its harmful effects on the bacterial cell membranes and nucleic acid structure as well as its ability to alter enzyme specificity and disrupt cellular functions (Roebbert et al., 2018).

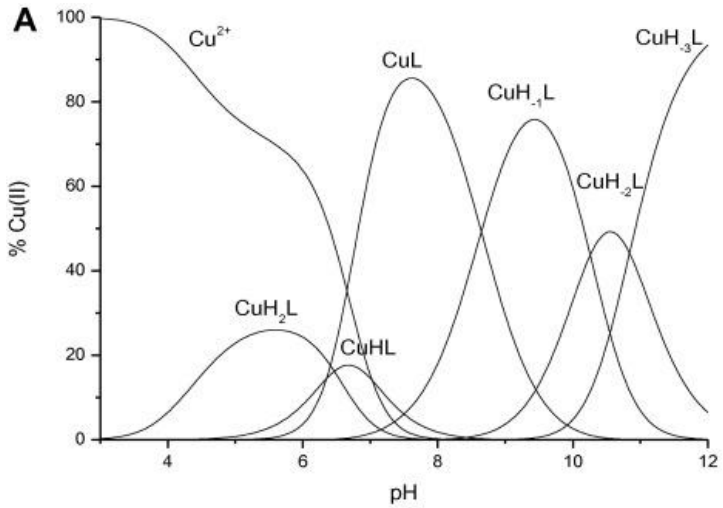

Figure 5: Speciation diagram for the copper, (Cuppett et al., 2006)

2.1.2.4 Cobalt

Cobalt is important in trace amounts for humans and other mammals as it is an integral component of the vitamin B12 complex; however, larger concentrations will be harmful. As for all divalent first-row transition metal cations, the Co^{2+} cation is octahedral coordinated with six water molecules. Although (Figure 6) indicates that at high pH the cation can undergo hydrolysis, the relevance of the hydrolysis species to the aqueous phase chemistry of Co in the environment is questionable. Most cobalt compounds released to the environment are adsorbed by sediment or soil particles and become immobile (Akcil et al, 2006; Collins et al, 2010). However, acidic environment, such as polluted/contaminated soils near mining site can lead to the remobilization of adsorbed metals and often rinse out to the surface and groundwater. Under this condition, the uptake by plants and animals is higher and accumulation in them may occur (Yousefi et al., 2015) Therefore, most risks from cobalt are associated with its forms that are accessible to the surface water and biologically available to plants (Gajda et al, 2012).

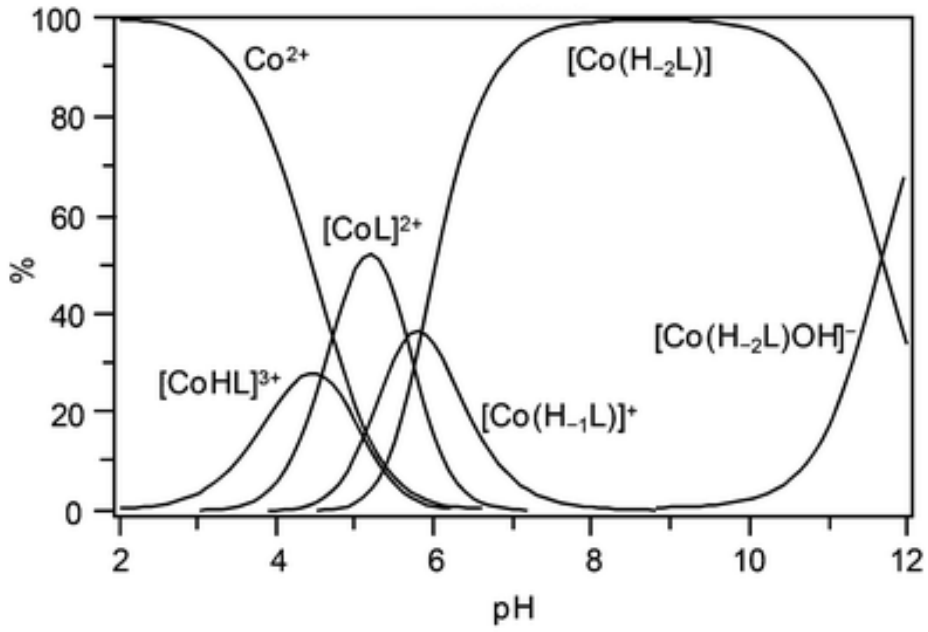

Figure 6: Speciation diagram for the cobalt, (Collins et al., 2010)

2.1.3 Technologies for the removal of trace metals

Several methods including chemical precipitation, coagulation, ion exchange, solvent extraction and adsorption can be used to monitor and recover trace metals from an aqueous solution (Fu et al., 2011). Among these, liquid-liquid solvent extraction is one of the most widely used technologies especially in hydrometallurgy processes (Gunatilake, 2015). Solvent extraction has been used for the processing of copper, nickel, cobalt, zinc, uranium, molybdenum, tungsten, vanadium, rare earths, zirconium, hafnium, niobium, tantalum, indium, gallium, germanium, the platinum metal group, reprocessing nuclear fuels, purification of wet process phosphoric acid and nitric acid recovery (Gupta et al., 2015). Generally, this method separates compounds based on their relative solubility in two different immiscible liquid mainly water and an organic solvent. However, this technology requires a large amount of an organic solvent that is not only expensive but also presents a major environmental and fire hazard due to the volatile, flammable, and toxic nature of these solvents (Sgarlata et al., 2008; Gupta et al., 2015). Indeed, solvent extraction can potentially lead to the evaporation of solvent and consume a large amount of energy, thus imposing significant environmental and health hazards (Ocampo et al., 2009). Hence, there is a need for alternative technologies to address these drawbacks. One such technology is membrane-based liquid-liquid extraction.

2.1.4 Liquid membranes

A membrane is a semipermeable barrier between two phases, where one component of a mixture moves through the membrane faster than another mixture component, a separation can be accomplished. If membranes are viewed as semipermeable phase separators, then the traditional concept of membranes as polymer films can be extended to include liquids. They are defined as liquid membranes (LMs). Liquid membrane system involves a liquid which is an immiscible with the source and receiving solutions that serves as a semipermeable barrier between these two liquid and gas phases (Kocherginsky et al., 2016). Due to the simple process and low energy consumption, it has become popular and preferable technology. It is applied in industrial application such as metal industries (metal recovery, pollution control,

air enriching for combustion), food and biotechnology industries (separation, purification, sterilization and by-product recovery). It is also applied in leather and textile industry (chemicals recovery and pollution control), pulp and paper industries, chemical process industries (gas separation, recovery, and recycle chemicals) and medical sector industries (Fenglianet al., 2011; Shahira et al., 2018).

There are many membrane processes including pressure driven membrane filtration, membrane distillation, liquid membrane and membrane bioreactor. These technologies are being expanded each day in various applications. For the last three decades, liquid membranes that integrate solvent extraction and membrane separation have been extensively studied (Chimuka et al., 2004; Eljaddi et al., 2017; Kiswandono et al., 2013; León et al., 2016). Studies reported to date in the literature demonstrate significant advantages over conventional solvent extraction techniques for trace metal monitoring and recovery (Kebiche-senhadji et al., 2008; Song et al., 2018). In general, there are three basic types of LMs namely, bulk liquid membranes (BLM), emulsion liquid membranes (ELM), and supported liquid membranes (SLM). LM provides a viable alternative for trace metal removal and monitoring; as they can achieve high permeate fluxes and high rejection coefficients at low energy costs and under mild conditions. LM play an important role in science and technology, and much effort is being put in for the development of these kinds of membranes. A LM is generally composed of a thin layer membrane containing an organic phase and separating two aqueous solutions. Also, the reverse configuration can be applied. The transport is based on liquid–liquid extraction and continuously operated membrane systems. A polymeric membrane can be used as a carrier, as a barrier, or not used. The mass transfer process through the LM basically consists of the solution-diffusion mechanism. The separation involves the solute diffusion through the membrane, due to a chemical/electrical gradient as driving force (Bringas et al., 2010; Resina et al., 2006).

2.1.4.1 Types of liquid membranes

Liquid membrane, depending on whether they contain only liquid phases or a polymeric support, is divided into two main categories: non-supported liquid

membranes (non-SLM) and SLM. In the case of non-SLM we have ELM and BLM. BLM consists of an aqueous and acceptor phases separated by a bulk organic liquid (Figure 7 a)). BLM are based on a simple design for carrying out liquid membrane operations, but present at the same time some disadvantages, such as small membrane surface, which limits its application at an industrial scale (Eljaddi et al., 2017). ELMs are made of an aqueous, internal stripping phase stabilized by oil soluble surfactants and dispersed droplets with very small dimension (1 - 10 μm) inside an oil phase. The resulting water/oil emulsion is further dispersed as globules of about 0.1–2 mm in another aqueous solution, which represents the donor phase (Figure 7 b)). This type of configuration offers a larger surface area, improving the transport rate through the membrane. The major problem of this type of liquid membranes is the difficulty of controlling the stability of the emulsion. However, it has to control multiple parameters simultaneously, such as ionic strength, pH, the stirring speed, and stirring time (Ling et al., 2017).

SLMs are based on the use of a porous, polymeric, or ceramic membrane that supports the organic phase and divides the donor phase and the receptor aqueous solution. By capillarity, the organic or carrier phase completely fills the pores of the solid membrane, leading to a relatively stable and heterogeneous solid–liquid membrane. This configuration is characterized by a high mechanical resistance, due to the presence of the solid support. Furthermore, when a solid membrane is hydrophobic, it promotes wetting by the organic solution and the rejection of the aqueous phases. The SLM operational systems commonly used are thin flat-sheet supports, hollow fibres, and spiral wound modules (Figure 7 c)) (Arous et al., 2010). It is difficult to obtain membranes which serve well for the purpose; hence, for specific chemical sensors they have to be synthesized according to the requirements of the researcher. Two routes for the preparation of the membranes include physical and covalent immobilization of required components in the polymer matrix (Mohapatra et al., 2006; Zawierucha et al, 2016 ; Zioui et al., 2017).

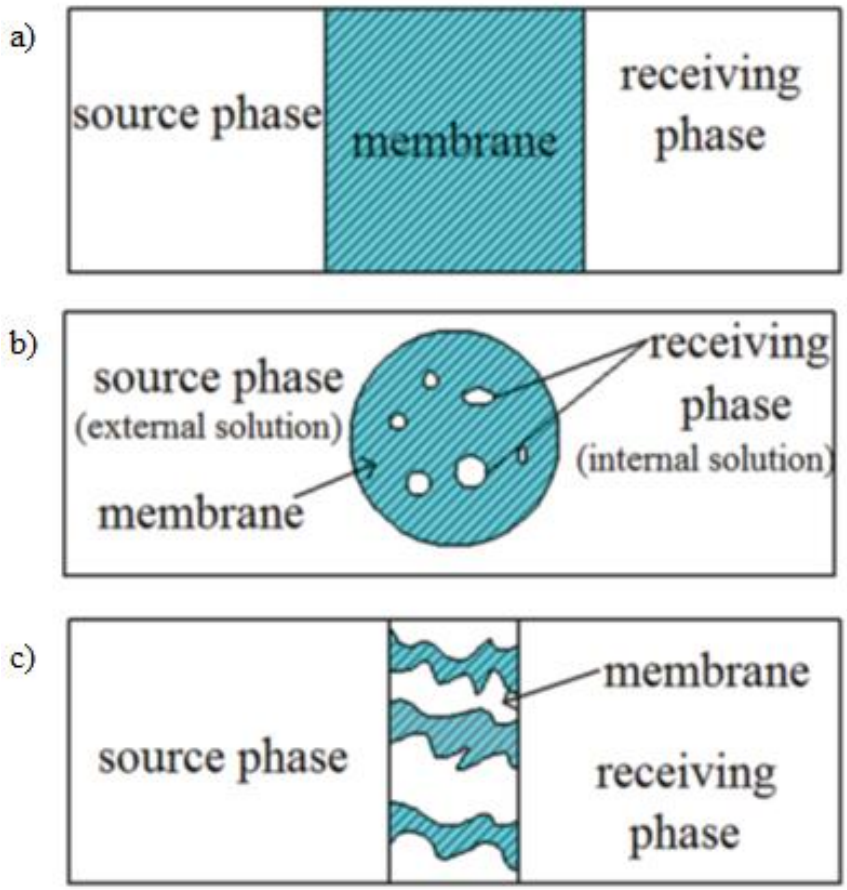

Figure 7: Types of liquid membrane a) bulk liquid membrane b) emulsion liquid membrane and c) supported liquid membrane, (Zawierucha et al, 2016)

Among the above membranes, SLM is the most widely studied. SLM consists of organic liquid which is embedded in small pores of a polymer support. This liquid contains an extractant which performs selectively separation as it binds with targeted components in feed solution and carries it to the other side of aqueous solution (stripping phase). Briefly, SLM involves three simultaneous processes that are extraction of the target species from feed phase to the SLM, diffusion through SLM and back-extraction of the target species to the stripping phase (Gega et al., 2014). The passage of the target ions from the source phase to stripping phase can be achieved by using different pH in both aqueous phases which will create different concentration gradient. This way, the targeted ions will be transported across the membrane against their concentration gradient and the process only uses

chemical energy as a driving factor and does not need any transmembrane pressure or voltage.

SLM exhibited high efficiency for the cation separation due to the fast transport rate and only need a small amount of the organic (Gega et al, 2014). However, the practical applications of SLM in industrial areas are limited due to several weaknesses. As a major concern regarding the long-term stability of SLM, the solvent and the organic extractant were found to be lost to the aqueous phase. The loss of extractant and membrane solvent should be reduced to increase the membrane lifetime and to assure their practical application in the future (Religa., et al 2015).

To improve the stability of SLM, (Nghiem et al., 2006; Salima et al., 2012) applied a thin cross-linked PVC gel layers on the feed side of the SLM. Their technique was effective for stabilizing the membranes for nitrate removal from water without any measurable influence on the flux. However, the reproducibility of their results was poor. This method is only suitable for flat sheet membranes. Several other attempts have been tested with varied level of success (Arous et al., 2010) but none of them have led to real significant improvements. Hence, more studies on immobilization of extractant were carried out. An alternative technique suggested by Masaaki Sugiura et al, (1987) has achieved some initial success. This technique used the plasticized cellulose triacetate (CTA) membrane containing extractant where the liquid plasticizer acts as an organic solvent like that used in SLM. The new alternative approach which synthesizes membrane with extractant incorporated in a plasticizer thermoplastic polymer is called polymer inclusion membranes (PIMs) and has of late retained so much attention, due to its better stability in comparison to other forms of liquid membranes. The chemical and physical properties of membrane polymers can be tailor made for specific applications. It is difficult to obtain membranes which serve well for the particular purpose; hence, for extraction of metal ions in wetlands the membranes were synthesized according to requirements in this study. Two routes for the preparation of the membranes

include physical and covalent immobilization of required components in the polymer matrix (Meng et al., 2017).

2.2 Polymer inclusion membranes

The polymer-based liquid membrane concept emerged about 50 years ago, but only recently have such membranes been termed "polymer inclusion membranes" (PIMs) (Almeida et al., 2017). These membranes were initially used as the sensing component in ion-selective electrodes and optodes (Figure 8). The interest around them has been growing exponentially as PIM-based separation has been also proving to be an attractive greener alternative to solvent extraction. PIMs are a type of liquid membranes composed of a liquid phase and a base polymer (Mostazo et al., 2017).

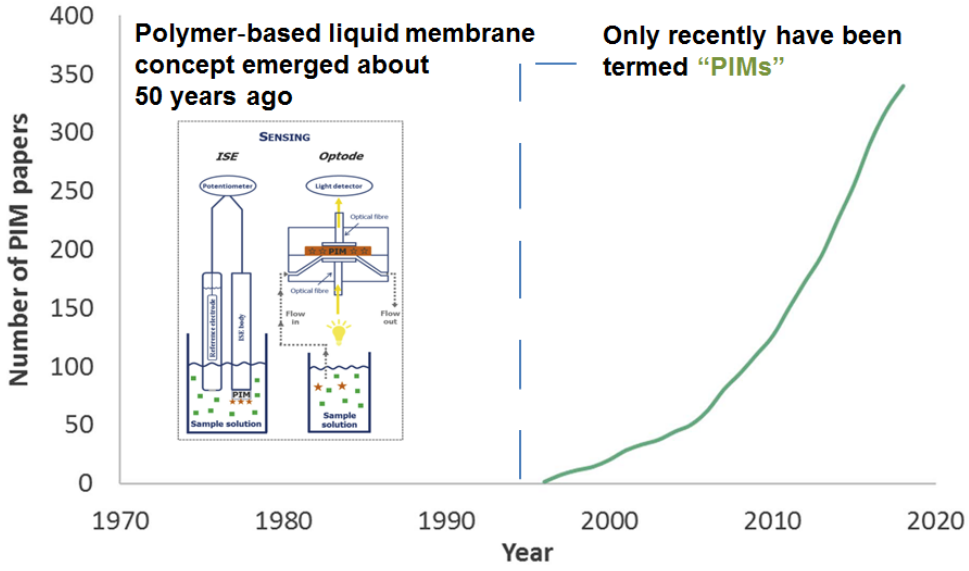

Figure 8: Evolution of PIM and number of papers produced, (Almeida et al., 2017)

In literature, PIMs are also known as polymer liquid, gelled liquid, polymeric plasticized, fixed-site carrier and solvent polymeric membranes (O'Rourke et al., 2009). The polymer-based liquid membrane has been proposed as a possible alternative to conventional solvent extraction. Polymer inclusion membranes are homogeneous, transparent, flexible and novel type of LM system and are usually

composed of an extractant, a base polymer (commonly used are PVC or CTA as shown in (Figure 9 a) & b)) and a plasticizer (Garcia-Rodríguez et al., 2015).

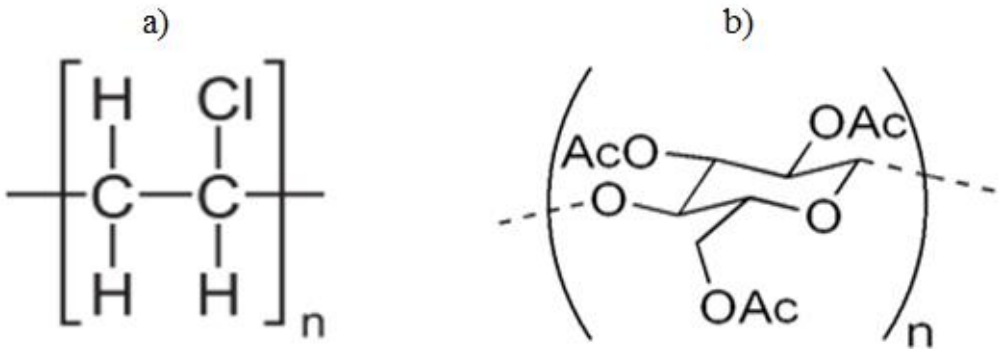

Figure 9: Structures of a) PVC and b) CTA

The base polymer provides the membrane with mechanical strength and the plasticizer provides elasticity and flexibility. Such a membrane form eliminates the problem of carrier elution to aqueous phase. PVC is used as polymer backbone in membrane because of its strength, inertness and compatibility with variety of plasticers (Yildiz et al., 2014). It is a non-flammable, light weight, durable polymer formed from a vinyl chloride monomer. The intermolecular interactions which dominate the C-Cl functional groups in PVC are nonspecific dispersion forces, which results in an amorphous structure. The carrier is essentially a complexing agent or anion-exchanger, responsible for binding with the species of interest (analyte) and transporting it across the PIM (Figure 10). This process relies on the concentration gradient of the species/carrier complex or ion-pair formed within the membrane, which acts as the driving force enabling transport across the membrane (Ling et al., 2017). Carrier mobility is limited because of mutual interactions between the carrier and the plasticizer, but movement in the plasticizer carrier particles and ion transfer takes place (L. Nghiem et al., 2006).

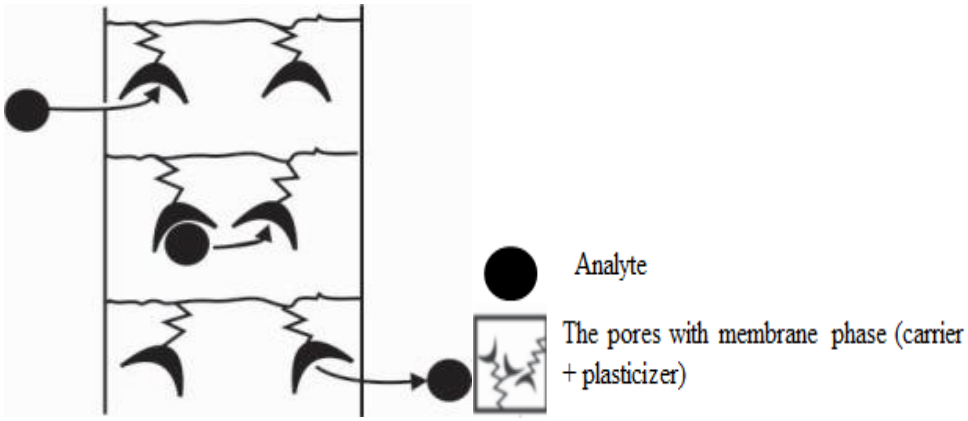

Figure 10: PIM, the idea of carrier transport, (Rajewski et al., 2016)

The plasticizer decreases the glass transition temperature of the membrane and improves the compatibility of the membrane components. A modifier (e.g. ethanol, 1-tetradecanol} is occasionally added to the membrane composition to improve the solubility of the extracted species in the membrane liquid phase. The use of PIMs for extraction and/or transport does not involve the use of toxic and volatile organic solvents. The amount of extractant required is very small, these membranes are considered environmentally friendly and separations using expensive extractants are economically viable. After casting the solution over a flat surface, the solvent is allowed to evaporate to form an optically transparent membrane. Each of these components contributes to important features that affect the overall performance of the polymer inclusion membrane and its transport mechanism as shown in (Figure 11) (Konczyk et al., 2010).

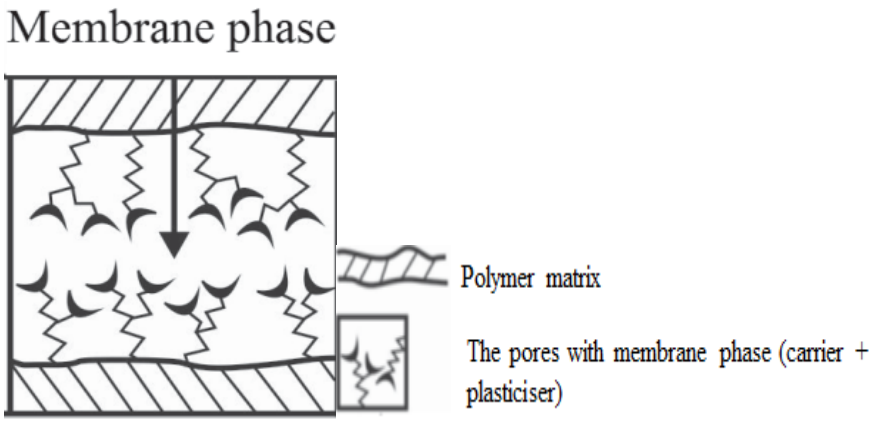

Figure 11: Simplified scheme of PIM matrix, (Rajewski., 2016)

The resulting membrane is used to separate source and receiving phases. This way, PIMs can effectively separate two aqueous phase without utilizing organic solvent to maintain phase separation. This makes the membrane easy to handle and promotes membrane durability (Nghiem et al., 2006). It should be noted that the simplicity of PIM fabrication makes it particularly attractive for developing low-cost separation/analytical technologies. To successfully cast a PIM, a good miscibility between the membrane components is imperative. Poorly miscible combinations will phase-separate upon drying, resulting in a brittle and inhomogeneous membrane, that will consequently contribute to the poor extractive performance of the PIM-based system. PIM components may only be miscible in specific or limited formulations, or exclusively in the presence of plasticizers or modifiers. If the PIM composition has been well designed, the resulting film should be mechanically stable, hydrophobic and safe to handle (Casadellà et al., 2016).

A comprehensive review by on the preparation and physiochemical properties of PIMs and their use in extraction and transport of various species has been published and demonstrate that research on PIMs has been largely focused on metallic rather than non-metallic species (Nghiem et al., 2006). This is undoubtedly due to the importance of extraction-based separation processes in the metallurgical processing of minerals and in the clean-up of metals from polluted natural waters and industrial and domestic wastewaters. It should be noted that PIMs have been used extensively for many years as the sensing membranes on ion-selective electrodes. Generally, for this application the amount of carrier in the membrane is around 1 wt%, whereas membranes used for extraction and transport typically contain 20 wt% or higher concentrations of carrier. The membrane performance in separation processes is strongly influenced by the membrane diffusion coefficient of the target chemical species, while membranes used for sensing require fast ion exchange or complexation at the membrane/solution interface to quickly establish the electrical potential difference across the membrane (Almeida et al., 2017).

PIMs are generally more stable than SLM mainly because of the reduced carrier loss to the aqueous phase, but they can suffer from lower fluxes as a results of their lower diffusion coefficients (Pawel et al., 2015). However, this can be offset to some extent by using thinner membranes to increase the flux of the target species. In a number of cases, it has been observed that a carrier concentration lower than 20% the membrane transport has been negligible (Almeida et al., 2012). But the transport rates increase exponentially above this value, referred to as the percolation threshold, as the carrier concentration is increased to a maximum of around 50%. Similarly to SLM, PIMs is also used to separate the source and receiving phase but does not contain any organic solvent (Konczyk et al., 2010). Instead, the extractant that sustains the transport of the ionic species through PIM is immobilised within the polymer matrix. Thus, PIMs are much more chemically and mechanically stable than SLMs. The question arises as to whether it is possible to simultaneously separate and concentrate two or more metal ions using PIMs. The simultaneous separation of multiple metal ions has the considerable advantage of being able to scale down the treatment scheme thus lessening the process time (Almeida et al., 2014, 2012). In addition, this would make the process more economical and would reduce significantly the possibility of environmental pollution.

2.2.1 Classification of carriers used in PIM

Transport in PIM is accomplished by a carrier that is essentially a complexing agent or an ion-exchanger. The complex or ion-pair formed between the metal ion and the carrier is solubilized in the membrane and facilitates metal ion transport across the membrane (Vázquez et al., 2014). A study showed that in the absence of extractant in CTA based-PIMs, no transport of cadmium was detected from the extraction phase to the receiving phase (Kebiche-senhadji et al., 2008). There are several classes of extractant namely as basic, acidic, chelating, neutral, solvating, macrocyclic and macromolecular that has been successfully used along with targeted metal ions (Radzyminska-lenarcik et al, 2015).

2.2.1.1 Acidic extractant (di-ethyl hexyl phosphoric acid) in PIMs

Di-ethyl hexyl phosphoric acid (D2EHPA) is a non-volatile organophosphorus compound with the formula $(C_8H_{17}O)_2PO_2H$) as shown in (Figure 12). It is used as a cationic carrier and in membrane processes presents a great selectivity towards Zn, in relation to other metals such as Cu, Ni, Ca, Mn, Fe, Al and Cd (Resina et al., 2006). This carrier has a hydrophobic character and is soluble in many organic solvents. It often acts as a transport agent following a counter-transport mechanism; in PIM, a crossed transport of protons and metallic ions takes place. In addition, D2EHPA has some suitable characteristics such as high loading capacity of metal charge, good selectivity, high mass transport rates, high chemical stability and low cost (Vellaichamy et al, 2017). It is used in the solvent extraction of trace metals, as well as rare-earth metals.

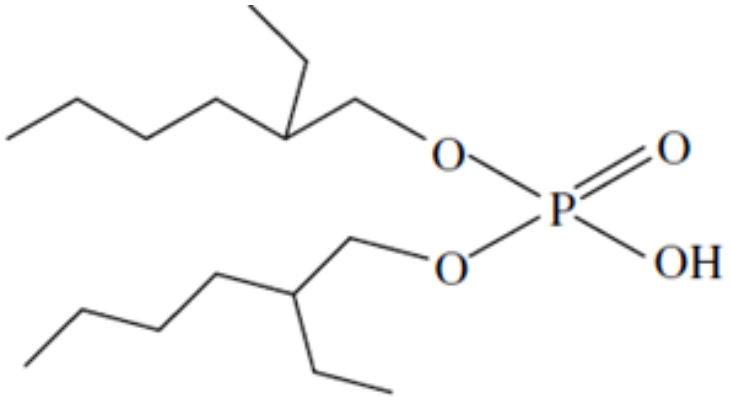

Figure 12: Structure of D2EHPA.

The organophosphoric acid, D2EHPA, is a very efficient and versatile extraction agent in liquid-liquid extraction processes for the purification, enrichment, separation and recovery of metal salts e.g. rare earths, extraction of uranium separation of cobalt and nickel and the extraction of zinc, vanadium and beryllium (Croft et al., 2018; Vellaichamy et al., 2017). D2EHPA replaces the carboxylic acids in metal extraction because of smaller extractant losses, higher metal loadings and faster equilibrium rates (St John et al., 2012). The extraction chemistry is shown in the following example where adduct is formed (Eqn 5).

$$4RH_{(org)} + M^{2+} \leftrightarrow R_2M\ 2RH_{(org)} + 2H^{+} \quad 5$$

Where RH(org) is the carrier D2EHPA, M2+ is the metal ion and R2M 2RH(org) is an adduct. Carboxylic acids can be used for the extraction of copper, cobalt, cadmium and nickel. D2EHPA can be used to extract a wide variety of metals. Careful pH control is required to achieve reasonable metal separation (Gega et al., 2014). For this reason, this extractant was chosen as being a viable method of selective metal extraction for this study.

2.2.1.2 DE2HPA complex formation with copper, cobalt, cadmium and nickel

D2EHPA was able to form different complex species with Ni (II), Co(II), Cu(II) and Cd(II).

Nickel-D2EHPA complexes form square-planar, tetrahedral or octahedral complexes. To obtain the octahedral configuration, two bidentate units of D2EHPA surround the Nickel ion and two water molecules must occupy the axial positions of the complex (Figure 13). This means that [$ML_2.2H_2O$] Ni-D2EHPA complexes are formed. In literature (Voorde et al., 2008), the formation of octahedral Ni(II) complexes [$(NiL_2.2H_2O)_3$] was proposed during the extraction of Ni (II) from sulfuric acid solutions with D2EHPA dissolved in hexane. Ni (II) is bivalent, although it assumes other valences with extractant D2EHPA. It also forms several complex compounds. Cobalt-D2EHPA complexes common geometries are tetrahedral or octahedral. The formation of Co tetrahedral complexes [ML_2] is therefore more justified (Figure 14). The formation of tetrahedral Co (II) complexes [$CoL_2.2H_2O$] was also proposed for the extraction of Co (II) ions from sulfuric acid solutions with D2EHPA dissolved in hexane as already discussed above. The existence of water molecules was found in the Co-D2EHPA complex, although less strongly bound compared to the Ni (II) complex (Gega and Otrembska, 2014). For

Copper-D2EHPA complexes [CuL_2] formation is normally the square planar configuration, which is highly preferred by Cu (II) as seen in (Figure 15). Cadmium-D2EHPA complexes stiochemistry of Cd (II) to carrier is 1:2; Cd (II) with D2EHPA carrier forms a square planar complex as seen in (Figure 16).

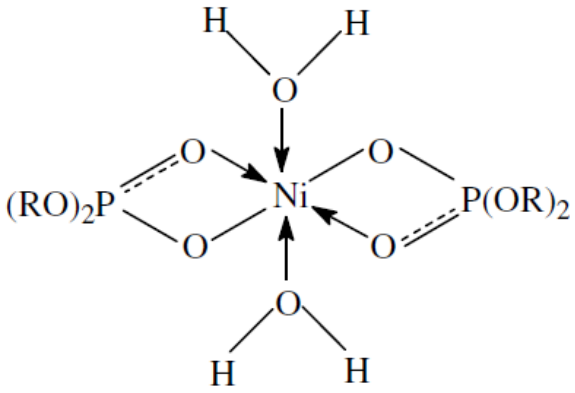

Figure 13: Octahedral coordination of nickel with D2EHPA, (Van de Voorde et al.,2007)

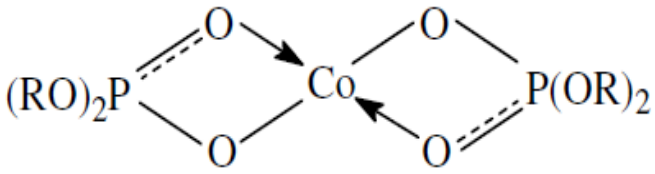

Figure 14: Cobalt-D2EHPA tetrahedral complex, (Van de Voorde et al., 2007)

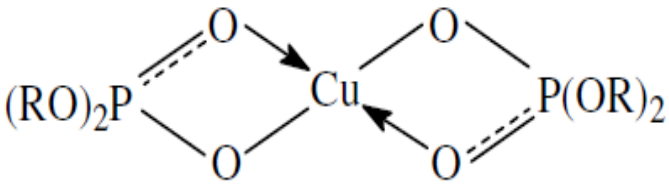

Figure 15: Square-planar complex of copper with D2EHPA, (Van de Voorde et al., 2007)

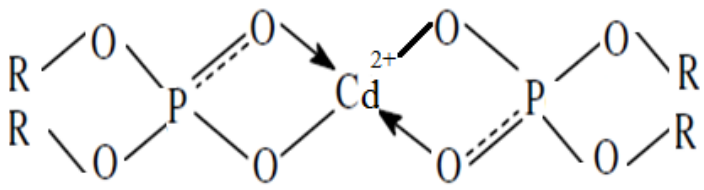

Figure 16: Square-planar complex of cadmium with D2EHPA

2.2.2 Transport mechanism across the PIM

To understand the way in which the extraction occurs in the membrane it will be important to examine the current theories of transport phenomenon. The information will then be able to be used to propose the way in which the mechanism of extraction takes place. There are four basic types of transport systems, each of which has its own mechanisms and carrier types. The four systems are cation transport, anion transport, neutral guest transport and switchable transport. However, in each of these systems, regardless of the mechanism the complexes that are formed must maintain charge neutrality (Casadellà et al., 2016; Kagaya et al., 2012). The PIM facilitated transport allows transport of the extracted species from a source solution with a lower concentration to a receiver solution with a higher concentration (Garcia-Rodríguez et al., 2015). Thus, it is possible to transfer quantitatively the extracted species.

Transfer of analytes from the source to the receiver phase occurs through a carrier mediated mechanism. D2EHPA is used as the cationic carrier molecule that targets the cationic metal ions in solution. Extraction and transport of a metal cation by an acidic carrier D2EHPA is directed by the exchange of the metal ion for protons of the carrier (Eljaddi et al., 2017). D2EHPA can also act as bidentate chelating agents. Therefore, counter-transport of protons is the driving force and is achieved by maintaining a suitable pH difference between the source and receiver solutions. In addition, careful pH control in the source solution can result in good selectivity as is the case in PIM-based passive samplers system using acidic reagents. When the

extractant exhibits acidic properties, coupled counter transport takes place and the extraction reaction proceed.

PIM transport mechanism is studied in (Figure 17). The overall transport mechanism across a typical PIM consists of the following three steps: In the first step, the target solute after diffusing through the aqueous stagnant layer at the source solution/membrane interface reacts with the carrier at this interface to form a complex, which is then transported across this interface and replaced by another molecule of the carrier. In the second step, the complex diffuses across the membrane toward the receiving solution. The last step, at the membrane/receiver solution interface, the complex dissociates, and the target solute is released into the receiving solution, which is essentially the reverse of the process occurring at the source solution/membrane interface. Thus, the source phase metal ion concentration is its total analytical concentration which is the sum of the concentrations of all chemical species containing this metal ion. Within the membrane phase, there is a concentration gradient of the target solute/carrier complex or ion-pair acting as a driving force for its transport across the membrane, even though the total analytical concentration of the target solute in the source solution can be substantially lower than in the receiving solution. In other words, uphill transport only takes place with respect to the total analytical concentration of the solute, while in the membrane phase it is downhill transport regarding the actual chemical species diffusing across the membrane. Many permanently charged compounds, especially metal ions can also be efficiently transported through PIM membranes by ionic carriers. In these cases, a gradient of counter ions from the receiving phase to the source phase provides the driving force for the transport. Therefore, the metal carrier complex is transported through the membrane from the source to the receiver phase, and the counter ions are transported in the opposite direction (Zawierucha et al, 2016). The rate and selectivity of a PIM-based passive sampler separation is determined mainly by the membrane thickness, membrane, source and receiving composition.

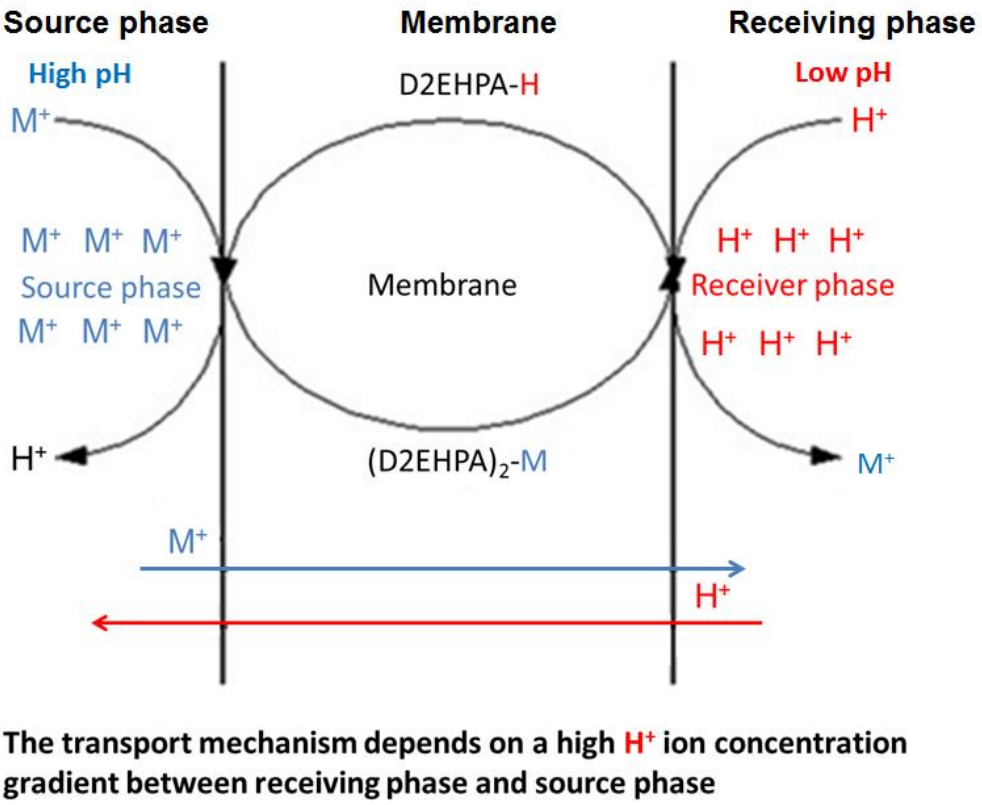

Figure 17: Transport mechanism through PIM

2.2.3 Extraction and transport of target ions by PIMs

The extraction studies in PIMs have been carried out in batch experiments by immersing the PIMs in an aqueous (Source) phase containing target species as described in the literature (Almeida et al., 2014, 2016). A PIM-based passive sampler is composed of a PIM, which separates the aqueous phase from a receiving phase which is placed inside a small container as illustrated in (Figure 18) After the deployment period, the device was removed from the solution and the receiving phase was taken for analysis.

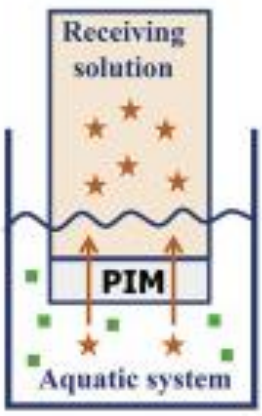

Figure 18: Polymer inclusion membrane passive samplers, (Almeida et al., 2017)

The extraction process across PIMs involves ion exchange via extractant and metal ions complexes which can be achieved by using suitable ionic solution in the extraction phase. The reactions that take place between the metal ions and extractant vary depending on the type of the extractant used. For example, HNO_3 solution can be used in the extraction phase for Co (II), Cd (II), Ni (II), Fe (II) and Cu (II) because they can readily form nitrates complexes. In the case of PVC/D2EHPA PIMs, D2EHPA will form an ion pair with a metal cation complex from the aqueous solution. (Vera et al, 2018). As results in a nitrates matrix, the availability of a metal nitrate complex carrying one positively charge is crucial for the extraction of the metal ion to the membrane. Several researchers, have reported that PVC PIMs with low D2EHPA content, resulted in lower extraction of metal (Meng et al., 2017; St John et al., 2012). They also showed that there exists a critical D2EHPA content in PIMs of 30 to 55 %w/w for the transport of metals to occur. However, it is noteworthy that PVC PIMs with D2EHPA content higher than 50 %w/w is mechanically weak and thus unsuitable for any extraction evaluation

2.2.3.1 Metal flux determination

Metal fluxes across the membrane are determined by monitoring their concentrations in the receiver and source phase. Flux (J) is a measure for characterizing the performance of a PIM in an extraction experiment, target

analytes move from one side (source) to the other side (receiving phase), (St John et al., 2012).

The value of the flux intake ($J, mol\ m^{-2}s^{-1}$) at the PIM/solution interface was used to assess the extraction rate of the PIMs using the following (Eqn 6):

$$J = \left(\frac{V}{A}\right)\left(\frac{\Delta[M^{2+}]}{\Delta t}\right) \qquad 6$$

Where V is the feed solution volume, A is the membrane area exposed to feed solution, $\Delta[M^{2+}]$ is the change in the metal ion concentration in receiver phase ($mol\ m^{-3}$) at elapsed time (s).

2.2.4 Morphological structure and properties of PIM

The homogeneity of the PIMs has been a focus of several recent studies (Benosmanea et al., 2018; Witt et al. 2018; Ling et al. 2017). Generally, PIMs are assumed as chemically homogenous when they are visually homogenous, transparent and free of any extractant droplets. These assumptions may not always be appropriate. Even SLM looks transparent and homogenous although they are filled with organic liquids in their pores. Several techniques have been used to characterize the morphology and properties of PIMs to identify the homogeneity and to have better understanding on their extraction and transport mode. However, most of them are surface characterisation techniques and they can only offer limited insight toward the homogeneity of PIMs. Apart from morphological and chemical studies, successful PIMs must also have an appropriate mechanical strength and thermal stability to resist any mechanical stress and high temperature operation without easily tearing off or deteriorating (Syazana et al., 2016).

Gherasim et al., (2011) investigated the membrane composition and the type of the interactions which established between their components, characterized the PIM by scanning electron microscopy (SEM) and Fourier transform infrared (FTIR)

spectroscopy. The mechanical and dielectric properties were also analysed with an emphasis on the interactions between the PIM components and the plasticizing role of the used carrier D2EHPA. The investigation allowed the author to explain the relationship between the membrane structure and their properties. Because the PIM under study did not contain added plasticizers, the enhancing of the extraction and transport properties were concurrent with the lowering price and easy-manufacturing process. The characterization by SEM and FT-IR revealed that the PIM contained the carrier D2EHPA dispersed in physical form in the polymer matrix. Also, the carrier D2EHPA molecules are organized in continuous liquid micro-domains which cross the membranes and explain the PIM's sorption and transport properties.

By using atomic force microscope AFM, Witt et al. 2018 investigated the dependence of the physical and chemical properties of two types of PVC-based membranes on their chemical composition and their efficiency in Zn(II) ion separation in transport across the membranes. Acetylacetone (ACAC) and D2EHPA were used as the cation carriers. The author discovered that PIMs based on PVC with no carrier form a thin film with no visible pores. The membranes have a porous structure only after an addition of ACAC or D2EHPA. The pores are irregular and few micrometres in size. In the case of membranes with ACAC as carrier, pore sizes increase with increasing content of ACAC in the membrane. In contrast, in the case of membranes with D2EHPA as carrier, pore sizes slightly decrease as the D2EHPA content in the membrane increases. Ling et al. (2017) performed a thermogravimetric analysis (TGA) analysis by measuring the weight loss of PVC, bis-(2-ethylhexyl) phosphate (D2EHP), dioctyl phthalate (DOP) and PIM (PVC: D2EHP: DOP) as a function of temperature in a controlled atmosphere. The calorimetry TGA (%weight loss against temperature) for PVC, D2EHP, DOP and PIM (PVC: D2EHP: DOP) each showed a different in the curve since PIM had three main steps to lose weight while the other components had only one or two steps to lose weight. Based on the methods mentioned above, the characterization of PIM membrane has been studied (Ling et al., 2017). So far not much work has

been focused on study on PIM before and after extraction by SEM, FTIR, AFM and TGA.

2.2.5 Advantage of PIM

PIM have attracted considerable interest in metal ion transport. PIM have high selectivity, long term stability and durability of the membrane. It is possible to prepare a PIM with negligible carrier loss during the membrane extracting process. The PIM provides low mass transfer rate, low energy consumption and low operating cost. One of the important aspects of PIM is the distribution of organic carrier in the polymer matrix, which determines their transport efficiency (Baczynska et al., 2015)

2.2.6 Stability of PIM

Stability has been the main advantage attributed to PIM in comparison with other liquid membranes. Several researchers have studied the stability of PIM and their reusability by performing repeated transport experiments with the same membrane, which involved renewing both the source phase and receiver phase solutions each time (Li et al., 2017; Mahanty et al., 2016). Overall, the stability of PIM was proved to be quite good with flux or permeability values varying only slightly within the first several cycles and with no signs of structural weakening of the membrane. Zaheri et al., 2017 investigated the stability of PIM for seven consecutive experiments by using PIM with 35.16 wt% (D2EHPA, Cyanex272) as a carrier, 18.52 wt% POE as a plasticizer and 46.31 wt% PVC as a base polymer. Receiver phase consisted of 1 M HNO_3, feed phase pH 6.5. Seven experiments were conducted under the same conditions without changing the membrane. The source and receiver phases were renewed for each experiment. The results indicate that the transport efficiency was over 90% in the first five experiments. After that, the transport efficiency decreases, this may be caused by the leaching of the extractant to the aqueous phase (Kagaya et al., 2012). All these PIM features have been found to attract interest in chemical analysis as they are able to assist with improving its sensitivity as well as selectivity.

2.2.7 Application of PIM

PIMs have been used for other applications in analytical chemistry such as sensing (e.g ISEs, optodes), sample pre-treatment (e.g separation, pre-concentration) and to sampling (e.g passive sampling). For this study the focus will be on passive sampling (Almeida et al., 2017). PIM application has also been used in passive sampling for determination of organic compounds such us antibiotics and Garcia-Roderguez et al (2015) investigated the pre-concentration of antibiotics in environmental water sample. Other organic compound that has been studies in literature is the application of dyes. Salima et al (2012) investigated the removal of cationic dye using PIM-based passive sampler in aqueous solutions (Salima et al., 2012). Ling et al (2017) investigated the malachite green from synthetic and real wastewaters solution (Ling et al., 2017). While separation of inorganic compounds such as metal ion analysis in aqueous solutions have also been reported in literature, Yildiz et al (2014) use the PIM-based passive sampler for the of separation of Cd (II), Co (II), Ni (II) and Cu (II) from aqueous solution.

2.3 Sampling strategies to monitor metal ion in water

2.3.1 Grab sampling

Most of the monitoring systems currently used to control concentrations of metal ion in the aquatic environment are performed by grab sampling, which consists of collecting discrete grab samples at specific points of the study area (Mitina, 2015). This approach is fairly popular because it is efficient, cheap, and easy to perform (Garcia-Rodríguez et al., 2015). However, some shortcomings are also associated with grab sampling. The sample only represents the concentrations of metal ion at the specific time and sampling point, giving an incomplete picture of the pollutants concentration that do not consider inter- and intra-day variations. A high sampling frequency is required to overcome the previous problem, especially in water bodies where metal ion concentrations are susceptible to fluctuation over relatively short periods of time (Garcia-Rodríguez et al., 2015). Large sample volumes are needed to obtain enriched extracts during sample treatment and thus, adequate concentrations prior to analysis, which is required due to the low concentrations at

which metal ion are usually found (Zabiegała et al., 2010). Consequently, obtaining representative data on metal ion concentrations over time using the grab sampling approach requires many samples, which increases cost and time of both sampling and analysis. However, the limitations of traditional water monitoring methods cannot be underestimated and thus many monitoring programmes are now evaluating alternative methods to monitor metal ion in the aquatic environment. Among them is the use of passive sampler devices that fulfil the requirements of long-term monitoring (Almeida et al., 2014; Garcia-Rodríguez et al., 2015).

2.4 Passive sampling

2.4.1 Passive sampling background

Passive sampling is a sampling technique for use in environmental chemistry which measures the time-weighted average (TWA) concentration of an analyte in an aquatic system such as lake, river or dams. This technique combines analyte collection and pre-concentration in one step at the sampling site and it can be classified as kinetic or equilibrium according to its mass transfer regime. This technique is particularly useful in the detection of point sources of pollution thus avoiding the need to collect numerous spot (grab) samples in order to detect the pollution source. (Goreckiet al., 2002; Vrana et al., 2005). In most aquatic monitoring, it is common practice to collect grab, spot or bottle water samples at specific sites and a given time. There are a few concerns regarding these monitoring methods. Firstly, in situations where pollutants are found in trace amounts, large volume samples must be collected in order to make better assumptions on the levels that are present. Secondly, there is a possibility of contamination and changes in metal speciation during storage and transport of samples (O'Connor Šraj et al, 2018). Furthermore, spot sampling provides information on the total amount of pollutant present and not the dissolved, bioavailable fraction (Vrana et al., 2005). In order to overcome some of these sampling issues, various methods were developed, and passive sampling proved to be the one with the greatest potential. Passive samplers have been used to gain understanding of the species of metals in the aquatic environment. Sampling technologies in environmental analysis are

gaining more importance these days as a presence of certain chemicals in the environment, which includes air soils, and waters, can have adverse effects on the organisms including humans.

Passive sampling techniques have been applied to monitor pollutants in the environment (Figure 19). The figure indicates that the passive samplers are getting more popular and recognized as alternative approach for environmental monitoring. Figure 20 shows the number of citations on passive samplers in published papers on water monitoring. The citations have also been increasing especially from 2005. In passive samplers, analyte molecules are progressively accumulated within the passive sampler against a concentration gradient (Vrana *et al*., 2005). Passive samplers have advantages over other sampling and sample pre-treatment techniques in that they measure the average concentration as they are deployed for longer periods such as two weeks or more (Figure 21). They combine sampling and sample pre-concentration thus allowing detecting even trace amounts of pollutants in water. They require no energy input during deployment and thus can be deployed over a wide area. They measure the bioavailable fraction and thus very important in assessment of the potential health risk assessment of the concerned aquatic water bodies.

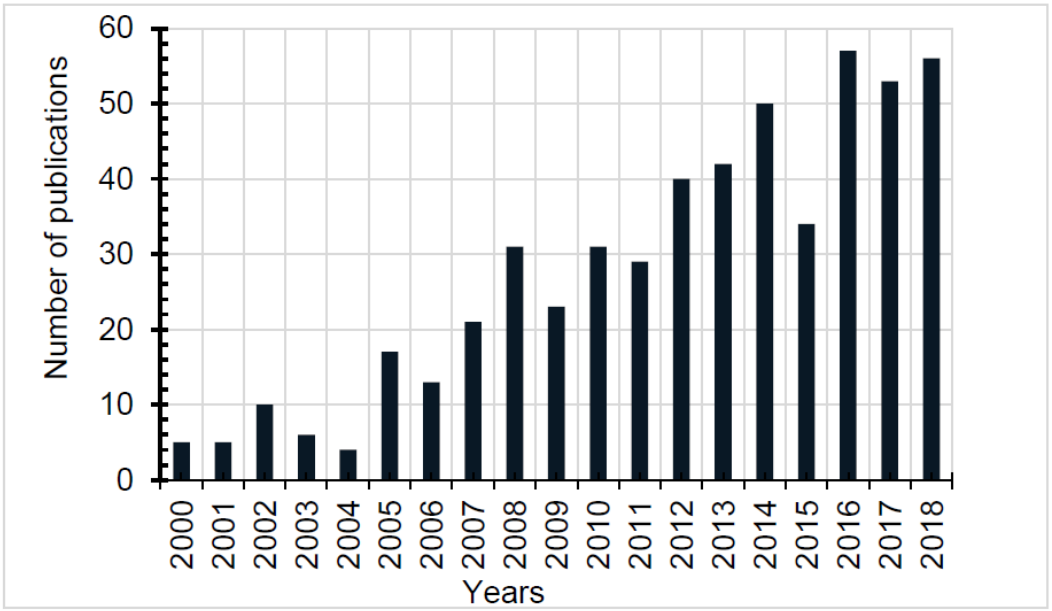

Figure 19: The number of publications on passive samplers for water monitoring

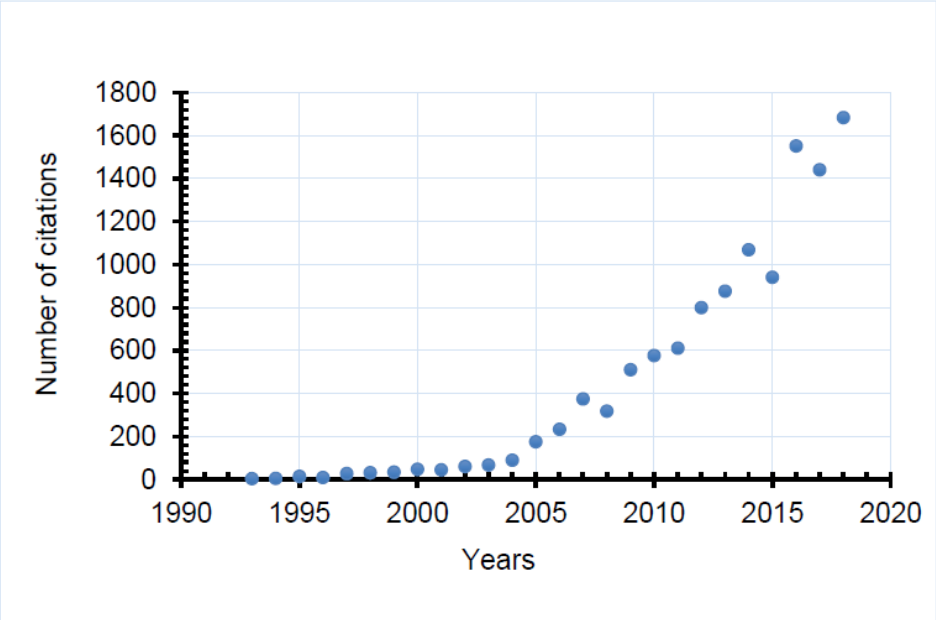

Figure 20: The number of citations per year of passive samplers for water monitoring

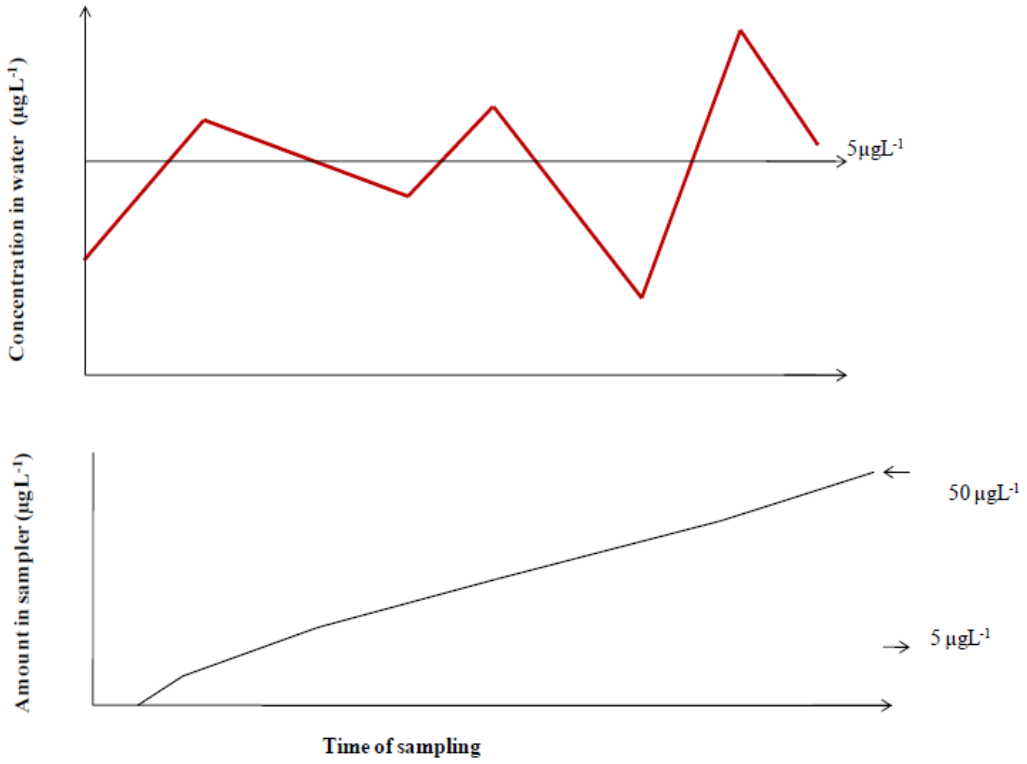

Figure 21: An Illustration of the uptake of the passive sampler in the water body where the concentration changes all the time. Passive sampler measures the integrative average concentration since sampling is performed continuously.

2.4.2 Theory of the passive sampler

Passive sampling is a technique based on the principle of free-flow. Analyte molecules travel from the sampled medium to the receiving phase within the passive sampler due to the difference in chemical potential between the two media. Sampling can proceed without the need of an external energy source besides the chemical potential (Tadeusz Gorecki, 2002; Vrana et al., 2005). As analyte molecules continue to travel through the passive sampler, they are retained within a reference or receiving phase. This can be a solvent, chemical reagent or a porous adsorbent. The reference phase is in contact with the water phase. The exchange kinetics between water and the sampler follow first order kinetics according to (Eqn 7)

$$Cs(t) = Cw\frac{k_1}{k_2}(1 - e^{-k_2 t}) \qquad 7$$

Where Cs (t) is analyte concentration within the sampler at exposure time t, Cw is the analyte concentration in the water phase, k1 and k2 represent the uptake and offload rate constants respectively (Allan et al., 2007). The way analytes are adsorbed from water onto the receiving phase of the passive sampler is illustrated in (Figure 22). Molecule uptake is controlled either kinetically or through equilibrium.

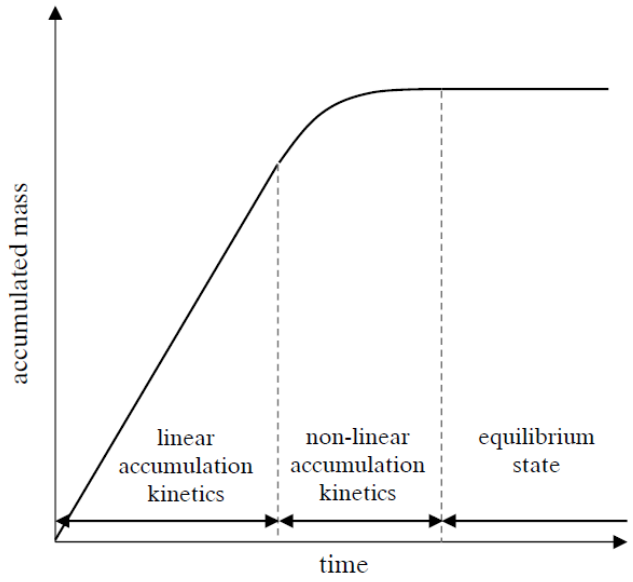

Figure 22: Representation of the different accumulation regimes during exposure of a passive sampler, copied from (Vrana et al., 2005)

2.4.2.1 Kinetic and Equilibrium passive sampling

The type of analytical information obtained because of the use of passive sampling technology depends, to a large extent, on the accumulation regimes in which passive samplers operate during field exposure.

In kinetically controlled passive samplers, it is assumed that the rate of uptake is linearly proportional to the chemical potential between the water and reference phase. During the initial phase after exposure, the rate of desorption becomes negligible in comparison to the rate of uptake, and equation above is simplified to (Eqn 8):

$$C_{S(t)} = C_W k_1 t \qquad 8$$

(Eqn 9) can be rearranged to an equivalent relationship:

$$M_{S(t)} = C_W R_{S(t)} \quad 9$$

Where Ms(t) is the mass of analyte accumulated in the receiving phase after time (t) and Rs is the proportionality constant. This proportionality constant is a product of the first-order rate constant k1 and the volume of water that gives the same chemical activity as the volume of the receiving phase. If the value of Rs is known then CW, which is the time weighted average (TWA) of pollutant in water, may be calculated from Ms(t), (t) and Rs. The value of Rs does not vary with CW for samplers operating in the kinetic region. This value is however, affected by turbulences, temperature and biofouling. Kinetic passive samplers can sequester contaminants from episodic events which are commonly not detected with spot sampling and can therefore be used where water concentrations are variable. They allow measurement of ultra-trace, yet toxicologically relevant, contaminant concentrations over extended periods (Vrana et al., 2005).

Equilibrium passive samplers require a longer period of incubation to allow the establishment of thermodynamic equilibrium to take place between the water and reference phase. (Eqn 9) re-arranged to (Eqn 10) as follows:

$$C_S = C_W \frac{k_1}{k_2} = C_W K \quad 10$$

The concentration of dissolved analyte can be estimated from the phase-water partition coefficient (K). One fundamental requirement of equilibrium-passive sampling is that stable concentrations are obtained after a known, specific time (Vrana et al., 2005).

A barrier between the sampled medium and the receiving phase is a common characteristic shared by most passive samplers. The barrier is an important aspect of the passive sampler because it determines the rate at which the analyte can be sequestered into the receiving phase at a given concentration. The barrier also

ensures the selectivity of the sampling device where certain groups of analytes will be selected more than others. The rate of analyte uptake depends on the sampler design, physicochemical properties of the analytes as well as environmental variables such as water turbulence, water temperature and biofouling (Vrana et al., 2005).

2.4.3 Types of passive samplers

2.4.3.1 Chemcatcher (Passive Sampler using Empore Disk)

The chemcatcher's system uses a diffusion-limiting membrane and inside a commercially available solid-phase empore disks as a receiving phase. A diffusion-limiting membrane and the solid-phase receiving material are supported and sealed in place by inert plastic housing (Figure 23). Several designs are available with different combinations of receiving phase and a diffusion-limiting membrane. Accumulation rates and selectivity are regulated by the choice of both the diffusion-limiting membrane and the solid-phase receiving material. In this case two separate prototype systems have been described, one suitable for the sampling non-polar organic compounds with Log *K*ow (partition coefficients) values greater than 4 and the other for polar species with Log *K*ow values between 2 and 4. Both systems use the same receiving phase but different rate - limiting membranes. The use of well-known and commercially available receiving phase makes this sampler promising. (Vrana et al., 2006) reported to have calibrated the Chemcatcher passive sampler for monitoring of priority organic pollutants in water. Environmental factors such as turbulence and temperature were studied in

a flow-through system under controlled conditions. PRCs were also used to correct for environmental factors. The results revealed that the absorption of test compounds on the sampler was like their desorption under the same exposure conditions. Therefore, in situ calibration of the sampler is possible using PRCs. The sampler has been calibrated for monitoring polar or nonpolar organics, some persistent organic pollutants (POPs) such as organochlorine pesticides, PCBs and polycyclic aromatic hydrocarbons (PAHs) in water (Nyoni et al., 2010).

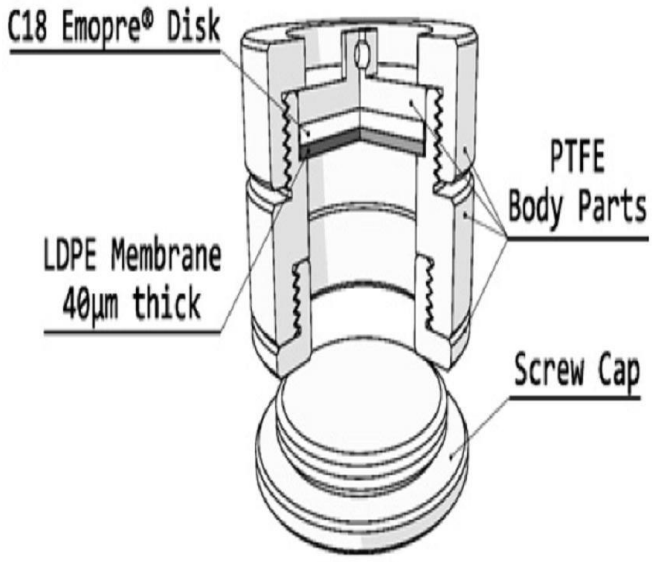

Figure 23: Views of the prototype Chemcatcher device, used during sampler development. The PTFE body parts (1st generation) support the receiving phase and the diffusion membrane and sealed them in place. The sampler is sealed by means of a screw cap for storage and transport (Nyoni et al., 2010).

2.4.3.2 Diffusive Gradients in Thin-films Technique (DGT)

The technique of diffusive gradients in thin-films technique (DGT) was developed by the Zhang group (Davison and Zhang, 1994) at Lancaster University as a means of *in situ* measurement of labile trace metal species in natural water. *In situ* measurements mean that contamination problems normally encountered during sampling and transport are eliminated (Davison and Zhang, 1994; Zhang and Davison, 1995). During the deployment of DGT, metal ions are gradually accumulated according to a diffusion gradient. Metal ion accumulation in DGT is based on Fick's first law of diffusion as shown in (Figure 24). The total mass of metal accumulated after a specific period can then be calculated (Davison and Zhang, 1994; Zhang and Davison, 1995). The fact that DGT operates on the fundamentals of a concentration gradient means that it is kinetically controlled. This is advantageous because it can be deployed for extended periods unlike equilibrium techniques (Li et al., 2002).

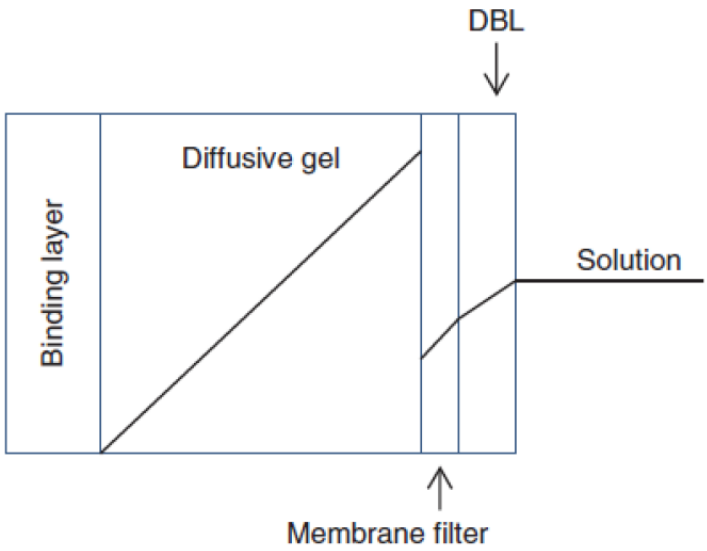

Figure 24: A representation of the free ionic species in a gel assembly that's in contact with natural water. The DBL is the diffusive boundary layer (Davison and Zhang, 2012).

DGT is a 25 mm diameter plastic device that looks like a small piston as shown in (Figure 25). The top cap has a 20 mm diameter window (Allan et al., 2008; Mengistu et al., 2012). The functional part is made up of three layers: a cellulose acetate filter membrane with a pore size of 0.45 μm, a layer of polyacrylamide hydrogel, on top of a Chelex 100 cation-exchange resin layer. The layers within the device are compact and sealed such that only the filter membrane interacts directly with the external environment; it helps protect the hydrogel from external particles. Both the filter membrane and the hydrogel make up the diffusive layer (Li et al., 2002; Mengistu et al., 2012; Zhang and Davison, 1995). DGT can operate under varying ionic strengths and temperature; however, ideally, for more comprehensive data, the temperature should remain constant, within ± 2 °C. The Chelex 100 resin in the binding layer is the limiting factor in DGT. The cation-exchange resin is affected by pH below 5 (Zhang and Davison, 1995). Therefore, sampling at a pH below 5 is not recommended.

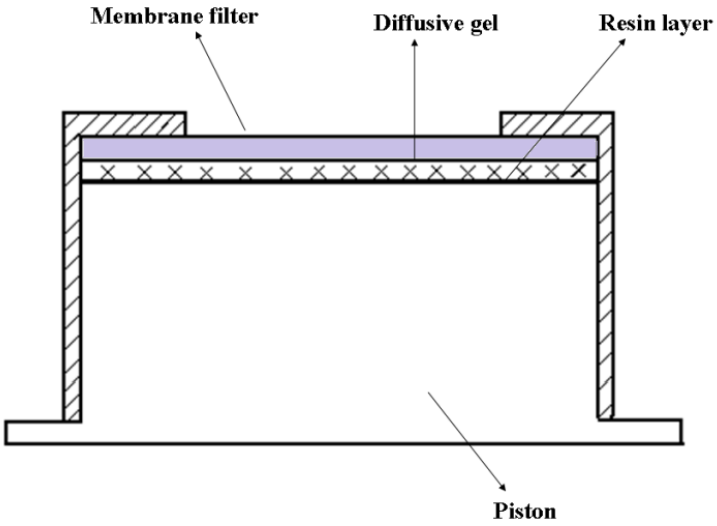

Figure 25: A simple representation of the DGT device with the functional components as indicated (Mengistu et al., 2012).

2.4.3.3 Polymer inclusion membrane-based passive sampler

DGT despite being the most popular for metal ions it has its own limitations. The major limitation is that target metals bound onto the sorbent have been re-desorbed using a suitable solution mostly acids are used. This has led to the development of other passive samplers with aqueous receiving phase. One such that is getting a lot of attention is polymer inclusion membranes (PIMs) as already discussed in section 2.2. PIMs are a type of liquid membranes, where a suitable carrier or ion-exchanger is immobilized within the chains of a plasticized thermoplastic polymer often referred to as base polymer. The polymer is synthesized in the presence of a carrier that is physically trapped in the polymer matrix. The carrier is essentially a complexing or ion-exchange reagent, responsible for binding the species of interest (i.e. analyte) at the membrane/source phase interface and transporting it across the PIM. The analyte is back-extracted into the receiving aqueous solution by a suitable stripping reagent thus releasing the carrier that diffuses back to the membrane/source phase interface where it can bind another analyte ion/molecule. The transport of the analyte across the membrane continues even when the total analyte concentration in the receiving phase becomes higher than that in the source phase this process is known as the facilitated transport.

The analyte concentration in the receiving phase of the passive sampler can be measured by a suitable analytical method either directly or after derivatization. Due to the facilitated membrane transport outlined above PIM-based passive samplers are expected to provide a high level of pre-concentration of the analyte in the receiving phase, thus allowing the use of less sensitive analytical methods.

In PIMs, the transport of analytes mimics biological membranes and thus there is no need of a diffusion gel like in DGT. Passive sampler based on PIMs thus measures the bioavailable fraction just like DGT and in all passive samplers. This is because uptake of analytes in passive sampler mimics biological membranes. Hence in this work we introduced the polymer inclusion membrane (PIM) passive sampler, which eliminates the drawbacks mentioned above.

2.4.4 Technical developments and optimisation in passive samplers

Passive samplers are designed to mimic living organisms in the transport of chemicals to the receiving or trapping medium (Pesavento et al., 2009). It is one of the analytical methods that measure the free and labile fractions of the chemical within the water bodies just like aquatic living organism. Typical compartments of the passive sampler for metals consist of a hydrophilic membrane that allows the passing of water and metals through its pores. Thus, any bigger particulates are excluded from going through. Next is the diffusion gel which allows metals to diffuse through just like in cell membranes. After this is a trapping media embedded in agarose or same gel used as diffusion media. The embedding of trapping particles in a gel helps to make sure that chemicals can diffuse all-round the particles and get trapped. The polarity of the membrane can influence transport across of the metals thus should be polar enough not limit the transport across into the diffusion gel. The diffusion gel thickness needs be controlled as this allows the passive sampler to mimic living organisms.

The actual trapping of the metals is determined by the type of sorbent used. Because of diverse metal ions and in different chemical forms, this is an area that is very active currently. The sorbent must be tailored towards the target metals. Critical is also the possible interferences from other metals or chemicals within the sample. Metals like Ca, Na, Mg and K are found in very high amounts, and if trapped, they can reduce the capacity of the sorbent and thus the deployment time. Thus, calibration of the passive sampler in the laboratory before final deployment is very critical. Calibration typically allows one to study the most important parameters that will influence passive sampler performance such as exposure time, sample pH, turbulence, elution solvent and its volume and possible interfering matrices (Dabrin et al., 2016; Turner et al., 2012). When finally, the passive sampler is applied is common to take few grab samples to compare the total versus free and labile fraction obtained in passive samplers.

2.4.4.1 Calibration of the passive samplers

The major purpose of every research is to give precise and accurate picture of the investigate object. In case of passive sampling, it is an actual conditions and composition of studied environmental area. In this regard, good precision (<5%) can be obtain if samplers are calibrated in the laboratory rather than in the field. For example, in the review of the passive sampling devices made by Chimuka et al. 2005, was noted that the average percentage relative standard deviations for aquatic passive samplers ranged from 10%-32%. However, calibration process itself may take a lot of time even though it is not so complicated. To calibrate the passive sampler, an appropriate exposure system with constant temperature conditions and water flow in the calibration system should be build.

2.4.4.2 Passive sampler exposure area

The purpose of the study is to determine source solution metal ion concentration; hence it is required to calibrate the passive sampler in the laboratory before its application to the field. This involves an estimation of the impact of surrounding

conditions on the performance of the sampler. To calibrate the passive sampler, it is necessary to construct an appropriate exposure area in the laboratory. Generally, samplers are exposed to continuous flow of analytes through the exposure area with a constant flow rate (Vrana et al., 2005). To have maximum sensitivity, a sampler design should have high (area and length) A/L ratio where A is the area and L is the length of the active device. Whatever design is employed, passive samplers mostly have a barrier between the sampled medium and the receiving phase. The barrier determines the rate at which analytes molecules are collected in the receiving phase. Some barriers have defined openings resulting into diffusion-based samplers. Others have the barrier in form of a non-porous membrane, referred to as permeation-based samplers (Vrana et al., 2005). Some factors that influence the uptake rate are sampler design, physio-chemical properties of the analytes and environmental variables (water turbulence, temperature and fouling) (Nyoni et al., 2010). Hence for this study we first started by constructing two passive samplers with different window opening size for a non-porous membrane. The dimensions for the receiver solution chamber did not change; the only dimensions that changed were the screw cap exposure area. The dimensions for screw cap with the small exposure area was 10 mm (Figure 26 a) while the larger exposure area is 20 mm wide (Figure 26 b). The optimisations of these windows opening are discussed in the results and discussion section.

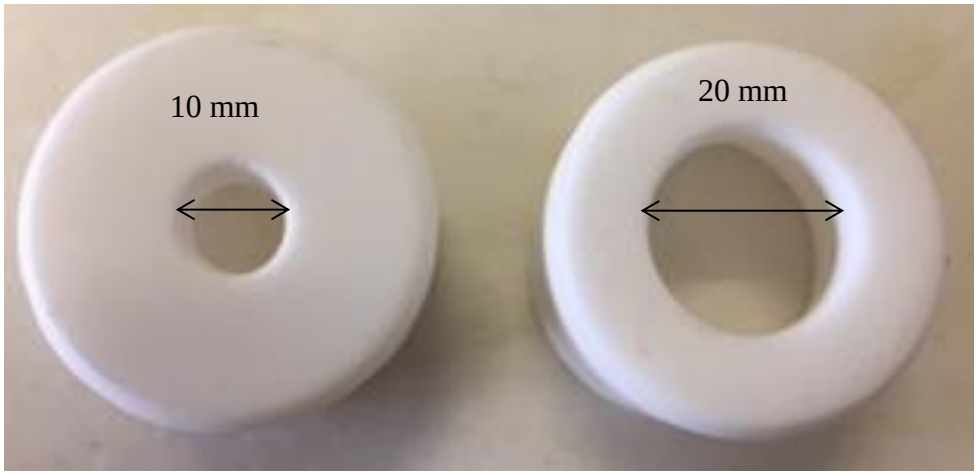

Figure 26: Dimensions of the a) small exposure area and b) large exposure area

2.4.5 Sampling/application area

In this study dams near tailing dumps in Johannesburg area will be used. Spot or grab samples will also be taken to compare the total concentration with what is obtained from passive samplers. Grab samples of the waters will be taken from same spot where passive samplers will be deployed. Passive sampler will be deployed above the sediment in the water. The bioavailable fraction of the toxic trace metals will thus be measured in the water. Hence in this study we attempted to monitor and recover the metal ions using an organophosphorus carrier D2EHPA. To monitor the valuable metals and reuse in their pure metallic form, a relatively simple, low cost and low energy consumption technology like passive sampling technique was adopted for the recovery of cadmium, copper, cobalt and nickel and iron.

CHAPTER 3

The aims and objectives of the research work are presented in this chapter. The novelty and the motivation behind this project are also discussed.

3 Aims and Objectives

3.1 Aim

The main aim of this research was to design a passive sampler based on polymer inclusion membrane (PIM) for studying the transport and fate of metals from AMD imparted water.

Objectives

- To design a simple but effective passive sampler based on polymer inclusion membrane for extraction of metal ions in AMD imparted water samples.
- To optimise important factor such as sample pH, exposure time, membrane thickness, stirring rate and receiver phase composition in PIM sampler for effective extraction of Ni (II), Co (II), Cu (II), Cd (II) and Fe (II).
- To deploy the PIM-based passive sampler in AMD imparted water.

3.2 Novelty

The innovation in this project was development of new passive sampler design that can be reused and can withstand harsh environmental conditions compared to other available passive samplers so far. The membrane barrier composition that also transported the metals across the source to the feed/ receiver phase consisted of PVC impregnated with D2EHPA which acted as a cationic carrier to facilitate transfer of metal ions from the source solution to the receiver phase. The combination of a PVC membrane and D2EHPA is very compatible hence; there was no need of a plasticizer and a modifier during synthesis. The presence of the acidic D2EHPA in the membrane gives the membrane bactericidal properties and therefore avoids fouling of the membrane when deployed in the environment. The developed passive sampler was then used for extraction and studying the behaviour of nickel Ni (II), Cd (II), Cu (II), Co (II) and Fe (II) in environmental natural water samples.

3.3 Motivation

Passive samplers are ideal for measuring the fate of pollutants like toxic metals in wetlands polluted by mining activities in the surrounding areas (Manzak et al., 2015) and natural water. For passive sampling of metal ions, DGT is the most popular and is commercially available but expensive (Turull et al., 2016). There is need to develop passive samplers that are cheaper than DGT but effective using locally available materials. In this study we have developed a new passive sampler design and material containing polymer inclusion membranes to monitor the fate of five metals in wetlands polluted by acid mine drainage in Johannesburg area. This study encompasses a technical aspect which is followed by laboratory optimisation and application in acid mine drainage and natural waters.

CHAPTER 4

This chapter focuses on the design, optimisation and application of the polymer inclusion membrane passive sampler.

4 Research methodology

4.1 Chemicals and calibration standards

All chemicals used in this study were purchased as analytically pure reagents, and no further purification was done. Polyvinyl chloride (PVC), di-(2-ethylhexyl) phosphoric acid (D2EHPA), tetrahydrofuran (THF), nitric acid (HNO_3), sulphuric acid (H_2SO_4), hydrochloric acid (HCl), nickel(II) nitrate $Ni(NO_3)_2$, cobalt(II) nitrate hexahydrate ($Co(NO_3)_2 \cdot 6H_2O$), Copper(II) nitrate, $Cu(NO_3)_2$, cadmium (II) nitrate ($Cd(NO_3)_2 \cdot 4H_2O$) and iron (II) nitrate $Fe(NO_3)_2$ were purchased from Sigma-aldrich (Johannesburg, South Africa). Metal stock solutions were prepared by adding a suitable amount of their metal salt in deionized water. The pH of the solutions was adjusted by addition of 1 mol L^{-1} HNO_3 and 1 mol L^{-1} NaOH solutions.

4.2 Instrumentation

All metal ions measurements were performed on a Spectro Genesis inductively coupled plasma optical emission spectrometry (ICP-OES) (Spectro, Genesis, Germany). Conductivity and pH values in the samples were measured at several time intervals using a Hanna Combo pH/EC/TDS/C/PPM tester HI98129, Redox potential (ORP WP) both from Mettler Toledo (Johannesburg, South Africa). Deionized water was obtained from a Millipore water system (Massachusetts, USA), was used for the preparation of all solutions. All glassware was soaked for at least 24 h in 10% HNO_3 and washed three times with deionized water prior to use. The morphology, structural configuration and roughness of the synthesized membrane were studied using an atomic force microscope, AFM Veeco Di3100 (Bruker, Boksburg, South Africa) and scanning electron microscope (SEM) with inverted light microscope (Nikon Eclipse Ma200). Small representative pieces of the membrane samples were coated with carbon and gold prior to analysis with the SEM microscope. Fourier transform infrared spectrometry (FT-IR) (Tensor 27, Bruker, Germany) was used for the identification of functional groups present in the frequency range of 4000 - 400 cm^{-1}. Thermal stability of each of the PIM

sampler components was assessed by thermogravimetric analysis (TGA), using a TA Q600 SDT–Simultaneous Differential Scanning Calorimeter/thermogravimetric analyser. Phosphorus-31 NMR spectroscopy (^{31}P *NMR*) used for determining the presence of D2EHPA in the membrane was a Bruker Avance III 500MHz NMR spectrometer (Bruker, Rheinstetten, Germany). Water contact angle was measured using a Kruss Drop Shape Analyzer, DSA30 (KRUSS GmbH, Johannesburg). Film applicator was used for casting the membrane using Elcometer 4340 Motorised Film. The membrane thickness was further confirmed by electronic outside micrometre with a 0 – 25 µm and a 0.001 µm shut geometrical metrology (Trossingen, Germany).

4.3 Experimental

4.3.1 Preparation of membrane

The PIM was prepared by dissolving appropriate amounts of D2EHPA (carrier molecule) and PVC in 10 mL of THF in a 100 mL glass beaker. The mixture was stirred for 3 h to form a homogeneous casting solution. The solution was casted on a flat glass surface using the Elcometer 4340 Motorised film Applicator which was kept on a level surface (Figure 27). The film applicator was set at the desired membrane thickness. Once the membrane was casted, THF was allowed to evaporate over 24 h at room temperature, the membrane was then covered with a plastic sheet to prevent dust from settling on the membrane surface. With optimisation of the composition of the carrier and PVC, a transparent, flexible and mechanically strong membrane was formed. The membrane thickness was further confirmed by electronic outside micrometre. The PIM was then peeled from the glass plate and kept in a plastic bag, the membranes were all homogeneous and transparent with an oil free surface. A round piece with diameter of 21 mm was cut out from its central section and used in the extraction experiments. (Table 1) shows the different membrane composition of the carrier and PVC giving a total mass of 1 gram. The membrane was characterized for morphology and contact angle



Figure 27: Elcometer motorised film applicator with casted membrane

Table 1: Total PIM composition (mass = 1g)

Membrane	PVC (mg)	D2EHPA (mg)	Composition (%w/w)
1	900	100	90:10
2	800	200	80:20
3	700	300	70:30
4	600	400	60:40

4.3.2 Passive sampler design

The passive sampler was designed from the PTFE rod shown in (Figure 28). The design drawings were then used to machine the sampler holders. Machining was done by the Physics Department workshop at the University of the Witwatersrand using PTFE tubular rods. In this regard the designed passive sampler consists of a receiver solution chamber with a lumen as shown in (Figure 29 a)). The length of the receiver solution chamber was 24 mm and its lumen has the capacity to hold 5.5 mL of the receiver solution. The weight of the receiver solution chamber container is 41 g. The screw cap length was 21 mm. The enclosed screw cap (Figure 29 b)) has a window opening (Figure 29 c)) with a diameter of about 20 mm and tread depth of 1 mm which expose the membrane to the source solution and allow flow of the liquid from the source phase to contact the outer surface of the membrane. The screw cap has a weight of 31 g. The fully assembled passive sampler housing

is shown in (Figure 30). The length of the fully assembled passive sampler is 46 mm and weighs 72 g. With the aim of making the passive sampler lighter, easier to assemble and durable, the entire parts of the sampler were from PTFE material. Other studies have designed PIMs using glass and the disadvantage with using glass is that it can easily be damaged during field deployment and teflon tape was used to seal the glass threads to prevent leakage (Almeida et al., 2016). In this design, all parts were joined by screwing and thus had no chance of leakage.



Figure 28: Polytetrafluoroethylene rod

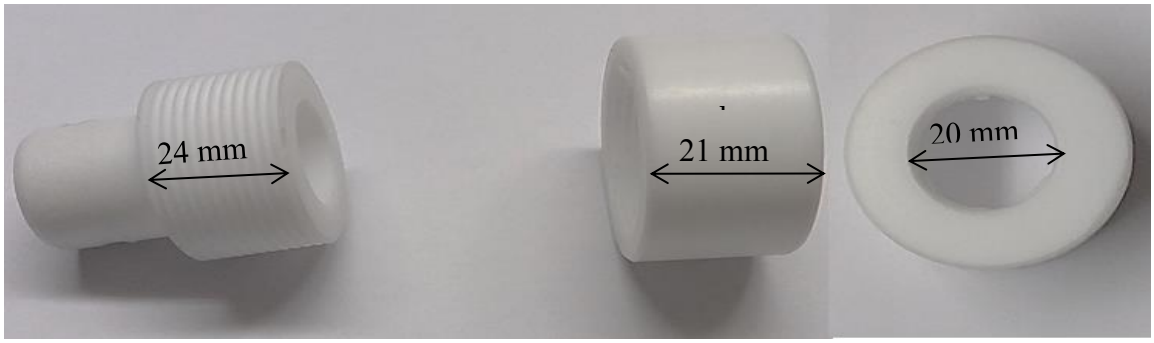

Figure 29: Components of the PIM a) receiver solution chamber, b) screw cap and (c) screw cap with a widow opening

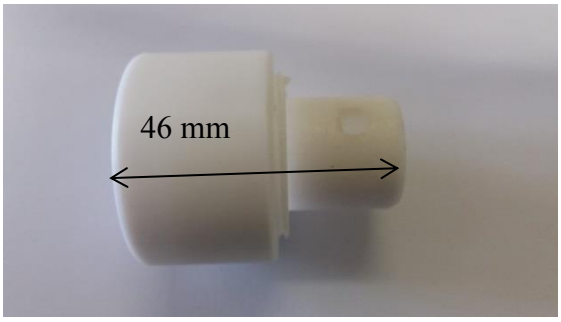

Figure 30: Fully assembled passive sampler housing

4.3.3 Assembling PIM-based passive sampler components

The unassembled PIM-based passive sampler with embedded membrane is shown in (Figure 31). About 5.5 ml of the receiver solution was poured in the receiver solution chamber and the PIM membrane was used as a sealer to seal the receiver solution. The screw cap was then screwed down the receiver solution chamber using the threats, until the membrane was visible by the screw cap window as in (Figure 32) and tightly bounded to the screw cap.

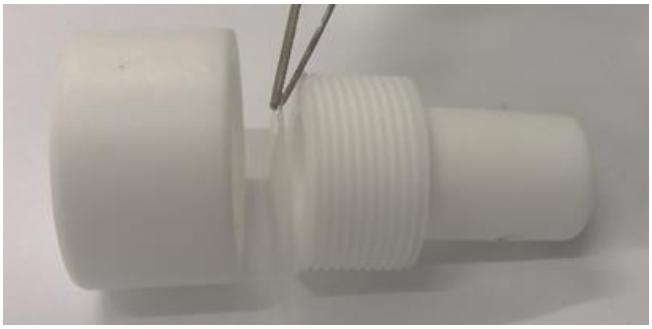

Figure 31: Unassembled PIM-based passive sampler

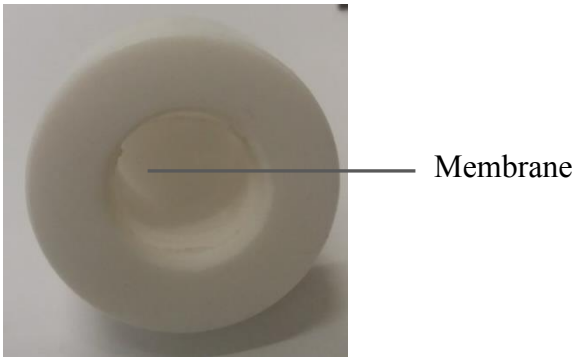

Figure 32: Assembled PIM-based passive sampler with exposure area

4.3.4 Experimental set up of PIM pasive sampler

These experiments were carried out in a system consisting of assembled PIM-based passive sampler and a glass beaker. During optimisation, typically, a volume of 3.5 L of deionised water was spiked with 1 mg L^{-1} of the metal ion concentration of Co (II), Cu (II), Ni (II) and Cd (II) in a 5 L glass container. The PIM-based passive sampler device exposure side was immersed 5 cm in the sample solution in a vertical position under stirring conditions. The receiver solution of the sampler contained 1 mol L^{-1} HNO_3. The assembled PIM-based passive samplers were then placed in a passive sampler holder to control the deployment in the sample container (Figure 33) and then dipped in the source phase. The entire set up is shown in (Figure 34). The solution in the source phase was continuously stirred at 200 rpm. The concentration of the target metal ion in the source phase and the receiver phase was monitored over time. The change in concentration in source phase and the receiver phase allows the determination of the rate of transport of the metal ion across the membrane (St John et al., 2012). During the PIM-transport experiments, the receiver solution was analysed for target metal ions after each exposure time interval using ICP-OES. All the experiments were run at 25°C. Triplicate measurements were made, and the standard deviations were used as error bars. The metal ion transport process is described by the first-order reaction as in (Eqn 11).

$$\ln(C_t/C_i) = -kt \qquad 11$$

Where C_t (mg L^{-1}) is the concentration of the metal ion in the source solution at a given time, C_i (mg L^{-1}) is the initial concentration of the metal ion in the source solution, k is the rate constant (h^{-1}), and t is the transport time (h).



Figure 33: PIM-based passive sampler holder

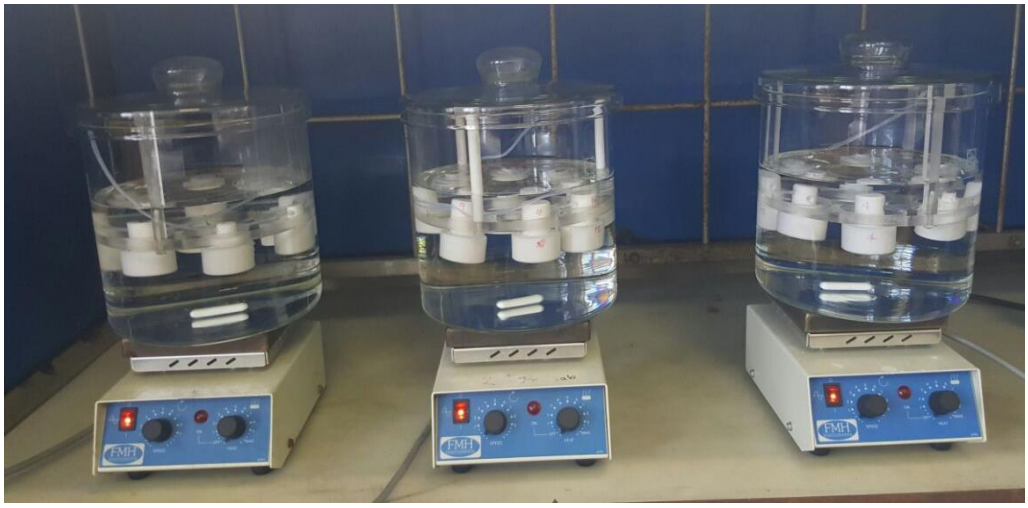

Figure 34: PIM-based passive sampler deployed

4.3.5 Optimization of the PIM composition

Various parameters that affect sampler uptake were studied such as carrier concentration, pH of the aqueous phase, membrane thickness, receiver phase concentration, and effect of deployment time, effect of turbulence and membrane stability.

4.3.5.1 Effect of the amount of carrier in PIM

The carrier concentration has a significant effect on the metal ion transport across the membrane. The effect of carrier concentration in the performance of PIMs was, investigated at 10, 20, 30, 40 and 50 %w/w D2EHPA. Parameters such as source pH 6, receiver concentrations of 1 mol L^{-1} HNO_3, stirring rate of 200 rpm and membrane thickness of 100μm remain constant.

4.3.5.2 Effect of source phase pH

The pH gradient between source and receiver phase generates the potential gradient across the membrane, which is the driving force for the permeation of metal complex towards the receiver phase. In order to assess the role of the source phase pH on the extraction of Co (II), Cu (II), Ni (II) and Cd (II), the pH of the source solution was investigated from (3-7). Parameters such as receiver solution of 1 mol L^{-1} HNO_3, membrane composition (60 %w/w PVC and 40 %w/w D2EHPA), stirring rate of 200 rpm and membrane thickness of 100μm remain constant.

4.3.5.3 Effect of membrane thickness

The effect of the membrane thickness was studied with different thicknesses of 50 to 250 μm. The thickness of a membrane was measured by the Elcometer film applicator during its preparation. Parameters held constant were membrane composition (60 %w/w PVC and 40 %w/w D2EHPA), source pH 6, receiver solution of 1 mol L^{-1} HNO_3 and stirring rate of 200 rpm.

4.3.5.4 Effect of receiver phase concentration

The concentration of the receiving solution plays an important role in the transport of metals across the membrane and the accumulation of metals in the receiving solution; it ultimately determines the accumulation capacity of the sampler. Hence, the effect of the concentration of HNO_3 in the receiving solution was studied in the range 0.25–1.5 mol L^{-1}. Other parameters held constant were membrane composition (60 %w/w PVC and 40 %w/w D2EHPA), source pH 6, stirring rate of 200 rpm and membrane thickness of 100μm remain constant.

4.3.5.5 Effect of stirring rate

Variation in stirring speed greatly affects the endurance, strength of the membrane and the transfer rate of metal ions from the source to the receiver solution. The effect of stirring rate was studied between 0 to 400 rpm. Parameters held constant were membrane composition (60 %w/w PVC and 40 %w/w D2EHPA), source pH 6, receiver solution of 1 mol L^{-1} HNO_3 and membrane thickness of 100µm remain constant.

4.3.5.6 Membrane stability (recycle)

The PIM stability studies were carried out in this study. To study the stability of PIMs, three experiments were conducted under the same conditions without changing the membrane. Parameters used for this experiment was membrane composition (60 %w/w PVC and 40 %w/w D2EHPA), source pH 6, receiver concentrations of 1 mol L^{-1} HNO_3, stirring rate of 200 rpm and membrane thickness of 100µm remain constant.

4.4 Field application of the developed passive sampler

4.4.1 Sampling sites for PIM deployment

PIM-based passive samplers were deployed at two different sites affected by previous mining activities. Both sampling sites are found in Roodepoort, Johannesburg West. The first sampling site was near a mine tailing, with active AMD production. The second sampling site is Fleurhof dam (Figure 35). The panoramic view shows that it is near a mine tailing. Fleurhof Dam is situated on the Rand Leases (Volgelstruisfontein) G.M. Co Property; located on the farms Roodepoort 237 and Volgelstruisfontein 231. There are two streams that bring in water into the dam. One stream has a huge tailing dump near it which leaches AMD into it. This then flows through some wetlands into the dam. The other stream comes from mostly residential areas bringing in relatively unpolluted water. These two streams meet just before both entering the dam. The pH of the dam generally changes as per input from these two streams.

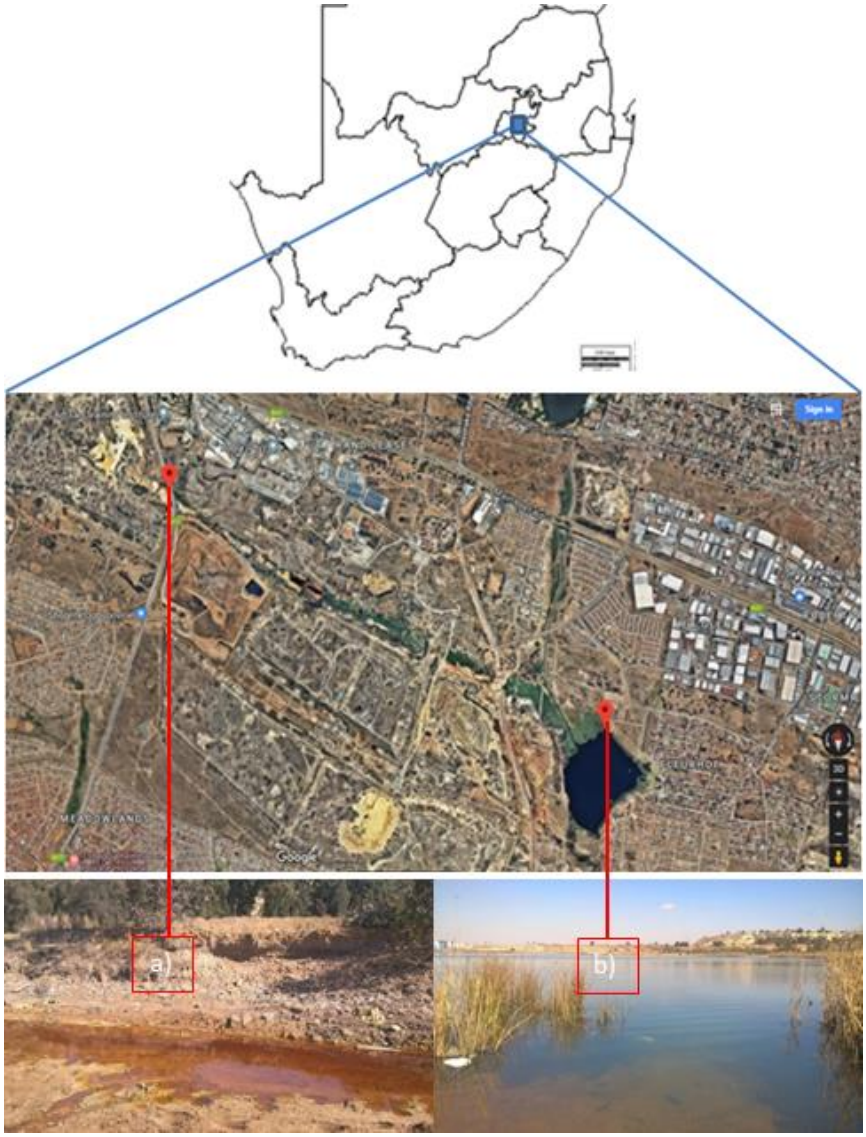

Figure 35: Sampling sites used for the deployment of PIM-based passive samplers, a) is the acid mine drainage impacted sampling site b) Fleurhof dam which is in close proximity to a mine tailing.

4.4.2 Construction of sampling cages

To protect the passive samplers at sampling sites during field deployment, the first step was to design cages that could house the passive samplers during deployment. The passive sampling cages were designed such that they used cheap material that could protect the passive samplers during deployment in the field (Figure 35). The skeleton was made of threaded steel rods (Figure 36 a) and a plastic mesh (Figure

36 b) was wrapped around the steel rod structure in order to seal the cage (Figure 36 c) while allowing water to flow through. The samplers were enclosed in stainless steel protective cages and taken to the field for deployment (Figure 36 d). The number of samplers placed in each cage was three and the total number of cages was four.



Figure 36: a) threaded steel rods and b) plastic mesh was wrapped around the steel rod structure in order to seal the Cages used for housing the passive samplers during field deployments, c) and d) deployment of the passive samplers, (e) picture of passive samplers submerged in the field.

4.4.3 Deployment of passive samplers in the dam and AMD

The cages were dipped approximately 10 cm below the water surface at random sites within the dam and AMD. Field parameters were recorded on the day of deployment and also on day 3, 5, 9 and 12 to check their variation during days of deployment of passive sampler. Grab samples were also collected on the same days and analysed for anions. It could be expected that anions might affect the transport of Cd (II), Co (II), Cu (II), Ni (II) and Fe (II) due to competition with the carrier molecule.

4.4.4 Collection of passive samplers and analysis of metal ions

The passive samplers were then collected after day 12 and taken to the laboratory where they were carefully disassembled by unscrewing the top screw out of the PIM-based passive sampler housing. The membrane that sealed the receiver phase solution was removed from the receiver solution chamber. The receiver solution was then poured inside the 15 ml plastic vial and immediately taken to ICP- OES for quantitation of metal ions. No further sample preparation steps were needed.

CHAPTER 5

In this chapter, design, optimisation and application results are presented.

5 Results and discussion

5.1 Polymer inclusion membrane-based passive sampler optimisation

The various parameters that affect PIM-based passive sampler performance were optimised. The optimisation was done by keeping other parameters constant while optimising one parameter.

5.1.1 Effect of D2EHPA composition

The effect of D2EHPA carrier concentration composition in the membrane was investigated at 10, 20, 30, and 40 and 50 %w/w D2EHPA for the extraction of Co (II), Ni (II), Cu (II) and Cd (II) ions as shown in (Figure 37). Results shows that only the 40 %w/w D2EHPA membrane transported appreciable amounts of metals over the 1 days sampling period. Results for the transport of metals across PIMs containing lower concentrations of D2EHPA indicated that either metals diffusion coefficients were too low to ensure appreciable trans-membrane transport during the sampling period. As shown in previous work by Zhu et al., (2012), the transport rate may be increased by adding a plasticizer to the membrane composition. However, adding the plasticiser increase fast trans-membrane transport was not essential for the PIM applications and could be even detrimental if it leads to rapid saturation of the receiving solution with the target analyte. Membrane containing 50 %w/w D2EHPA had limited mechanical stability as reported by (Kolev et al., 2009). The 40 %w/w D2EHPA composition was therefore selected for further experiments. This optimum D2EHPA composition has been reported by other researchers such as Almeida et al., (2014) in the development of a PIM-based passive sampler for Zinc (II) in urban pond waters.

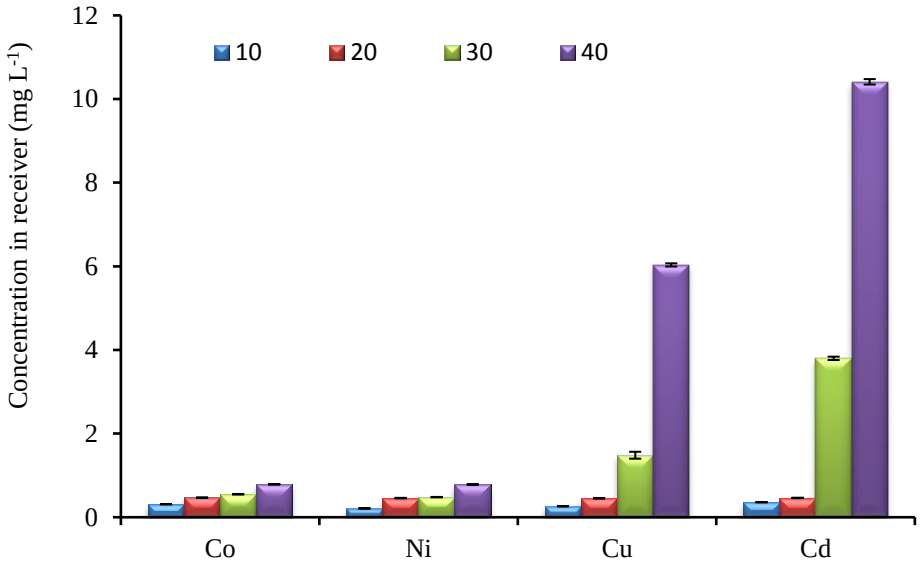

Figure 37: Effect of extractant (D2EHPA) concentration (%w/w) in the membrane (n = 3, SD) Source phase: 1 mg L^{-1} of the metal ion concentration, pH = 6.0, Stripping phase: 1mol L^{-1} HNO_3, Carrier: 40%, Operation temperature: 25°C, Time: 1 days, stirring speed of 200 rpm, Thickness of PIM: 150 µm.

5.1.2 Effect of receiver solution

Effective stripping of the membrane is necessary for the system to be used in practical situations. Three different receiver solutions containing 1 mol L^{-1} H_2SO_4, 1 mol L^{-1} HCl and 1 mol L^{-1} HNO_3 were used to evaluate the stripping of Co (II), Ni (II), Cu (II) and Cd (II) from PVC/D2EHPA PIM sampler. The PIM samplers were deployed for 2 days at pH 6 (Figure 38). It is notable that the stripping solution of HNO_3 gave the highest uptake of metal ions from the source to the receiver solution followed by HCl and H_2SO_4. It appears that facilitative transport of Co (II), Ni (II), Cu (II), and Cd (II) through PVC/D2EHPA PIMs can be achieved with H^+ concentration gradient across the membrane from nitric acid. Nitric acid has been has been reported in literature as a good metal ion stripping solution (Kim et al., 2001). Further experiments were conducted using 1 mol L^{-1} HNO_3 as receiving solution.

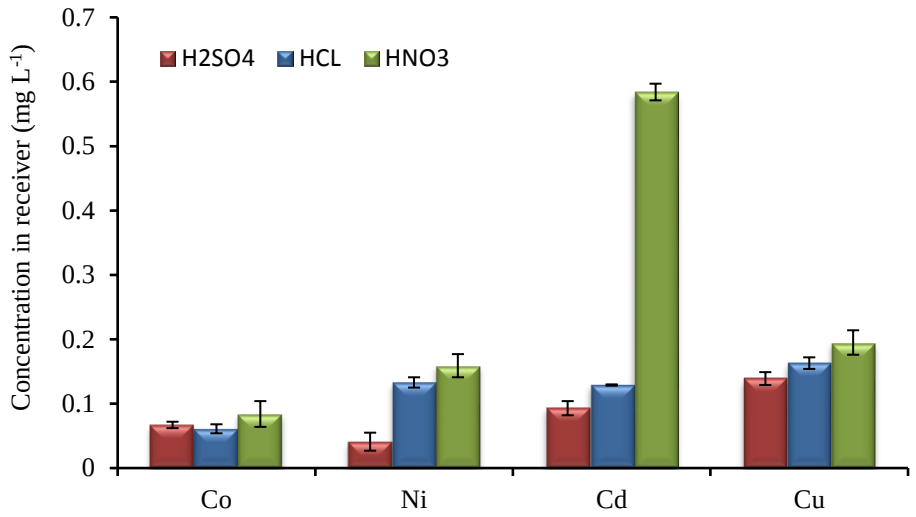

Figure 38: Effect of various acids on the receiver solution set at pH 6 (n = 3, SD) Source phase: 1 mg L^{-1} of the metal ion concentration, pH: 6.0, Carrier: 40%, Operation temperature: 25°C, Time: 1 day, Stirring speed: 200 rpm, Thickness of PIM: 150 µm.

5.1.3 Effect of receiver phase concentration

For a membrane composition of 40 % w/w D2EHPA/ 60 %w/w PVC, the effect of the nitric acid concentration in the stripping phase on the of metal ion concentration was studied from 0.25 – 1.5 mol L^{-1} after 5 days of deployment. As shown in (Figure 39) the metal ion uptake through the PIM increases with increasing HNO_3 concentration up to 1 mol L^{-1}, this could be attributed due to high concentration of protons in the receiver phase which leads to an increase in the driving force, which accelerates the separation of the metal ion-D2EHPA complex at the membrane-receiver interface**.** However, the optimum concentration was 1 mol L^{-1}, as from 1.5 mol L^{-1} HNO_3 the metal ion uptake reduces. This might be related to poor ionisation of the acid at high concentration

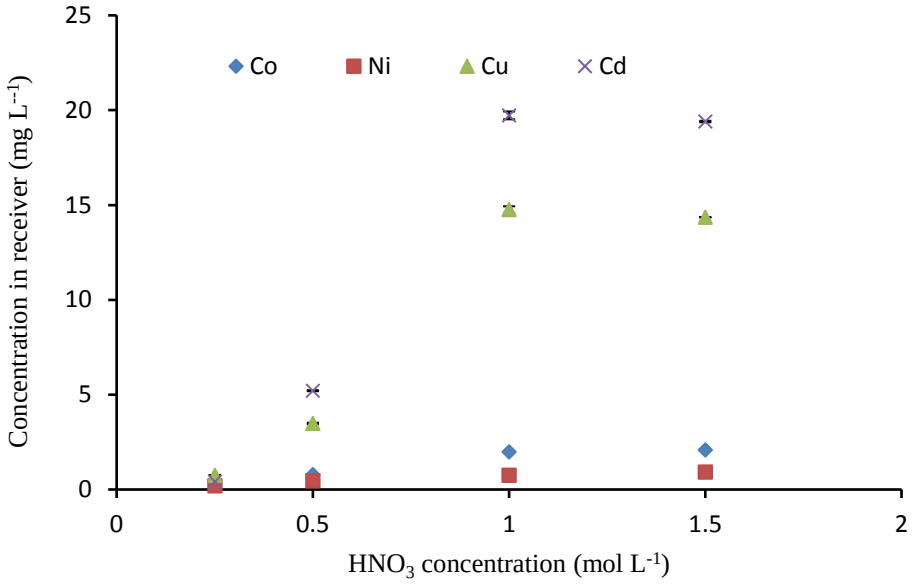

Figure 39: Effect of stripping phase concentration on the extraction of metal ions (n = 3, SD) Source phase: 1 mg L^{-1} of the metal ion concentration, pH: 6.0, Carrier: 40%, Operation temperature: 25ºC, Time: 1 day, stirring speed: 200 rpm, Thickness of PIM: 150 µm.

5.1.4 Effect of pH in the source solution

The pH of the source solution plays an important role in the complex formation by acidic extractant. The influence of pH is related to the form of metal ions in solution, as well as the functional group of the extractant. Since D2EHPA is an acidic extraction reagent it is expected that the extraction concentration can be enhanced by increasing the pH of the receiver solution since H^+ are the driving force in the extraction and the bigger is this difference H^+ concentration between the source and receiver solutions the better is the expected transport. In this study the effect of pH on the extraction of the membrane containing 40 %w/w D2EHPA and 60 %w/w PVC was investigated at pH range of (3–7) (Figure 40). The deployment time in this case was 24 hours. The extraction could be interpreted from the general extraction Eqn 12 between divalent metal ions and D2EHPA molecules.

$$M^{2+}{}_{(aq)} + (2+P)/(2+P)/2(HR)_{2\,(org)} \leftrightarrow MR_2(HR)_{p\,(org)} + 2H^+{}_{(aq)} \quad 12$$

Where $(HR)_2$ is a dimeric form of D2EHPA and P is the number of molecules of D2EHPA engaged in the reactions. In these cases, P has a value of 2 for Cd (II), Cu (II), Ni (II) and Co (II) when DE2HPA is used. According to Eqn 12, as the pH increases there are is a decrease of H^+. It was observed that the amount of metal ion extracted decreased beyond pH 6, because an increase of pH higher than 6 leads to the precipitation of the trace metal ions. Once metal ions precipitate, then are no longer bioavailable.

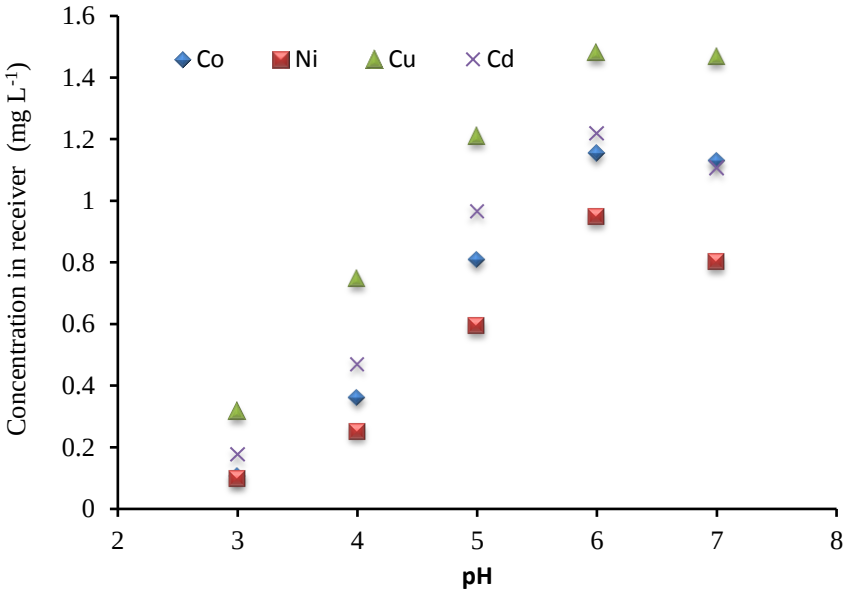

Figure 40: The effect of pH on the membrane extraction capacity (n = 3, SD) Feed phase: 1 mg L^{-1} of the metal ion concentration, Stripping phase: 1 mol L^{-1} HNO_3, Carrier: 40%, Operation temperature: 25^oC, time: 1 day, Stirring speed: 200 rpm Thickness of PIM: 150 µm.

5.1.5 Effect of membrane thickness

The diffusion of the complex formed by metal ion with D2EHPA across the membrane is a critical process of the PIM transport. Membrane thickness is one parameter that influences the transport rate of the formed metal ion-D2EHPA complex. The influence of membrane thickness was investigated at four different thicknesses (50, 100, 150 and 200 µm). It was observed in (Figure 41) that transport slightly increased and then decreased with membrane thickness. The slight increase

with membrane thickness for some metals in somewhat surprising because this deviates from Fick's first law of diffusion in Eqn 13 (Kaya et al., 2013; Zaheri et al., 2017). Thus, slight increase could be attributed to huge time lag in the PIM transport since deployment time was done for 24 hours. This is within the passive sampler time lag, which was about 5 days. Thus, the effect of membrane thickness influence could not be properly observed until after 1 µm membrane thickness. Thus 1 µm membrane thickness was therefore accepted as optimum and used in further studies.

$$J = D\frac{C_{f,o}}{d} \qquad 13$$

Where d is the membrane thickness and D is the apparent diffusion coefficient of metal ion studied through the membrane and $C_{f,o}$ are the initial and final concentration (Zaheri et al, 2017).

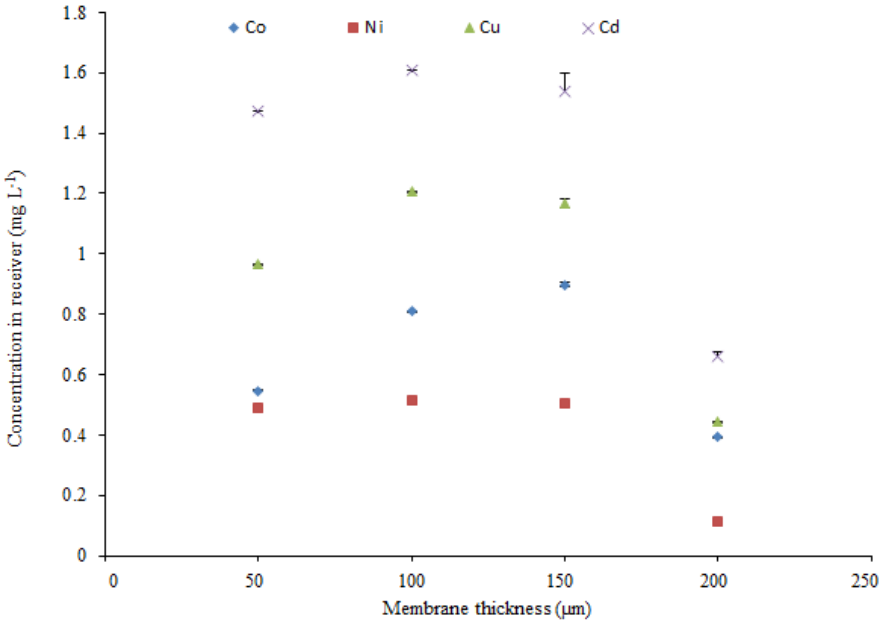

Figure 41: Effect of the thickness of PIM on the transport (n = 3, SD) Feed phase: 1 mg L^{-1} of the metal ion concentration, pH = 6.0, Stripping phase: 1mol L^{-1} HNO_3, Carrier: 40%, Operation temperature: 25°C, Time: 1 day, stirring speed: 200 rpm

5.1.6 Effect of stirring rate

The passive sampler with a different stirring rate speed of the source solution was performed with the aim of investigating any turbulence effects on the rate of accumulation of metal ion in the receiving solution (Figure 42). With no stirring, the metal uptake was very low and a significant increase was noticed once the stirring rate was increased to 200 rpm. Thereafter a decrease at 400 rpm was observed. The increase can be attributed to the aqueous boundary layer thickness decreasing continuously with increasing stirring speed up to 200 rpm. The increase of stirring speed to 400 rpm leads to stirring rate which then causes the release of the DE2HPA out from membranes (Benosmane et al. 2015). Hence, the stirring speed of 200 rpm was selected for further experiments. The increase in metal uptake with stirring speed in membrane extraction is consistent with other previous fundings (Kiswandono et al., 2013; Kolev et al., 2013).

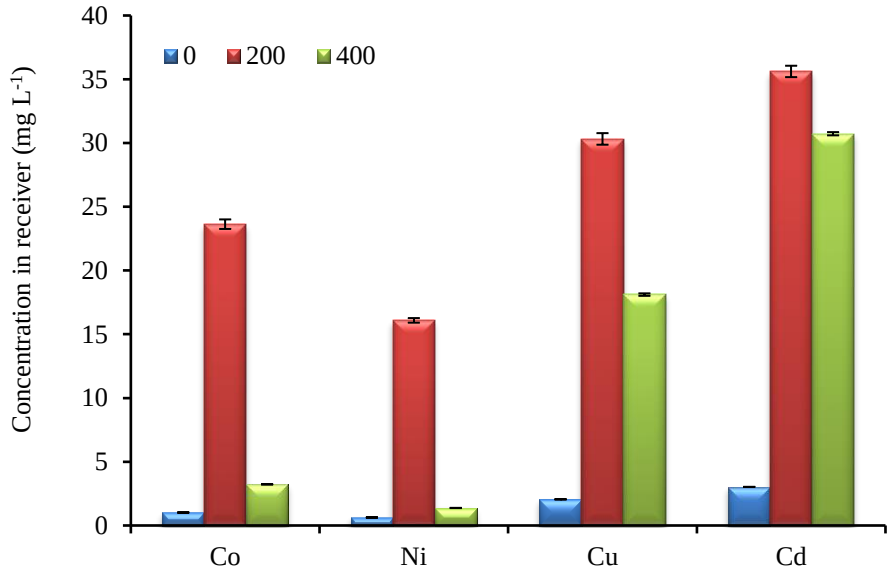

Figure 42: The effect of different stirring speed on concentration in the receiver solution of the passive sampler was investigated at 0, 200 and 400 rpm (n = 3, SD) source phase: 1 mg L^{-1} of the metal ion concentration, pH: 6.0, Stripping phase: 1mol L^{-1} HNO_3, Time: 5 days, Carrier: 40%, Operation temperature: 25°C, Thickness of PIM: 150 µm.

5.1.7 Effect of passive sampler exposure area

PIM-based passive sampler exposure area was tested. The study was performed using the optimum conditions which are 40 %w/w D2EHPA, 1 mol L^{-1} HNO_3, 100 µm, sample pH 6 and 200 rpm stirring rate. The exposure period was for two days. The result in (Figure 43) shows that the larger exposure area of passive sampler was more effective, and its extraction was higher than that of the small exposure area of the passive sampler. These results are proving that the larger contact areas of the PIM-based passive sampler improve the rate of transport metal ion concentration uptake. However, for longer deployment beyond two weeks, a small exposure area might be ideal as can give equilibrium time due to slow uptake kinetics. In our case since the passive sampler was designed to be deployed for two weeks, bigger exposure area was chosen.

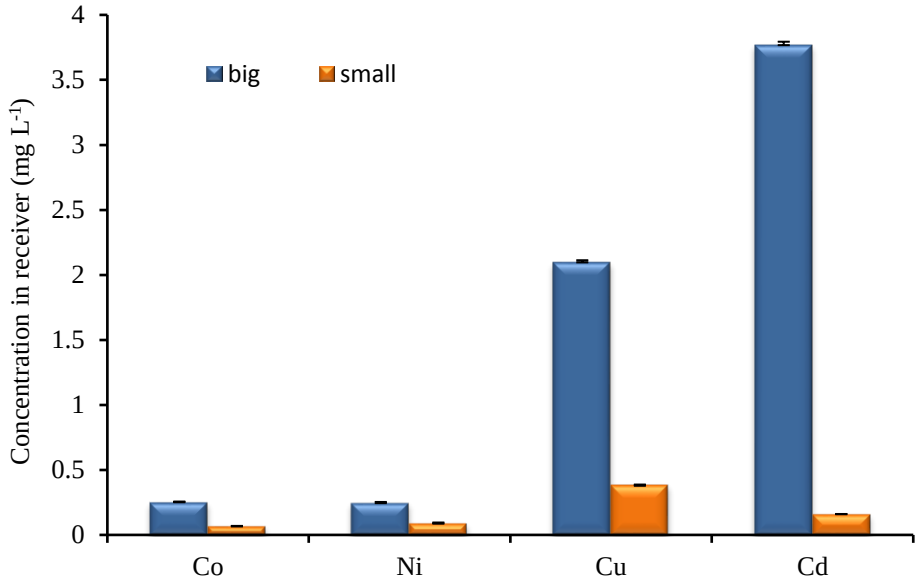

Figure 43: pH 6 PIM-based passive sampler window opening results after day 2 (n = 3, SD) Source phase: 1 mg L^{-1} of the metal ion concentration, pH: 6.0, Stripping phase: 1mol $L^{-1}HNO_3$, Carrier: 40%, Operation temperature: 25°C, Time: 1 day, stirring speed: 200 rpm, Thickness of PIM: 150 µm.

5.1.8 Deployment time

The influence of sampling time on metal ions accumulation in the receiver phase was investigated over 13 days using the optimum parameters of the PIM-based passive sampler (Figure 44). Lower transport kinetics was observed up to day 5. The concentration increased after day 6 and an uptake was observed up to day 13 which showed that PIM containing D2EHPA as carrier and PVC as polymer can facilitate the transport of Co (II), Ni (II), Cu (II) and Cd (II). An uptake of metal ion was only obtained between day 6 and day 13. The passive sampler has a large time lag and stripping into the receiver solution is a rate limiting factor in this period. This means that any fluctuation of the external metal concentration will become apparent in the receiver with a delay of 5 days. Therefore, the time-weighted average concentrations provided by the PIM-based passive sampler apply only to the exposure period from 0 to (t-5) days. This also means that passive sampler is suited for deployed between 6 and 13 days which is the kinetic region of the passive sampler. This observation was also observed by Martınez et al 2008 where passive sampler was used for the uptake of organotin compounds. They author discovered that the lag-time could be due to either the delay caused by the slow diffusion of an analytes across the rate limiting barriers (Martıneza et al., 2008). Nyoni et al., (2011) also observed time lag of days for some triazines when a passive sampler based on silicone rubber was developed (Nyoni et al., 2011).

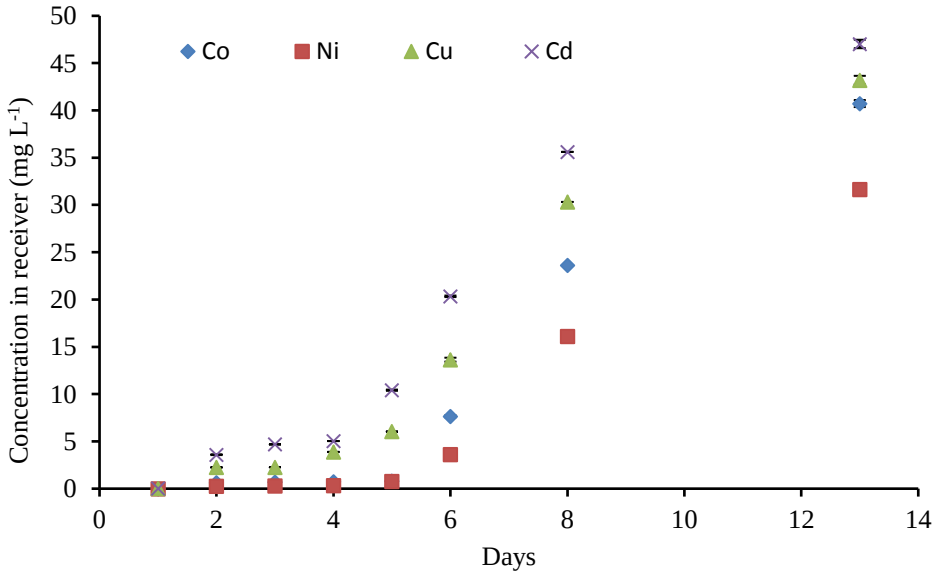

Figure 44: Transport of metal ion across PIM (n = 3, SD) Source phase: 1 mg L^{-1} of the metal ion concentration, pH: 6.0, Stripping phase: 1mol $L^{-1}HNO_3$, Carrier: 40%, Operation temperature: 25°C, stirring speed: 200 rpm, Thickness of PIM: 150 μm.

5.2 PIM stability, re-use and characterisation

Membrane microstructure is one of major aspects affecting the separation of metal ions. PIM have a specific structure, depending on the particular type of polymer film. In the case of PIMs, which are prepared by pouring out a polymer solution containing a carrier, the resulting membrane may have a different structure, depending on the type and concentration of the reactants. Scanning electron microscopy (SEM) provides information on how the carrier is distributed within the base polymer. By means of these techniques the actual picture of membrane morphology can be obtained. The stability of the PIM was further tested using thermogravimetric analysis (TGA) and nuclear magnetic resonance (^{31}P NMR). Contact angle measurements were studied.

5.2.1 PIM stability and re-use

To study the stability of PIMs, three experiments were conducted under the same conditions without changing the membrane. The source and receiving phases were renewed for each experiment while the used PIM was first soaked in water set at pH 3, shaken for 5 mins and allowed to dry at ambient temperature before reuse. The results in (Figure 45) indicate that the metal ion concentration was higher in the first cycle. After that, the transport efficiency decreases, which may be caused by the leaching of the extractant to the source solutions, the difference in percentage between first cycle and second cycle for Co (II), Ni (II), Cu (II) and Cd (II) is 20 %, 15%, 17% and 21% respectively. After the decrease between the first and the second cycle, the membrane was stable and there was no change between the second and third cycle. This means that the membrane can be reused especially in relatively clean water that has no fouling. The mass of membrane weighted after transport

was less than the one weight before transport. The percentage mass loss of the PIM from first cycle to second cycle was 5.1%. The visual observation of the membrane colour before transport is homogeneous, clear and colourless (Figure 46 a)), after transport the membrane colour changes to white and the membrane structure becomes visible (Figure 46 b)).

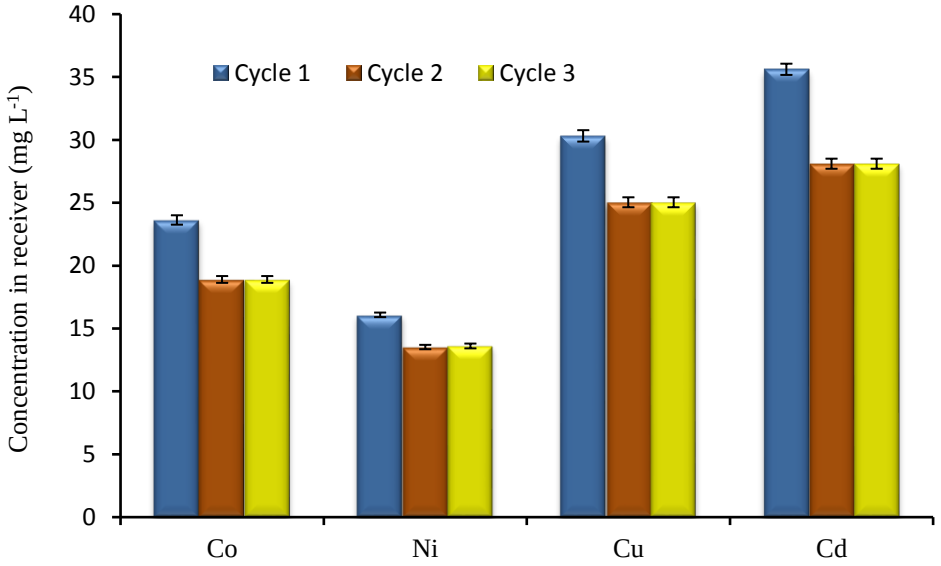

Figure 45: Stability of PIM for three consecutive experiments (n = 3, SD) Source phase: 1 mg L^{-1} of the metal ion concentration, pH: 6.0, Stripping phase: 1mol $L^{-1}HNO_3$, Carrier: 40%, Operation temperature: 25°C, Time: day 3, stirring speed: 200 rpm, Thickness of PIM: 150 µm.

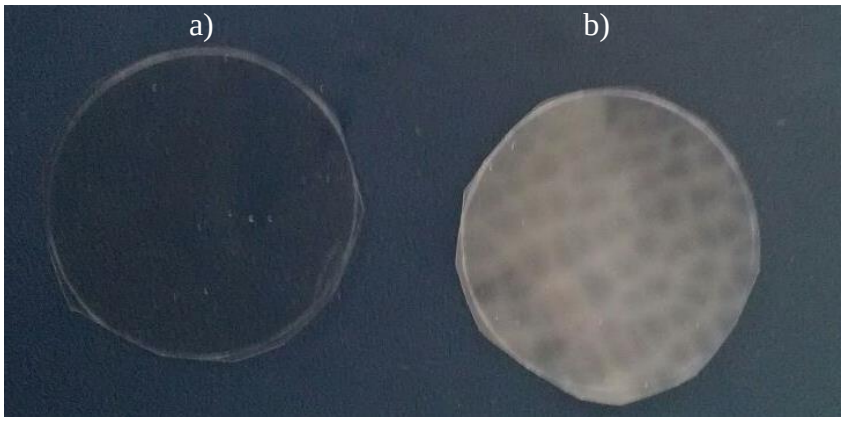

Figure 46: Membrane before a) and after b) extraction.

5.2.2 Scanning electron microscopy (SEM)

The SEM images of the PIM before application in (Figure 47 a)) show a homogenous membrane surface filled with liquid micro-domains containing the extracting agent. This observation supports the idea of coalescence of the aqueous carrier molecules to create liquid pathways that relay the analytes across the membrane (Gherasim et al., 2011). After extraction the membrane surface seems to collapse into irregular wells (Figure 47 b)). The membrane structures have also been lost exposing the structures. The absence of liquid carrier domains at these openings might be an indication that the carrier liquid now exists inside the membrane only. This might be responsible for the reduction in metal ion transfer across the membrane. When the PIM is reused for the third time, the transfer is not affected because the carrier liquid now exists inside the membrane and there is minimal loss.

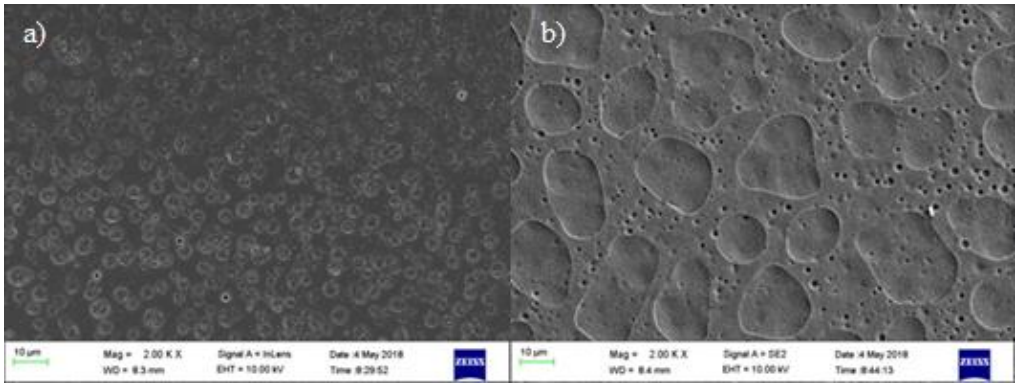

Figure 47: SEM image surface of the a) before extraction and b) after extraction of PIM.

5.2.3 Thermogravimetric analysis (TGA)

TGA analysis was done to determine the stability of PVC and the PIM (PVC impregnated with D2EHPA) before and after extraction as a function of temperature. The results are presented in (Figure 48). The thermogram curve shows that the thermal degradation of PVC and PIM before extraction have common degradation temperatures at 260°C and 400°C due to loss of the original weight followed by the decomposition of the polymer chain. This result was consistent with the thermogram of PVC and D2EHPA in a study by Ling et al. (2017). The

thermogram for the PIM shows degradation of D2EHPA at about 300°C. The PIM before extraction shows a total D2EHPA loss of about 35% while after extraction the percentage loss due degradation of D2EHPA was about 15%. These D2EHPA composition results affirm the observation seen with SEM images.

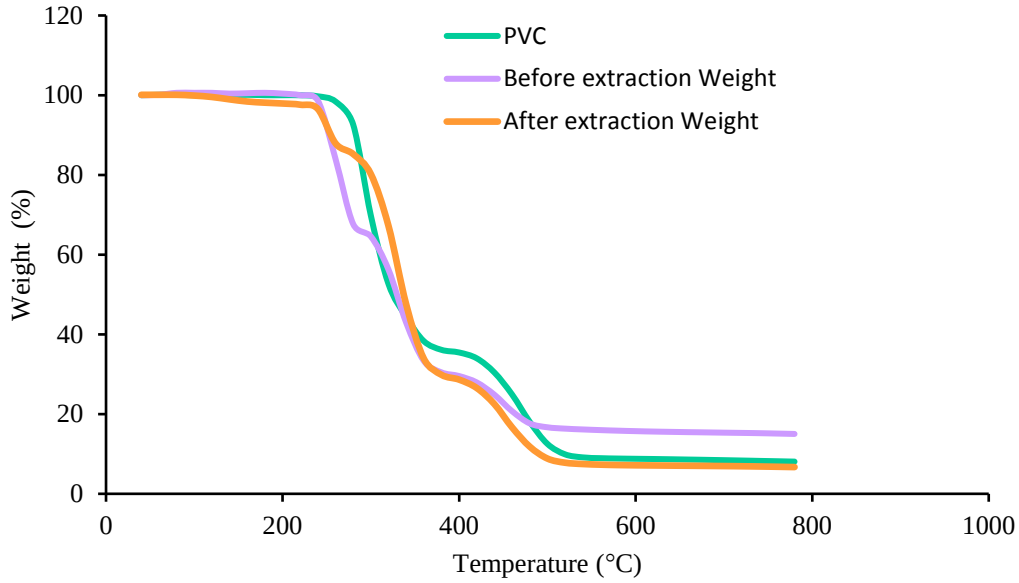

Figure 48: Thermogram a) PVC, b) before, and c) after extraction of PIM

5.2.4 Nuclear magnetic resonance (^{31}P NMR)

The presence of D2EHPA in the PIM was confirmed using ^{31}P NMR. The ^{31}P NMR spectrum for PVC, DE2HPA and the PIM before and after extraction are shown in (Figure 49). The PVC spectrum as expected did not show any phosphorus peak. The D2EHPA had a sharp peak, which was a clear indication of the presence of phosphorus atoms in its structure. The phosphorus peak was visible in the spectrum for PIM both before and after extraction. However, a chemical shift of 1.6 ppm for the phosphorus peak for D2EHPA in the PIM was observed. This might be because of THF that was used to dissolve the D2EHPA and the PVC. The peak also appears in the PIM spectrum after extraction as an indication that the extraction process did not remove D2EHPA from the membrane. The PIM can therefore be reused for more experiments as seen in the membrane stability studies. However, the intensity of the peak decreased and broadens as compared to that of the PIM before

extraction. This might be since a small amount of D2EHPA might be lost during extraction; this was confirmed by the TGA thermograms, SEM images and membrane reusability results.

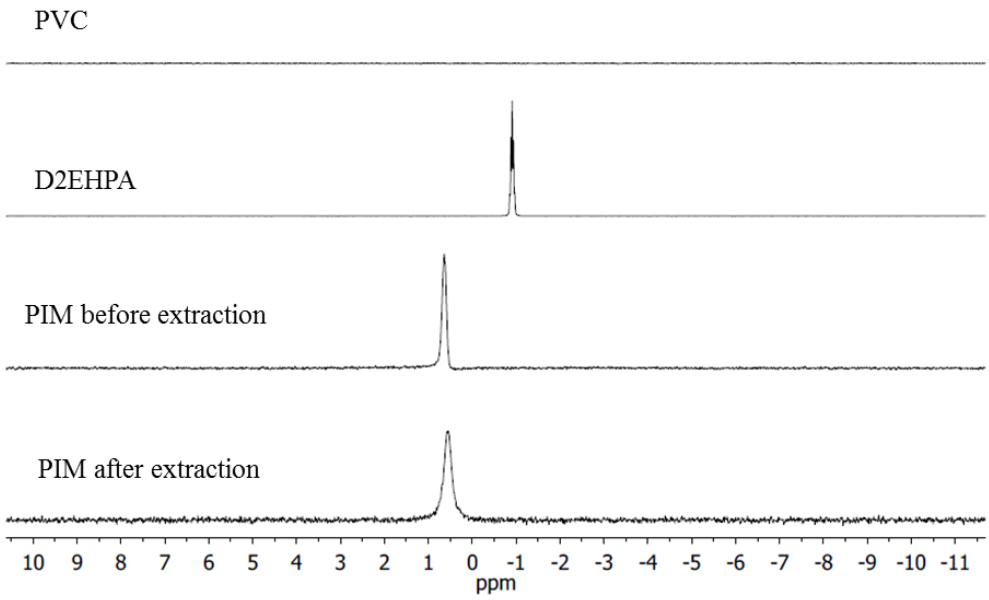

Figure 49: ^{31}P NMR spectrum of PIM Composition

5.2.5 Contact angle

The contact angle is a measure of the ability of a liquid to spread on a surface. The method is used to measure the angle between the outline tangent of a drop deposited on a solid and the surface of this solid. The contact angle measurements give the following information: The affinity of a liquid to a solid surface: if water is used to measure the contact angle one can deduce the hydrophobic (great angle, >90) or hydrophilic (small angle, < 90) character of the surface. In this study, contact angle measurements were taken at room temperature for PIM containing 40 %w/w D2EHPA of carrier. The angle was found to be 78.80 ± 2.58°C. When a solid surface is hydrophilic, the contact angle will be lower than 90°. This phenomenon can be the result of changes in surface morphology and the hydrophilic quality of carrier in the membrane

5.3 Studying the effects of sample matrix in laboratory experiment from field samples

5.3.1 Physical-chemical properties of dam water during lab PIM sampler deployment

Various physical-chemical properties of dam water were measured in the laboratory during sampler deployment (Table 2). Physical chemical parameters that changed drastically in the water during exposure controlled the changes in water chemistry during exposure in the laboratory. These parameters are pH, redox potential and nitrate. All these parameters increased with time during exposure and thus their behaviour is inter-related. The decrease in the pH of the source solution is a consequence of the transport process. As metal cations are extracted and back-extracted into the receiving solution, H^+ is released into the source solution. Since the experiment is done in a confined environment, this pH drop is significant, and it also affects the accumulation. However, when the sampler is applied in the field, this effect is not observed due to the large volumes of water available. This is one of the main challenges in calibrating a PIM-based passive sampler under laboratory conditions (i.e. to maintain the source solution pH and concentrations constant throughout the sampling period). Moreover, since DZEHPA is a cation exchanger, the species expected to affect the accumulation of metals ions are other cations which exist in higher concentrations (e.g. calcium, magnesium, sodium and potassium), and their effect should thus be taken into account.

Table 2: Physical-chemical properties of dam water during sampler deployment in the laboratory

Parameters	Day 0	Day 3	Day 5	Day 9	Day 12
pH	6.37	5.66	4.95	3.90	2.42
Conductivity (mS cm^{-1})	0.36	0.39	0.40	0.44	0.99
Total-dissolves solid (ppt)	0.16	0.19	0.22	0.30	0.48
Redox-potential (Mv)	317	325	335	353	385
F^- (mg L^{-1})	0.11	0.090	0.089	0.090	0.082
Cl^- (mg L^{-1})	19.68	20.43	21.27	20.16	20.49
Br^- (mg L^{-1})	0.053	0.059	0.073	0.067	0.060
SO_4^{2-} (mg L^{-1})	138.48	139.81	147.79	141.68	143.51
NO_3^- (mg L^{-1})	6.92	21.35	27.39	21.01	79.92

5.3.2 Effect of contact time in laboratory-based experiments from field samples

5.3.2.1 Spiked dam water

The passive sampler was deployed in water samples obtained from Fleurhof dam and spiked with 1 mg L^{-1} metal ions as shown in (Figure 50). A linear kinetic uptake of metal ion concentration was observed up to day 12. The measured pH of the dam water was 6 which coincided with the optimum source phase pH for efficient metal ion flux across the membrane. The metal ion concentration in the spiked source phase was corrected for concentrations already existing in the dam water. The uptake rate dropped significantly by a factor of between 4 and 9 lower than the values obtained for spiked deionized water. In environmental samples, metal ions exist as complexes with organic acids. Even though some researchers have observed that the formation of the D2EHPA-metal ion complexes is fast Li et al.,(2017) and Meng et al., (2017), noted that the impact of the metal-humic acid complexes on the D2EHPA/D2EHPA-metal complex equilibrium cannot be ignored.

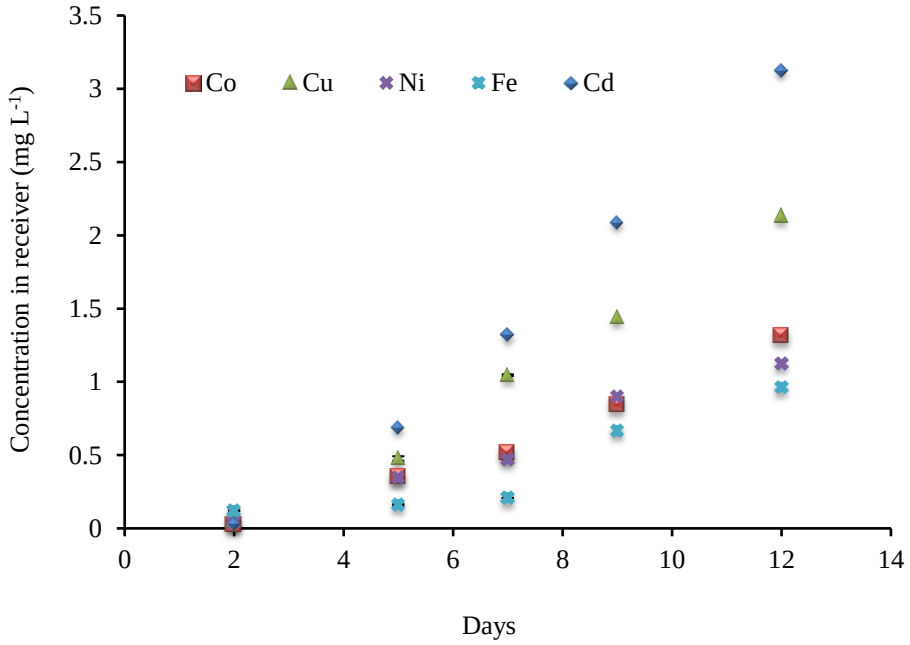

Figure 50: Uptake of metal ion in the laboratory using Fleurhof dam spiked with 1 mgL^{-1} metal ion (n = 3, SD) Source phase: 1 mg L^{-1} of the metal ion concentration, pH: 6.0, Stripping phase: 1mol L^{-1} HNO_3, Carrier: 40%, Operation temperature: 25°C, stirring speed: 200 rpm, Thickness of PIM: 150 µm.

5.3.2.2 Un-spiked dam water

The passive sampler was further deployment in un-spiked dam water (Figure 51 & 52). Results show Cu was far much more up taken than other metals followed by Fe, Co, Ni and Cd. A linear up take was observed this time all the way until day 12. However, linearity was not as step as in normal calibration where correlation coefficient is closer to 1.

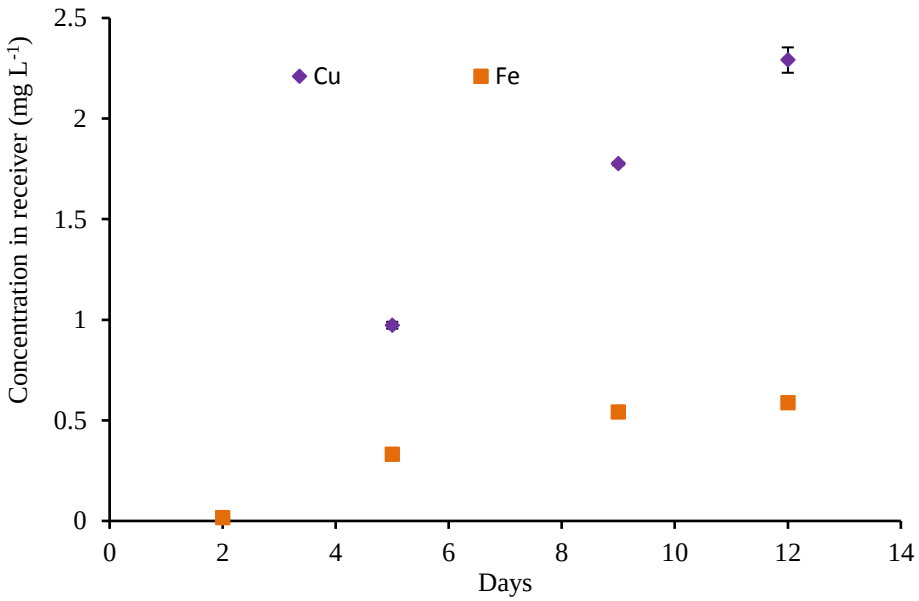

Figure 51: Uptake of Cu (II) and Fe (II) in in the laboratory using dam unspiked (n = 3, SD) Source phase: pH: 6.0, Stripping phase: 1mol L^{-1} HNO_3, Carrier: 40%, Operation temperature: 25°C, stirring speed: 200 rpm, Thickness of PIM: 150 µm.

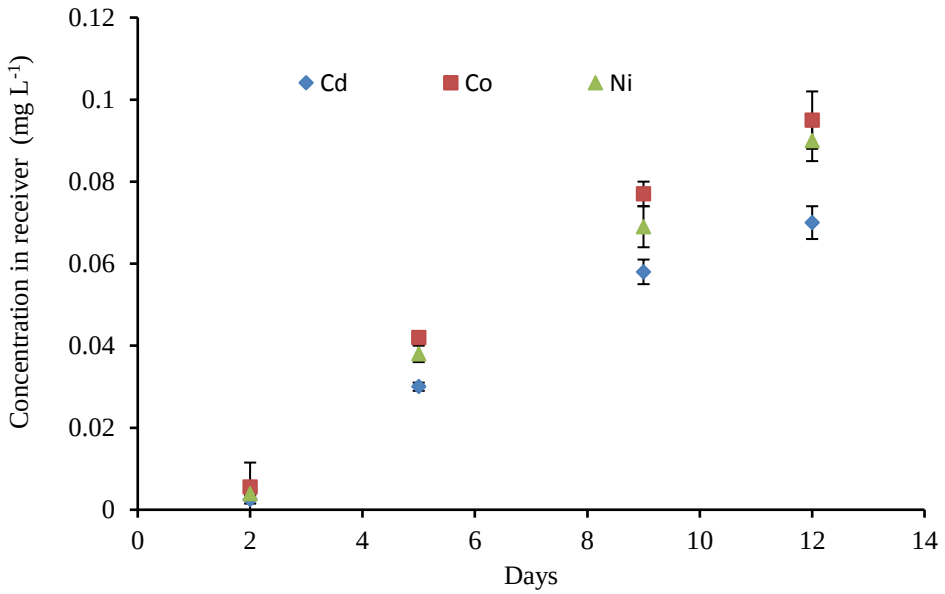

Figure 52: Uptake of Co (II), Ni (II) and Cd (II) in in the laboratory using Fleurhof dam unspiked (n = 3, SD) Source phase: pH: 6.0, Stripping phase: 1mol L^{-1} HNO_3, Carrier: 40%, Operation temperature: 25°C, stirring speed: 200 rpm, Thickness of PIM: 150 µm

5.3.2.3 Un-spiked AMD water

The AMD laboratory results are shown in (Figure 53). The result shows a drastic decrease of metal ions concentration after 5 days of deployment. The decrease in the total metal ion concentration after day 5 is attributed to precipitation reactions and pH because of the accumulation process. AMD water samples are susceptible to precipitation when kept stagnant due to changes in the water chemistry. The concentration of Fe (II) decreased from 48 mg L^{-1} to 22 mg L^{-1}. A lot of solid precipitate was observed settling at the bottom after 5 days and the colour also changed from a brown colour to an orange colour as shown in (Figure 54). For this reason, the experiment was only carried out for 5 days instead of 12 days. These results were also confirmed by the decrease of metal ions concentration of AMD water that was standing in the laboratory at room temperature for a period of 5 days as shown in (Table 3). This means precipitation reactions reduced the bioavailability of the metals. The decrease was much more observed with Fe which means Fe is a major driver of the precipitation reaction. Cd (II) and Co (II) seem

least affected but could be co-precipitated with Fe (II). The precipitation of Fe (II) to Fe (III) could be due to lack of oxygen, as samples are being stored in the laboratory. Thus, passive sampler optimisation in AMD can best be done in the field. In the laboratory, it can be used to study the metal bioavailability after system is perturbed.

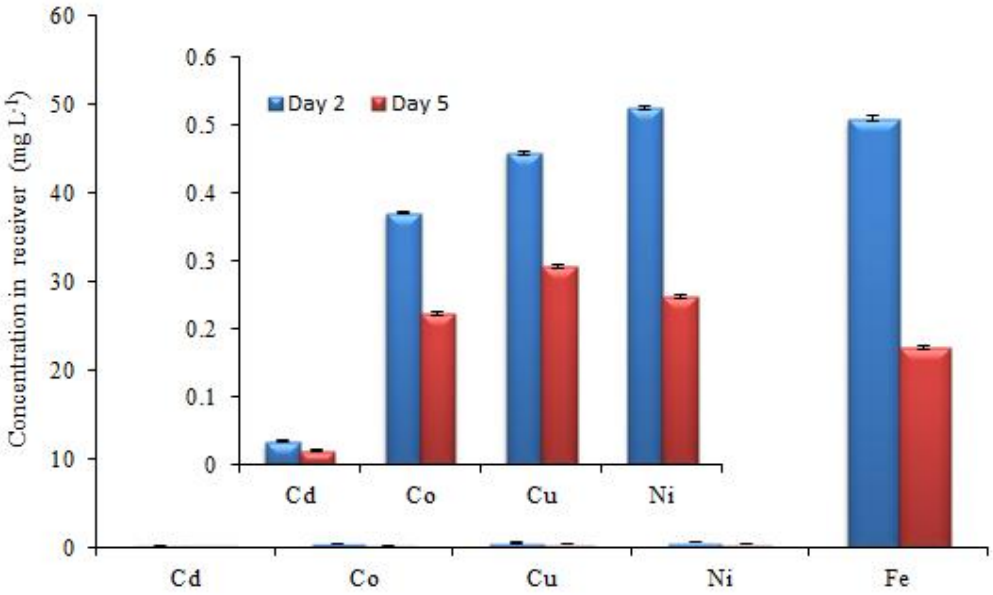

Figure 53: Metal ion deployed in AMD water in the laboratory (n = 3, SD) Source phase: pH: 2.83, Stripping phase: 1mol L^{-1} HNO_3, Carrier: 40%, Operation temperature: 20°C, stirring speed: 200 rpm, Thickness of PIM: 150 µm.

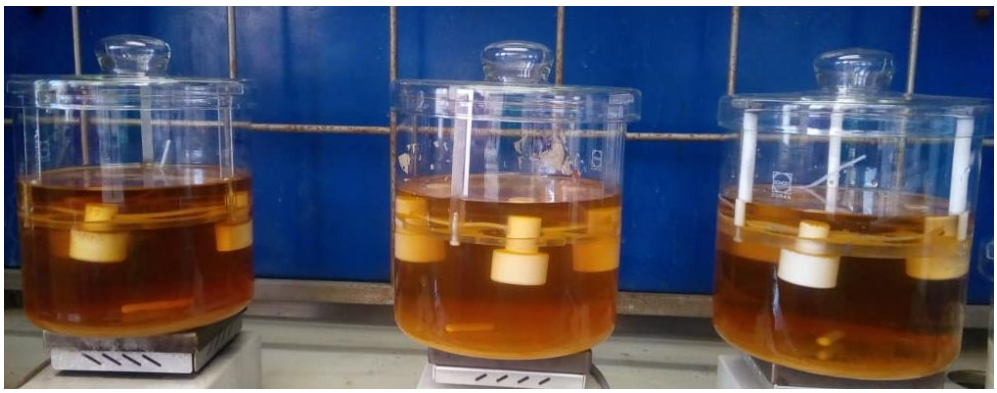

Figure 54: Fe precipitation after day 5 in the laboratory set up

Table 3: Metal ion concentration in the AMD sampled in one batch but analysed different days and kept at room temperature.

Metal (mg L^{-1})	Cd (II)	Co (II)	Cu (II)	Ni (II)	Fe (II)
AMD immediately after sampling	0.53	19.06	14.48	28.70	1142.50
AMD analysed after 5days	0.16	10.23	9.73	23.62	817.79

5.3.3 Effect of stirring rate in laboratory-based experiments

The effect of stirring rate in which dam water was used as the source phase was further investigated to ascertain performance of the PIM sampler (Figure 55). The dam water was spiked with 1 mgL^{-1} of Cd (II), Co (II), Cu (II), Ni (II) and Fe (II) besides what is already there. It was observed that just like in spiked deionized water, the optimum stirring rate was also 200 rpm. This was an indication that stirring rate was not affected by presence of potential matrices. However, application in real samples with varying turbulence still requires considerations of the turbulence. In our case, the PIM-based passive sampler was deployed where turbulence was very minimal due to the nature of the site with lots of reeds.

For AMD, the results are shown in (Figure 56). The stirring rate was only investigated at 0 to 100 rpm, due to Fe (II) precipitation. The hydrodynamic condition also had an effect on the concentration of Cd (II), Co (II), Cu (II), Ni (II) and Fe (II) transport. This effect was more observed in the AMD that had started to precipitate as stirring released the metal ions. Metal ions were made to be more bioavailable due to stirring since they were released from the precipitate. This observation was more pronounced in metals ions like Fe (II) and Cu (II), which were driving the precipitation process.

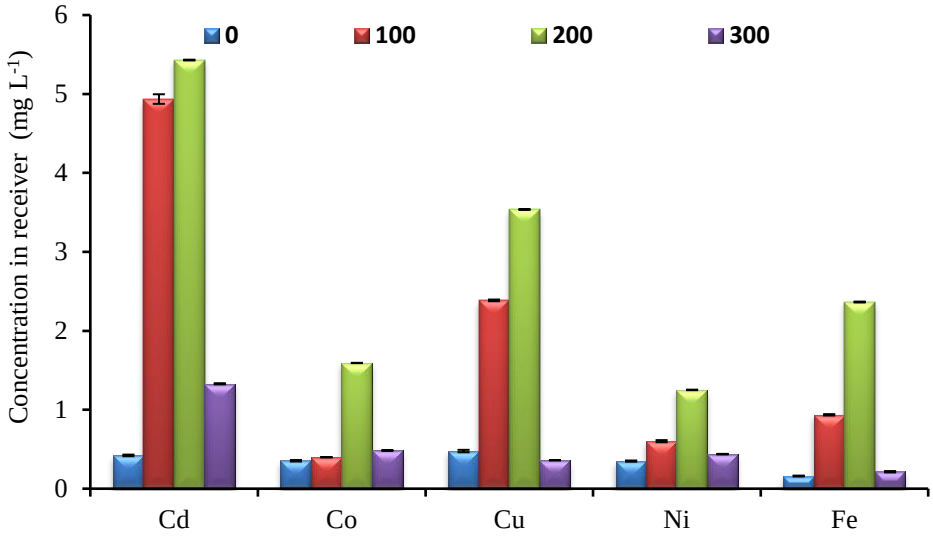

Figure 55: Effect of stirring rate using Fleurhof dam water spiked with 1 mgL^{-1} of each metal ion (n = 3, SD) Source phase: pH: 6.0, Stripping phase: 1mol L^{-1} HNO_3, Carrier: 40%, Operation temperature: 25°C, stirring speed: 200 rpm, Thickness of PIM: 150 µm.

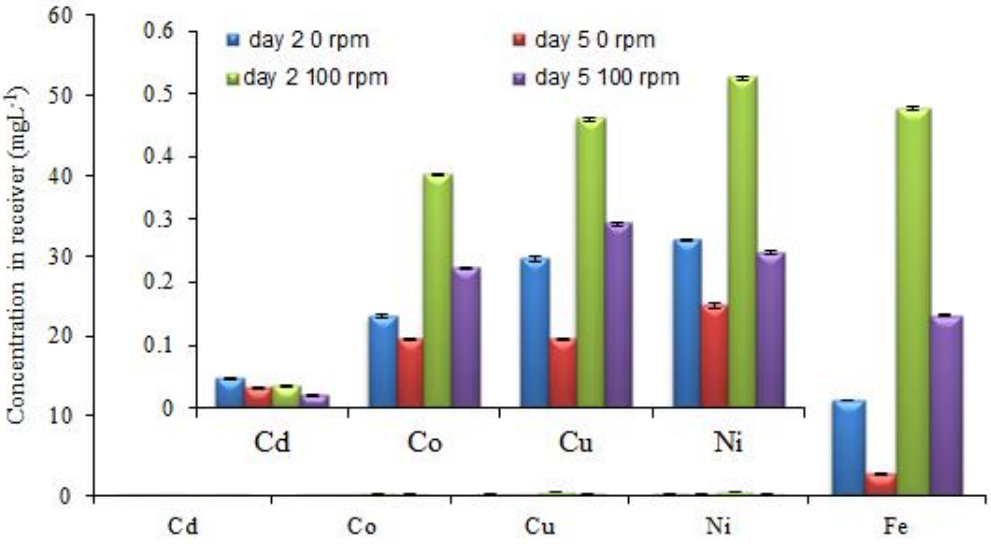

Figure 56: Effect of stirring rate on uptake of PIM-based passive sampler in AMD in the laboratory (n = 3, SD) Source phase: pH: 2.83, Stripping phase: 1mol L^{-1} HNO_3, Carrier: 40%, Operation temperature: 25°C, stirring speed: 200 rpm, Thickness of PIM: 150 µm.

5.3.4 Comparison receiver solution pH during sampler deployment in different sample matrix

The pH of the receiver solution was investigated between the dam water un-spiked, dam water spiked, and the AMD water as shown in (Figure 57, 58 and 59). The pH of the dam water un-spiked at day 12 was 0.64. When the dam water was spiked with the metal ions at 1 mg L^{-1}, the increase in pH of the receiver phase is more pronounced as shown in (Figure 57). For example, the pH of the receiver phase for the spiked sample at day 12 was 0.84 compared to 0.64 in the un-spiked setup. At higher metal ion concentration in the source phase, there are more metal ions that are transferred to the receiver phase, in turn, more H^+ ions are transferred in the counter direction resulting in an increase in the pH of the receiver phase.

The pH of AMD in (Figure 59) shows the same trend that was observed in the study where dam water was used. The pH in the receiver solution inceased as the number of days increased. The pH of the receiver phase for the AMD samples at day 12 was 0.95 compared to 0.64 in the un-spiked and 0.84 spiked setup. This might be due to low pH in the AMD and this accelerates the H^+ ions transfer resulting in an increase in the pH of the receiver phase.

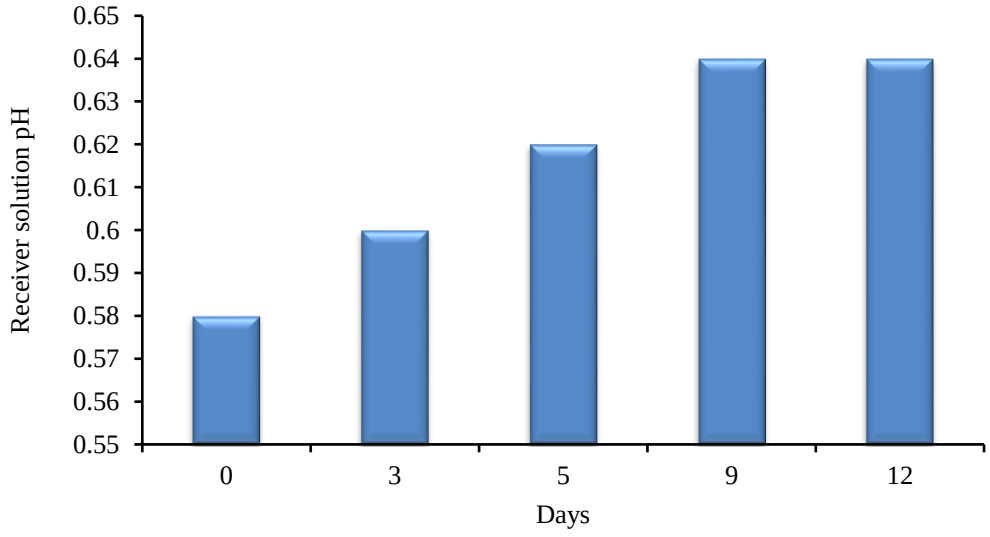

Figure 57: Un-spiked dam water receiver solution pH

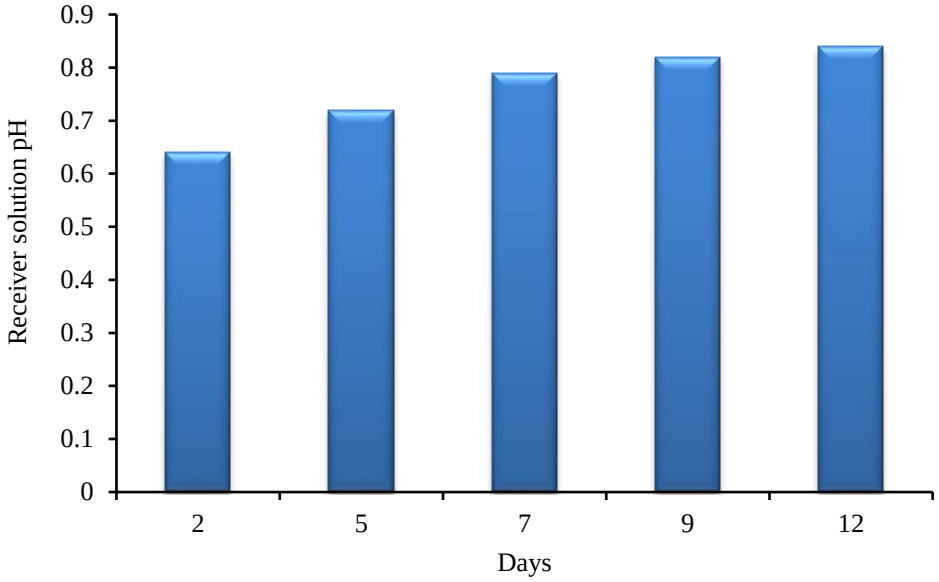

Figure 58: Spiked dam water receiver solution pH

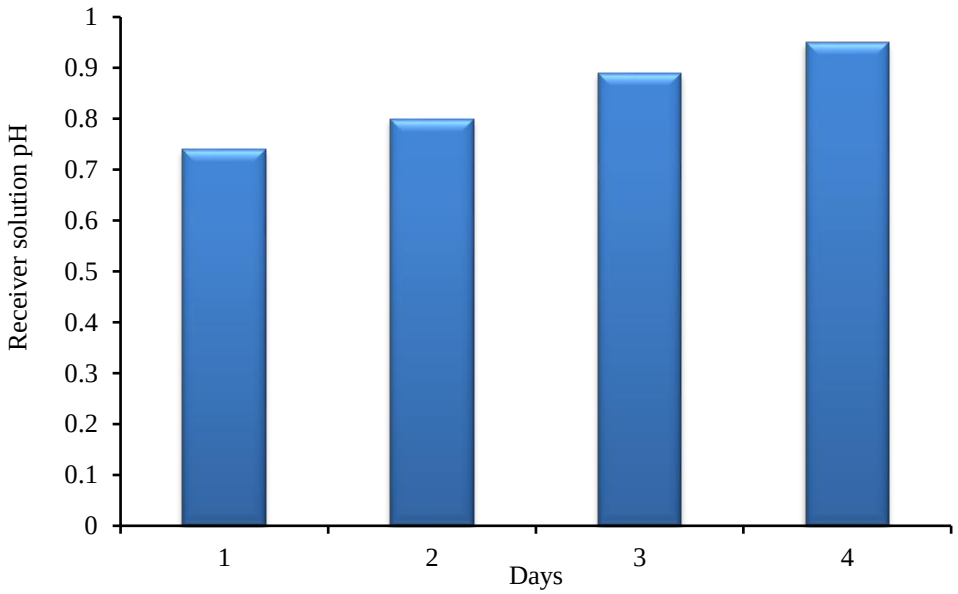

Figure 59: AMD receiver solution pH

5.4 Application in dam water

5.4.1 Total metal ion concentrations in Fleurhof Dam

Table 4 gives the concentration of study metal ions found at Fleurhof dam using the developed passive sampler after 12 days of deployment. The total metal ion concentrations found in dam water are compared to allowed limits of various local and international bodies such as WHO, EU and South African guidelines. All metal ions concentrations were well above the permissible levels. Cu (II) was most high in concentration followed by Fe (II) and Co (II) as least. Fe (II) is naturally more abundant than Cu (II) thus presence of high Cu (II) indicate pollution of dam water from tailing materials. The total metal concentration exceeded the amounts allowed by various bodies. Despite the AMD leached from the tailing dumps passing through some wetland before reaching the dam, it means not all metals are trapped by the natural wetland. Input of these metals into the dam could be more pronounced in summer when rainwater increase the amount of AMD reaching the dam. Since the Fleurhof dam is near a number of gold mine tailing dumps and the dam might be acting as a sink for the metal pollutants that drain from these tailings. High metal ion concentrations in dams affected by mine dump tailings have been reported elsewhere (Baytak and Turker, 2009; Minello et al., 2009; Modoi et al., 2014; Mutlu et al., 2017; Nazir et al., 2015; Santisteban et al., 2015; Sim et al., 2016; Valente et al., 2016) For example, Nazir et al. 2015 has reported 0.129 mg L^{-1} Cd (II), 2.443 mg L^{-1} Fe (II), 0.659 mg L^{-1} Cu (II) and 0.007 mg L^{-1} Ni (II) among other metal ions at Tanda dam in Pakistan (Nazir et al., 2015).

Table 4: Total concentrations of target metals in the dam water and their comparison to various drinking water allowed limits.

Metals ions	Fleurhof Dam ($mg\ L^{-1}$)	WHO ($mg\ L^{-1}$)	European Union ($mg\ L^{-1}$)	South Africa ($mg\ L^{-1}$)
Ni (II)	0.114	0.02	0.02	0.07
Cu (II)	2.989	2.0	2.0	2.0
Fe (II)	0.616	-	0.2	-
Cd (II)	0.115	0.003	0.005	0.005
Co (II)	0.077	-	-	-

Adapted for Water Quality for Ecosystem and Human Health, 2006 (prepared and published by the United Nations Environment Programme. Water Programme for South African water affairs. Empty space means no data found.

5.4.2 Metal uptake during PIM sampler field deployment in dam water

The field metal ion uptake results are shown in (Figure 60 & 61). Results show Cu (II) was far much more up taken than other metals followed by Fe (II), Cd (II), Ni (II) and Co (II) respectively. The same trend was observed with lab deployment and follows the metal concentration in the source water, which in turn control the bioavailable fraction. The linear uptake of metal ions with deployment time was not that linear as compared to lab deployment except for Cu (II). Further linearity window was much smaller between days 2 up to day 9 for Cu (II). These results correlates with those reported by Singh et al, (2002), where Cu (II) was extracted quantitatively in the pH range 6 to 8 with using D2EHPA as a carrier. Fe (II) was most poorly up taken as far as linearity is concerned as Fe (II) seemed to reach equilibrium around day 5. The passive sampler in this case did not show much time lag as in deionised and dam water performed in the laboratory. The reason for this is unclear.

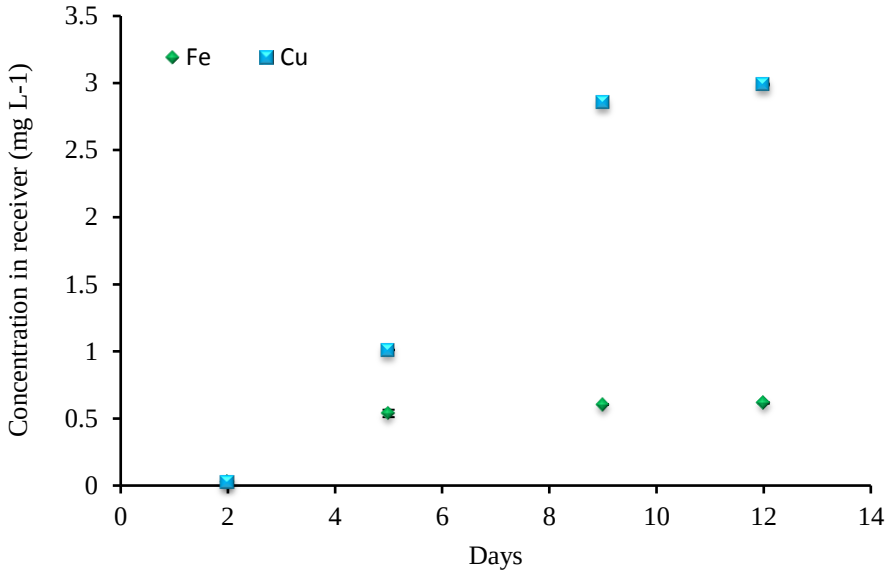

Figure 60: Uptake of Cu (II) and Fe (II) in PIM sampler deployed at Fleurhof dam (n = 3, SD) Source phase: pH: 6.0, Stripping phase: 1mol L^{-1} HNO_3, Carrier: 40%, Operation temperature: 25°C, stirring speed: 200 rpm, Thickness of PIM: 150 µm.

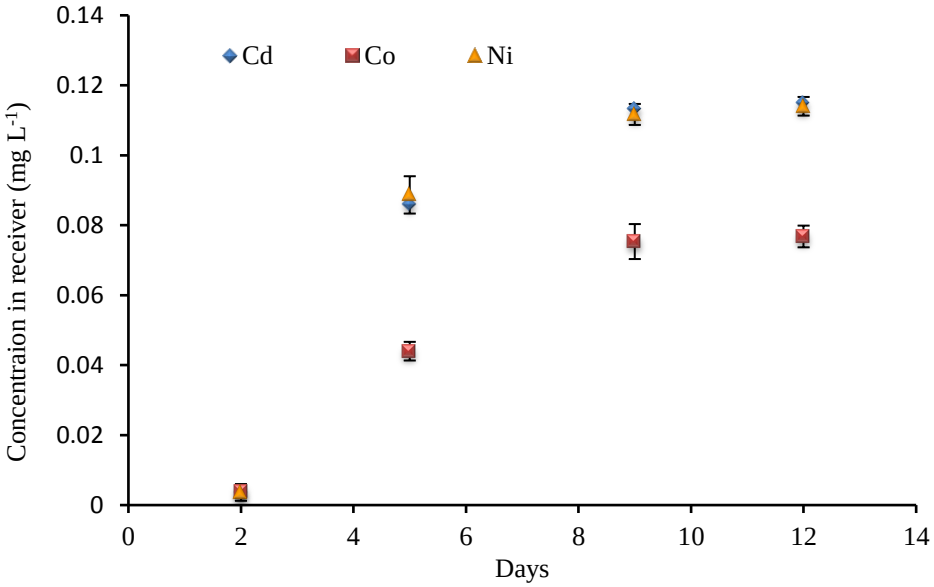

Figure 61: Uptake of Cd (II), Co (II) and Ni (II) in PIM sampler deployed at Fleurhof dam (n = 3, SD) Source phase: pH: 6.0, Stripping phase: 1mol L^{-1} HNO_3, Carrier: 40%, Operation temperature: 25°C, stirring speed: 200 rpm, Thickness of PIM: 150 µm.

5.4.3 Uptake of other metals by PIM-base sampler

In the field the source medium will almost certainly contain other cations which may potentially be transported together with Cd (II), Co (II), Cu (II), Ni (II), and Fe (II), across the PIM. Figure 62 shows uptake of other metal ions present in the dam and extracted into the receiver solution. The concentration of Zn (II) was the highest with 1200 mg L^{-1}.This preference towards Zn (II) has also been observed by (Almeida et al., 2014) in natural waters at pH above 6 and could also reflect its high concentration in the source water. Despite the presence of other metals in natural water, the passive sampler was still able to extract the target metals. This shows the versatility of the developed sampler.

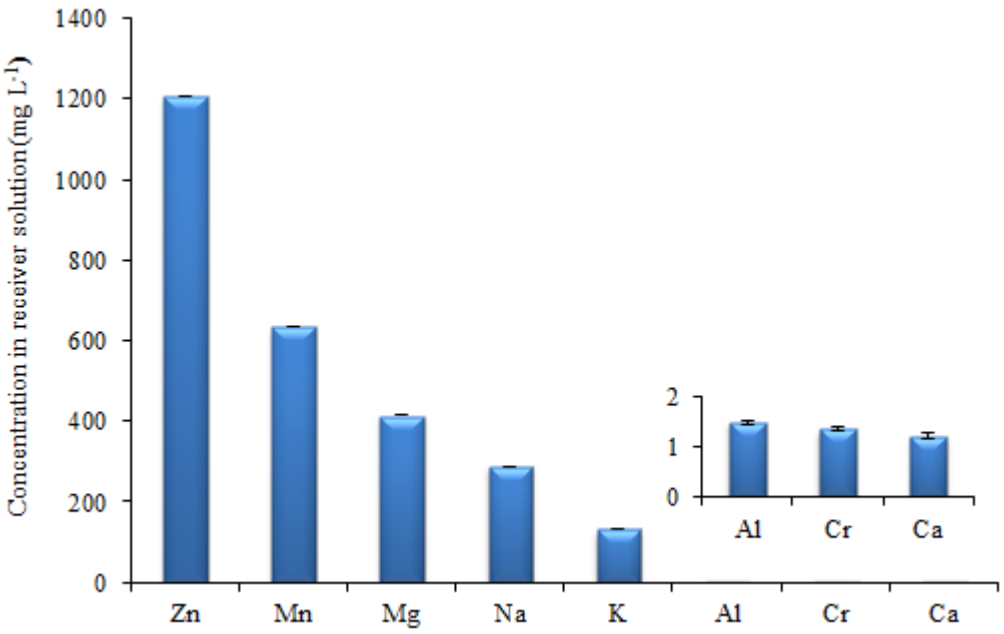

Figure 62: Other metal ion up take by PIM-based passive sampler after day 9 at Fleurhof dam (n = 3, SD) Source phase: pH: 6.0, Stripping phase: 1mol L^{-1} HNO_3, Carrier: 40%, Operation temperature: 25°C, stirring speed: 200 rpm, Thickness of PIM: 150 µm.

5.4.4 pH changes in the acceptor phase of the PIM-based passive sampler deployed at Fleurhof Dam for different days

The pH of the acceptor solution was measured for the acceptor solution before and after deployment for each period. The results in (Figure 63) show that the pH of the acceptor solution increased with deployment time and remained steady after 9 days of passive sampler deployment. The increase in pH is expected since the transport mechanism involves transporting H^+ to the source phase while transporting metal ions to the receiving phase. The H^+ in the receiving phase are therefore the driving process for the transport. Due to the continuous slow transport of the acid in the receiving solution across the membrane to the sample solution, it is expected that the pH at the interface between sample solution and membrane to be substantially lower than the bulk pH value of 6 of dam water. The steady state of acceptor pH change from day 9 coincides with steady state uptake kinetics of the metals in Figure 61. This could mean that at this point uptake kinetics moves from linear to equilibrium phase.

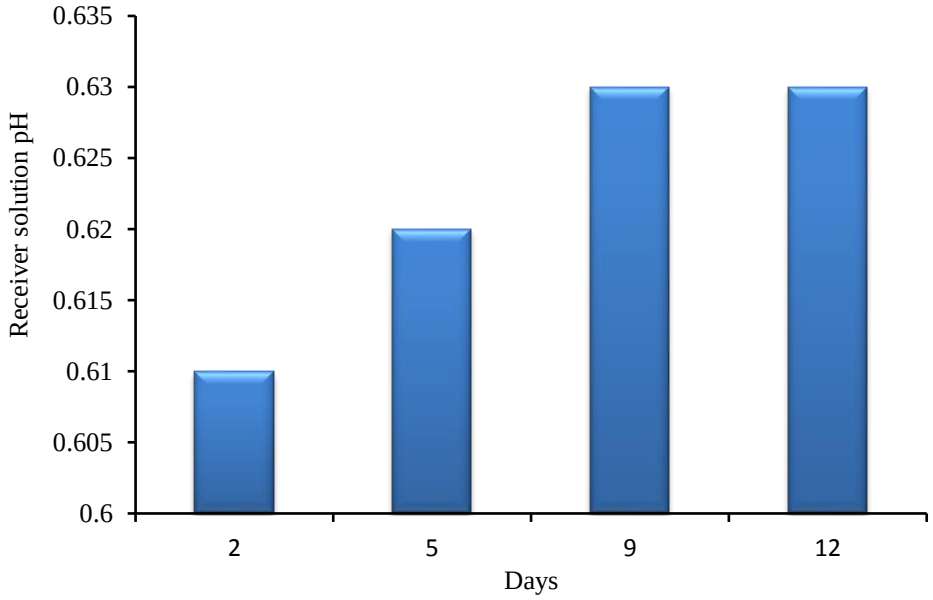

Figure 63: Comparison of the receiver solution pH in PIM sampler deployed at diferent days at Fleurhof dam (n = 3, SD)

5.4.5 Fouling on the passive samplers deployed at Fleurhof dam

PIM-based passive sampler cages on deployment day and on collection day (day 12) at Fleurhof dam are shown in (Figure 64 a) & b)). The cages still looked clean with very little fouling of the membrane after day 12. The PIM after 12 days in (Figure 65) was still transparent with no sign of precipitation or fouling on the membrane surface. FTIR was used to confirm that the functional groups observed before application of the membrane were still present after 12 days of deployment. The FTIR results are shown in (Figure 77). It was noted that in day 12, the wetland reeds that form part of the dam had been burned but the deployed passive sampler was not affected. This was a reflection of the challenges associated with passive sampler deployments in the field. In addition, the cages can be stolen by thieves for selling to metal scrap yards and that is why much cheaper materials were used.



Figure 64: Picture of PIM-based passive sampler cages a) on day of deployment and b) day 12 at Fleurhof dam

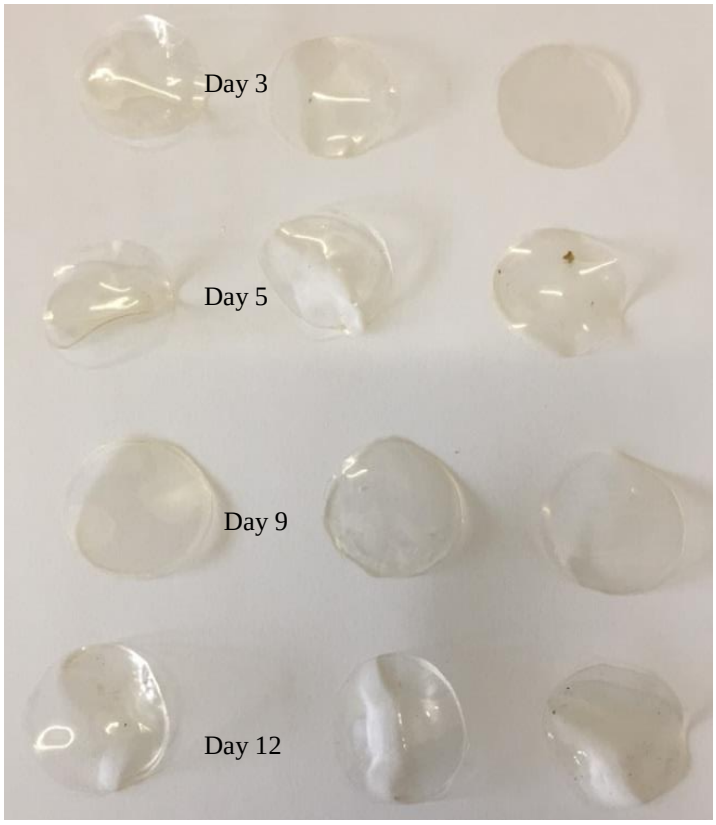

Figure 65: PIM pictures deployed different days at Fleurhof Dam

5.4.6 Comparison of the bioavailable fraction of the metals in PIM sampler deployed in the field and in laboratory from Fleurhof dam water

Passive samplers are often optimised in the laboratory under similar environmental condition so that they can be applied to estimate the bioavailable fraction in the field. Results of the comparison of the PIM-based passive sampler deployed in the field and in the same dam water in the laboratory are shown in (Figure 66). For most metals, the concentrations obtained in the PIM-based passive sampler while in the field and that in the laboratory are comparable. This shows the PIM-based passive sampler calibration in the laboratory was successful and can be used to estimate the bioavailable fraction in the field. However, for Fe (II) and Cu (II), the concentrations obtained in the field were much higher than in the laboratory. This means that taking the water samples from the field and leaving it standing in the laboratory perturbs the water system (Table 3). This probably makes Cu (II) less

bioavailable as it involved in redox reaction. This is why passive samplers are very good at studying the bioavailable fraction after a system has been perturbed.

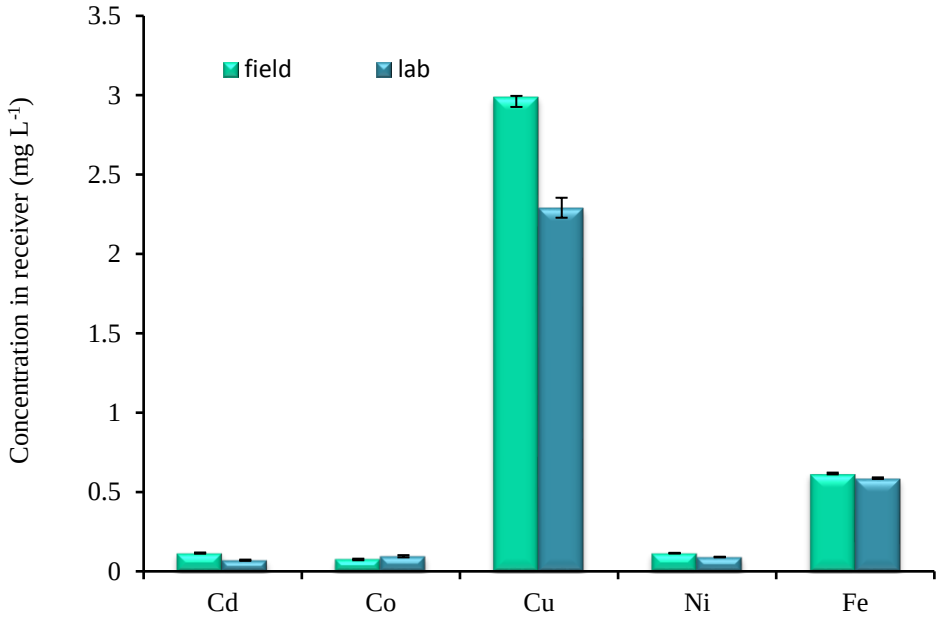

Figure 66: Comparison of the metal ion bioavailable fraction in PIM sampler deployed over 5 days in laboratory and field (n = 3, SD) Source phase: pH: 6.0, Stripping phase: 1mol $L^{-1}HNO_3$, Carrier: 40%, Operation temperature: 25°C, stirring speed: 200 rpm, Thickness of PIM: 150 µm.

5.4.7 Passive sampling vs grab sampling in dam water

To demonstrate the effectiveness of passive sampling, grab samples were collected on the day of deployment and the day of collection of the passive sampler. The results in (Table 5) show the fluctuation of the metal ion concentration from day 1 to day 12 using grab sampling. For example, Ni (II) concentration on day 1 was 0.293 mg L^{-1} while on day 12 it was 0.040 mg L^{-1}. The passive sampler concentration was 0.114 mg L^{-1}. This value lies in the 0.040 - 0.293 mg L^{-1} range. In this regard the passive sampler concentration can be viewed as a time weighted average over the 12-day period. However, in this study grab sampling was done on day of deployment and collection of the passive sampler only. A better comparison

of the results could have been achieved if grab sampling was done every day during the 12-day deployment period.

Table 5: Concentrations of metals ions collected from dam water and in the receiving solution after a 12-day sampling period

Metal ions	Grab sampling concentration (mg L^{-1})	
	Day 1	Day 12
Ni (II)	0.293	0.040
Cu (II)	0.195	0.072
Fe (II)	0.107	0.064
Cd (II)	0.058	0.023
Co (II)	0.073	0.048

5.5 Field deployment of the developed passive sampler in acid mine drainage

5.5.1 Physical-chemical properties of AMD

The concentrations of anions were 18728.76 mg L^{-1} for SO_4^{2-}, 2030.79 mg L^{-1} for PO_4^{2-} and 38.94 mg L^{-1} for Cl^{-}. The pH was 2.83 while conductivity and redox potential was 10.76 Ms cm^{-1} and 346 mV, respectively. The result shows the pH of the AMD was very acidic compared to dam samples (pH 6). The conductivity of the AMD was also about 30 times that of the dam water.

5.5.2 Total metal ion concentrations found AMD

5.5.2.1 Uptake of metal ions in PIM sampler deployed in AMD

The passive sampler's deployment results in AMD are shown in (Figure 67-71). The complexation rate at source phase/PIM interface increases and on the other site of the membrane the decomplexation rate also increases at the PIM/ receiving phase interface. Hence the result shows an increase in the metal ion uptake deployed in AMD. A linear up take was observed between 5 to 12 days. This can be explained by the fact that in acidic solutions the PIM is able to uptake metal ions. The

accumulation of metal ions follows a linear regression. This suggests that PIM-based passive sampler is operating within the kinetic region from day 5 to day 12. Between day 2 and 5 a time lag was observed. The time-lag could be attributed to either the delay caused by the slow diffusion of the analyte across the rate limiting barriers, or the time taken to saturate binding sites in the diffusion limiting membrane before breakthrough is achieved. This time-lag depends on experimental conditions (Aguilar-Mart´ınеza et al., 2008). The metal ions concentration in AMD is as follows: Fe (II) > Ni (II) > Cu (II) > Co (II) > Cd (II). Fe was expected to have high concentration since AMD has a lot of Fe.

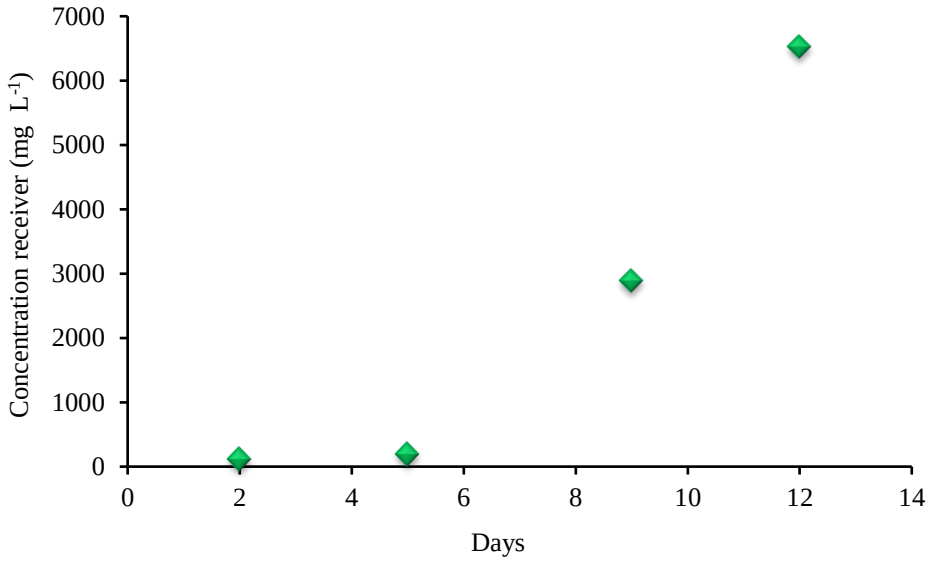

Figure 67: Uptake of iron at AMD site (n = 3, SD) Source phase: pH: 2.83, Stripping phase: 1mol $L^{-1}HNO_3$, Carrier: 40%, Operation temperature: 20ºC, stirring speed: 200 rpm, Thickness of PIM: 150 µm.

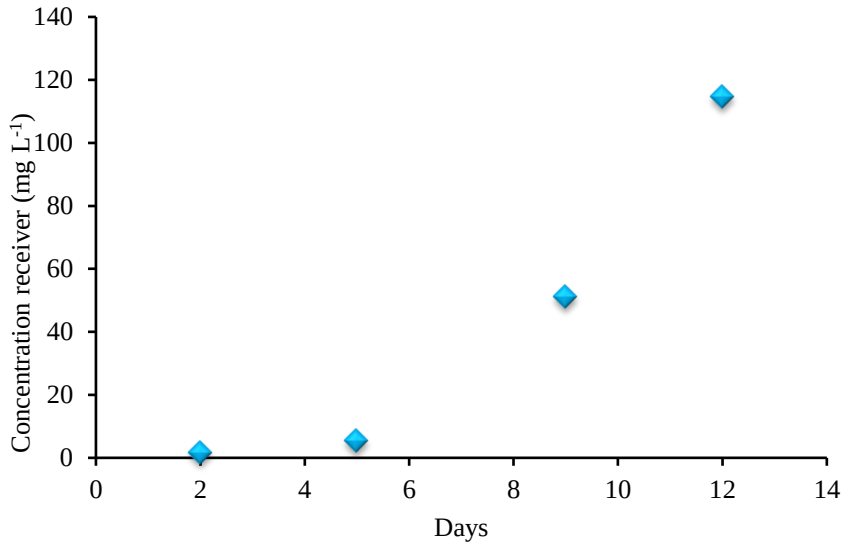

Figure 68: Uptake of copper at AMD site days (n = 3, SD) Source phase: pH: 2.83, Stripping phase: 1mol $L^{-1}HNO_3$, Carrier: 40%, Operation temperature: 20°C, stirring speed: 200 rpm, Thickness of PIM: 150 µm.

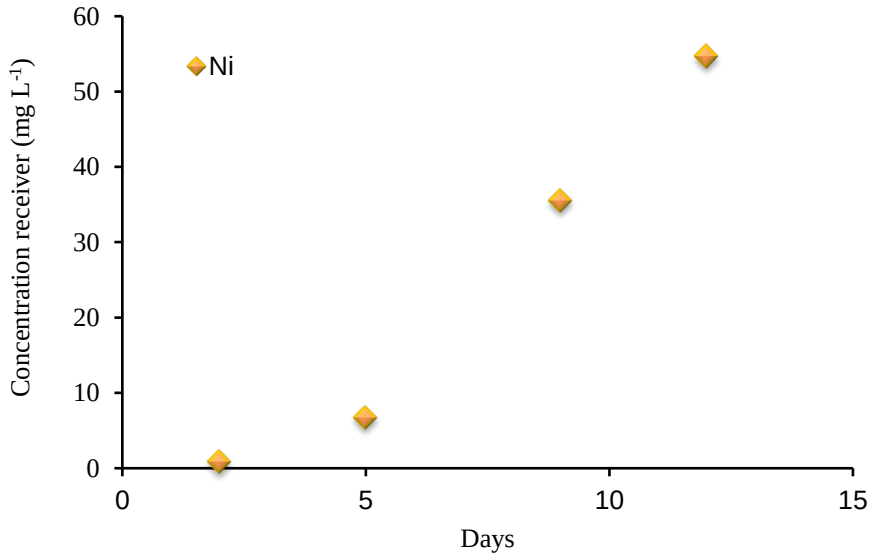

Figure 69: Uptake of nickel at AMD site (n = 3, SD) Source phase: pH: 2.83, Stripping phase: 1mol $L^{-1}HNO_3$, Carrier: 40%, Operation temperature: 20°C, stirring speed: 200 rpm, Thickness of PIM: 150 µm.

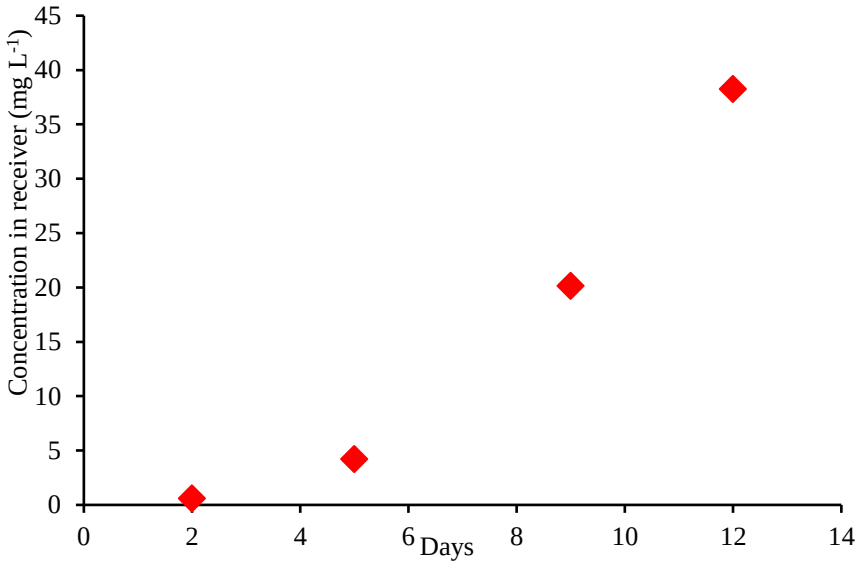

Figure 70: Uptake of cobalt at AMD site (n = 3, SD) Source phase: pH: 2.83, Stripping phase: 1mol $L^{-1}HNO_3$, Carrier: 40%, Operation temperature: 20°C, stirring speed: 200 rpm, Thickness of PIM: 150 µm.

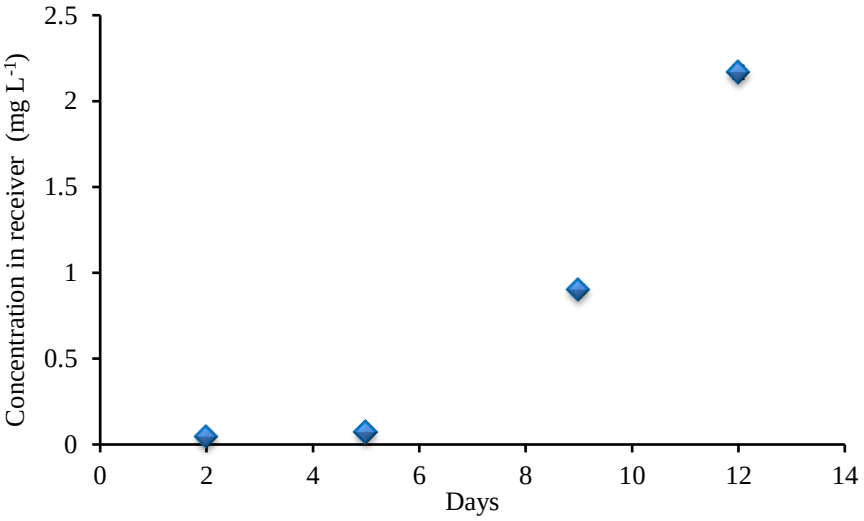

Figure 71: Uptake of cadmium at AMD site (n = 3, SD) Source phase: pH: 2.83, Stripping phase: 1mol $L^{-1}HNO_3$, Carrier: 40%, Operation temperature: 20°C, stirring speed: 200 rpm, Thickness of PIM: 150 µm.

5.5.3 pH changes in the acceptor phase at AMD site

The pH of the acceptor solution was compared before and after passive sampler deployment as in Fleurhof dam. Results in (Figure 72) shows the same trend that was observed in the study where passive sampler was deployed in the Fluerhof dam. The pH of the acceptor solution increased from day 2 up to day 12. The increase in pH again can be attributted to the transport of protons across the acceptor to the source solution.

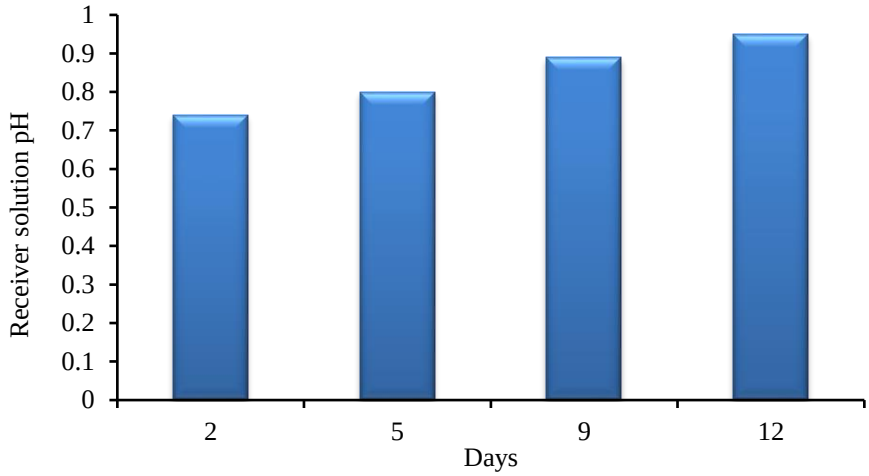

Figure 72: pH of the receiver solution in PIM sampler deployed at diferent days at AMD

5.5.4 Fouling on the passive samplers deployed in AMD

Rusting of the cages on the surface was seen (Figure 73) and fouling on top of a membrane surface after day 12 as shown in (Figure 74). The fouling is caused by the undesirable accumulation of solutes inside the membrane or on the membrane surface which can be attributed to the high hydrophobicity of the polymer. Which then result in a decline in the life span of the membrane, (Khalid et al., 2017). From theory, the PIM-based passive sampler is expected to transport the metal ions across the membrane to receiver phase until the protons in the receiver phase are nearly depleted or pH of the receiver phase is near that of the source phase. It also shows the versatility of PIM based passive sampler.

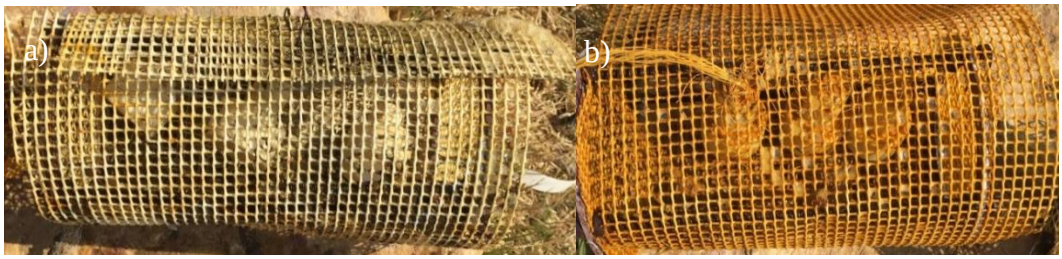

Figure 73: Rusting on cage surface after deployment of a) day 2 and b) day 12 at AMD

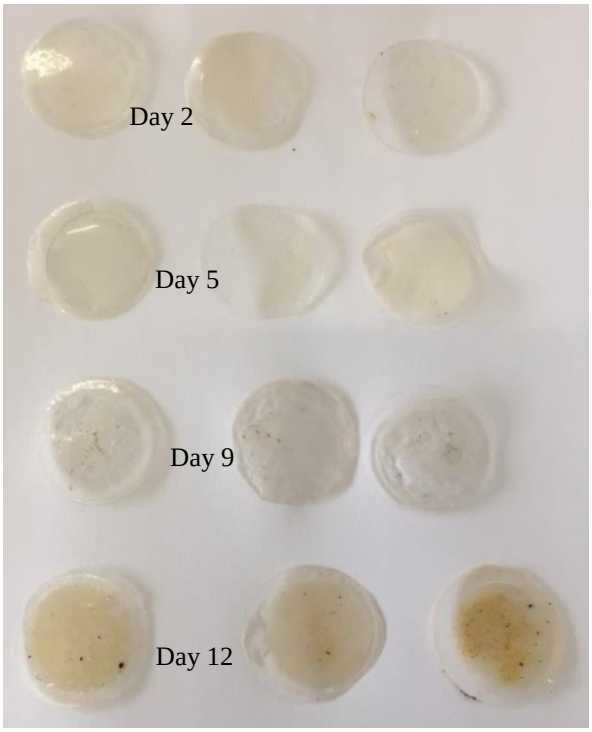

Figure 74: Fouling of polymer inclusion membrane after deployment at AMD site

5.5.5 Comparison of the bioavailable fraction of the metals in PIM sampler deployed in the field and in laboratory from AMD water

Figure 75 shows a comparison of the bioavailable fraction of the metals in the laboratory and in the field with similar exposure for AMD. Results support those in (Figure 53) as less amount of metal ions are bioavailable in the laboratory due to changes in water chemistry and pH. This result also proves that the PIM based passive sampler is more effective with field samples when they are deployed in the field rather than in the laboratory.

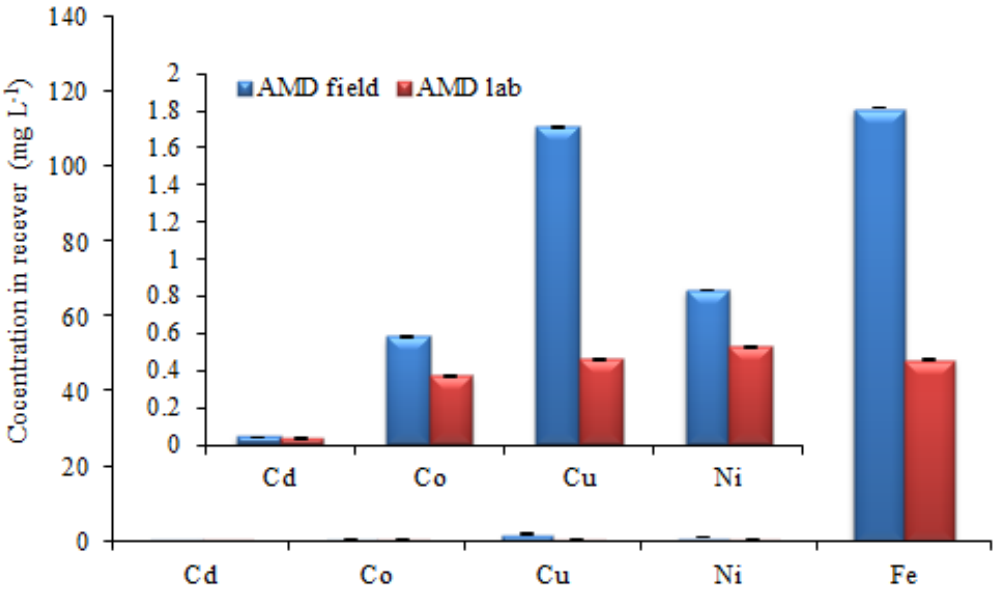

Figure 75: Comparison of uptake of metals in PIM-based passive sampler deployed in AMD water in the laboratory and in the field (n = 3, SD) Source phase: pH: 2.83, Stripping phase: 1mol $L^{-1}HNO_3$, Carrier: 40%, Operation temperature: 20°C, stirring speed: 200 rpm, Thickness of PIM: 150 µm.

5.5.6 Other metal ion uptake by PIM-based passive sampler in AMD for nine days exposure

There are a number of inorganic and organic ligands that may complex the metal ions and thus affect their transport across the membrane in low pH medium water. Figure 76 shows other metal ions that have been up taken by PIM-based passive sampler after day 9 of deployment. This show that the PIM-based sampler with carrier used can extract as much metals as well.

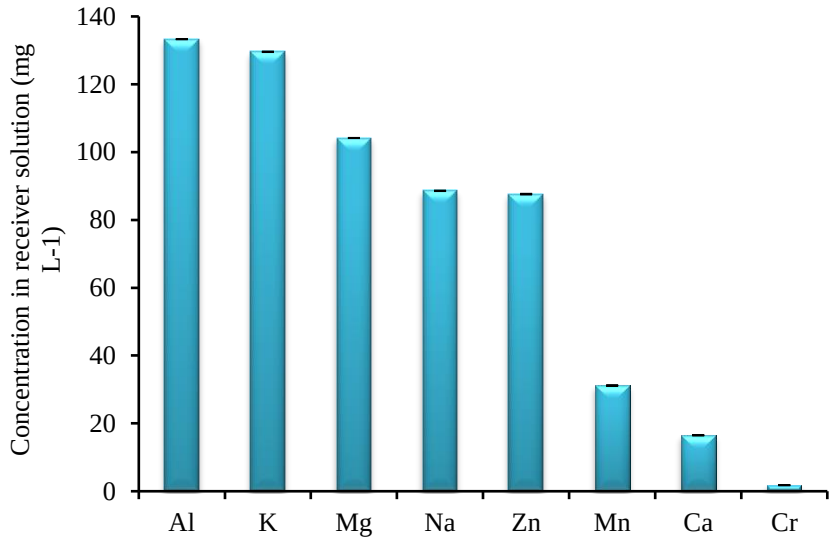

Figure 76: Other metal ions up take by PIM-based passive sampler after day 9 at AMD (n = 3, SD) Source phase: pH: 2.83, Stripping phase: 1mol $L^{-1}HNO_3$, Carrier: 40%, Operation temperature: 20°C, stirring speed: 200 rpm, Thickness of PIM: 150 µm.

5.5.7 Passive sampling vs grab sampling in AMD

The metal ions concentration found at AMD were studied. Passive sampling grab samples were collected on the day of deployment and the day of collection of the passive sampler. The results in (Table 6) show the fluctuation of the metal ion concentration from day 1 to day 12 using grab sampling. For example, Ni (II) concentration on day 1 was 28.70 mg L^{-1} while on day 12 it was 60.41 mg L^{-1}. The passive sampler concentration was 54.65 mg L^{-1}. This value lies in the 28.70 – 60.41 mg L^{-1} range. In this regard the passive sampler concentration can be viewed as a time weighted average over the 12-day period. However, in this study grab sampling was done on day of deployment and collection of the passive sampler only.

Table 6: Concentrations of metals ions collected from AMD and in the receiving solution after a 12-day sampling period

Metal ions	Grab sampling concentration (mg L^{-1})	
	Day 1	Day 12
Ni (II)	28.70	60.41
Cu (II)	14.48	79.67
Fe (II)	1142.50	4386.10
Cd (II)	0.53	1.88
Co (II)	19.07	33.09

5.5.8 Literature comparison of deployment time with other PIMs

Recent analytical applications that make use of PIMs for separation and pre-concentration involving passive diffusion-based transport for metal ions are shown in (Table 7). It is observed that PIM-based passive samplers have been applied for extraction of various metals including trace transition elements, precious lanthanides as well as actinides like uranium. The most common carrier molecule is D2EHPA impregnated in PVC while Aliquot 336 has also been used mainly for metal ions that exist as negative species. Deployment times for effective extraction of the target metals ranges from 3 h to 12 days. The observed wide deployment range might be related to the type and size of the passive sampler. It may also be related to receiver solution used with higher deployment times obtained when HNO3 is used as a receiver solution. While most studies deployed their passive samplers in spiked and simulated wastewater, in our study deployment was done onsite in a dam and AMD-imparted area. Two more studies have also reported deployment in real environmental samplers (Almeida et al., 2014; Guell et al., 2011).

Table 7: Recent examples of PVC/D2EHPA membrane and the maximum number of days the PIMs were deployed

Target species	PIM Composition	Receiving solution	Application	Deployment	Reference
Cu(II), Ni(II), Co(II), Cd(II), Fe(II)	40%D2EHPA/60%PVC	1 mol L^{-1} HNO_3	AMD, Dam water	12 days	Current study
Zn(II)	40%D2EHPA/60%PVC	0.1 mol L^{-1} HNO_3	Urban water	7 days	(Almeida et al., 2014)
Zn(II)	45%D2EHPA/55%PVC	0.1/1 mol L^{-1} HCl	Spiked water	24 h	(Kolev et al., 2009)
Yb(III), Gd(III), La(III)	45%DE2HPA/55%PVC	4.15 mol L^{-1} HCl	Spiked water	48 h	(Croft et al., 2018)
In (III)	69%D2EHPA/29%PVC	6 mol L^{-1} HCL	Spiked water	50 h	(Meng et al., 2017)
U(VI)	45% D2EHPA/55% PVC	6 mol L^{-1} H_2SO_4	Spiked water	50 h	(St John et al., 2012)
Cu(II)	D2EHPA/CTA/DOP	1 mol $L^{-1}H_2SO_4$	e-waste	14 h	(Kavitha et al., 2012)
As(V), As(III)	28.8% CTA /26.2% Aliquat 336/ 45% NPOE	0.1 mol L^{-1} HCl/NaCl	Wastewater	25 h	(R.Guell et al., 2011)
Cr(VI)	40% Aliquat 336/60% PVC	0.05 mol L^{-1} NaOH	Simulated industrial wastewater	3 h	(Gherasim et al., 2011)

5.6 Characterisation of PIM before and after field deployment

5.6.1 FTIR

The PIM membrane consisting of 60 %w/w PVC and with 40 %w/w D2EHPA was taken for FTIR analysis before Figure 77a) and after field exposure at Fleurhof dam Figure 77b) and AMD site Figure 77c) over 12 days. FTIR spectral characterization was used to determine functional groups present in each sample and to check for fouling. The functional groups of the polymer PVC and the carrier D2EHPA are present and this was confirmed by a band at 2959 cm^{-1}, indicating the C-H stretching of the aliphatic C-H group assigned to PVC, while the C-H band also exhibited from 2959 to 2861 cm^{-1} (Salima et al., 2012; Zioui et al., 2017). The peaks at 1228 cm^{-1} and 1018 cm^{-1} correspond to P=O and P-O stretching and are due to D2EHPA. The overlapping of some characteristic bands of PVC/D2EHPA was observed at 2959, 1228 and 1018 cm^{-1}. The PIM before extraction and after extraction at Fluerhof dam had the same intensities and wavelength shifts. This proves that there was no fouling of the membrane at Fleurhof dam after day 12.

After 12 days of metal ions extraction at AMD site, the intensities of the characteristic peaks decrease, suggesting that perhaps part of carrier was lost. The peak of 3239 cm^{-1} corresponding to the O-H stretching vibration could be caused by the depletion of the O-H groups of the D2EHPA molecules (Ling et al., 2017). The change in peaks intensity and shift in wavelength could be attributed to fouling. This may be responsible for the reduction in transport studies for AMD described earlier and may be due to solubility or degradation of the extractant because of the chemical conditions established by the source phase.

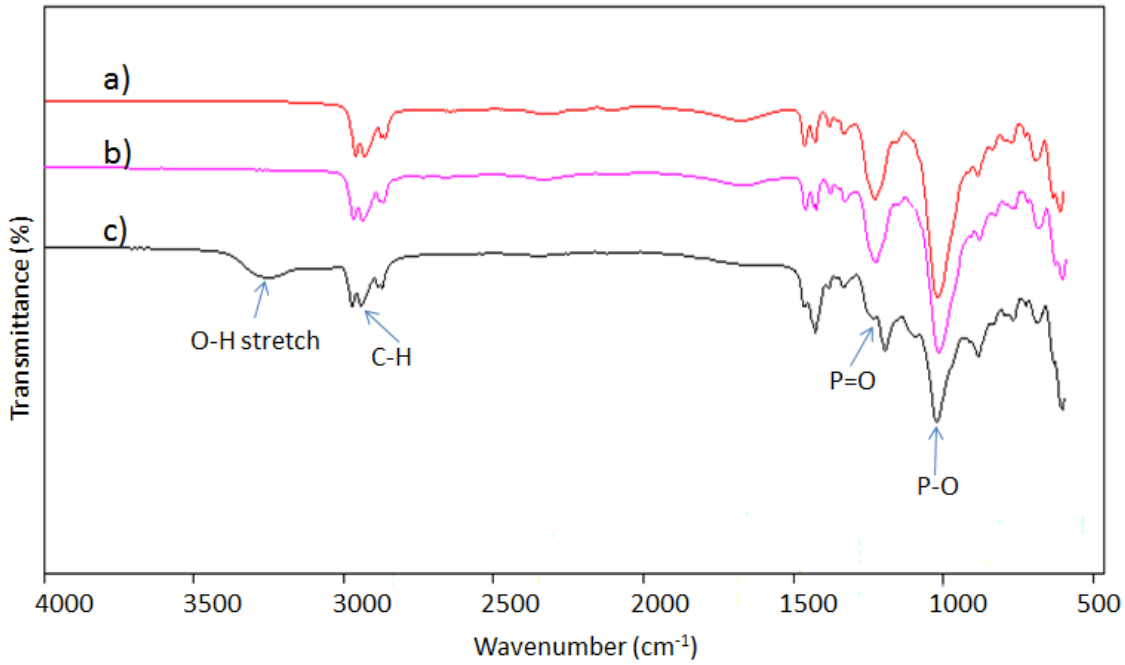

Figure 77: FTIR spectrum of PIM a) before extraction, b) after extraction at Fleurhof dam and c) AMD

5.6.2 AFM

The 2D and 3D AFM images are shown in (Figure 78, 79 & 80) which indicates the carrier distribution in the investigated membranes, after the evaporation of THF, the membrane is homogeneous throughout the entire surface. AFM has proved to be a useful tool in detecting the leakage of D2EHPA and the extracted complex from the surface of a PVC-based membrane. The performance of AFM analysis enables quantitative determination of membranes mean roughness (R_a) and membrane mean square roughness (R_q) (Ghazanfari et al., 2017). The membrane R_a value difference after extraction at Fluerhof dam was 1.00 nm while the (R_a) value at AMD was 102.28nm respectively. The lower R_a values for membrane after extraction at Fluerhof dam (Figure 83) indicate that the uniform parts of the membranes have well-defined membrane structure. A significant difference was noticeable with the AMD where high R_a values showed that the membrane structure have been deformed (Figure 84). The porosity and roughness of the membranes is determined by the kind and concentration of the ion carrier (Radzyminska-lenarcik et al, 2015).

Mean square roughness (R_q) values for membranes before and after extraction at Fleurhof dam and AMD site were calculated in (Table 8). There was a noticeable increase of mean square roughness after membrane extraction at AMD site; this confirms that there was membrane fouling with AMD samples (Figure 84). The metal ions transport happening within the membrane penetrates its irregular surface and caused its roughness. Membranes with rough surface are prone to fouling. Surface roughness is considered as the most important factor to improve antifouling ability of the membranes.

Table 8: Mean square roughness values after 12 days of sampling at Fleurhof dam and AMD

	Before extraction	After extraction	Difference
Dam $R_{q,\ nm}$	12.42	13.42	1.00
AMD $R_{q,\ nm}$	12.42	114.70	102.28

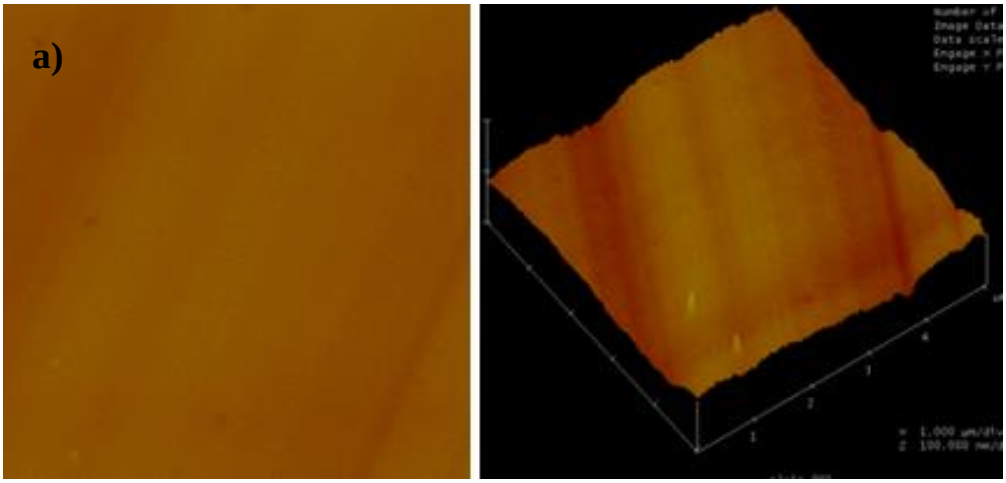

Figure 78: 2D and 3D-AFM images of PIM before extraction

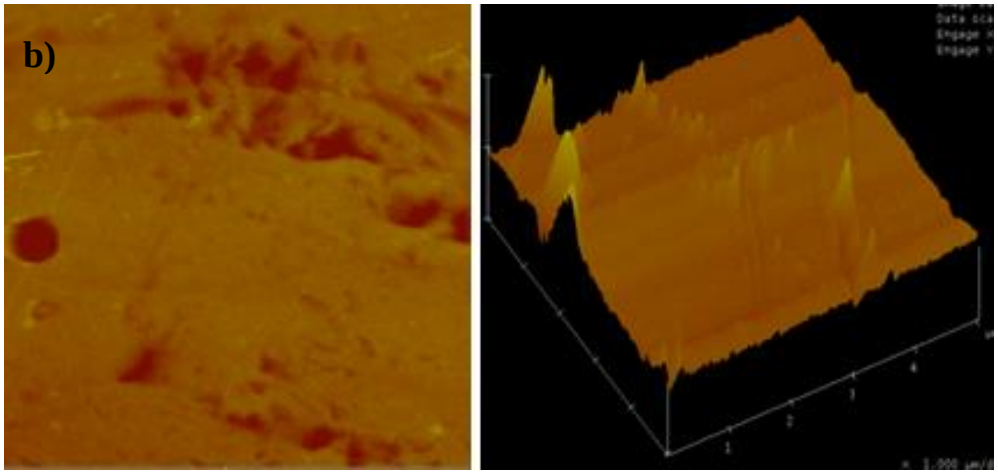

Figure 79: 2D and 3D-AFM images of PIM after 12 days extraction at Fleurhof dam

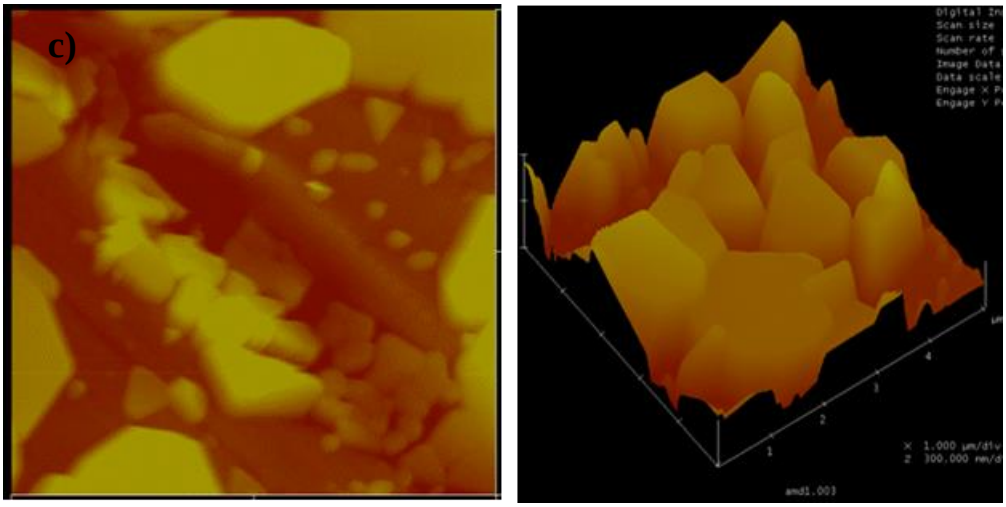

Figure 80: 2D and 3D-AFM images of PIM after 12 days extraction at AMD site

CHAPTER 6

This chapter highlights the Design of the newly developed PIM-based passive sampler the efficiency of the synthesized polymer inclusion membrane and their potential application in Fleurhof dam and acid mine drainage. Other potential future researches to improve the developed PIM-based passive sampler are also highlighted.

6 Conclusions and recommendations

6.1 Conclusions

A PIM-based passive sampler has been successful designed, optimised and field-tested in studying the uptake of metals in surface and AMD waters. The sampler holders made out of PTFE and screwed together proved to be very rugged and able to with stand harsh environmental conditions. The use of solid PIM barrier in the new sampler proved to be very stable with insignificant leaching of the membrane liquid phase. In addition, since that barrier has a permanent acidic surface from H^+ involved in driving the process and from D2EHPA used as carrier ensured bactericidal properties in the sampler (Almeida et al., 2014). This prevented fouling of the membrane and could be reused especially in surface water. The uptake of targets was linear from 5-12 days in deionised water, surface water and AMD. Thus, the developed PIM sampler is very versatile and rugged as it was able to tolerate harsh environment from AMD at pH 3 with high amounts of metal ions and anions. It was also able to uptake a lot of other metal ions. The PIM-based passive sampler was also able to relate the observed physical-chemical changes in the water during deployment to the uptake kinetics. This is very important as it can be used to study the transport and fate of the target metals in an aquatic system after outside perturbation.

6.2 Future studies and recommendations

Projected and currently running projects as well as studies aimed at testing the versatility and applicability of the developed passive sampler. The study on PIM-based passive sampler was found that the sampler is very versatile and rugged.

The following are recommended;

- Using the optimised PIM to quantify the bioavailable fractions of the target metals in both surface and AMD. In the study, sampling rates have been calculated as first trial but detailed determination of sampling rates is needed and using these to determine the amount of bioavailable fractions in the waters.

- The passive sampler demonstrated that it could take many other metals along with target metals. Thus, it is proper to check whether some of these are linearly taken in the sampler and what is the maximum deployment time for them before equilibrium is reached.
- Seasonal changes leads to the perturbation of the aquatic systems and this affects metal transport and behaviour. Thus, deployment of the passive sampler in various seasons to study the transport and fate of metals in mining polluted water system within South Africa could be of interest. In summer, surface water in these areas has high evaporation rate and the water chemistry is dramatically affected as seen from the preliminary study.
- Building pilot plant versions of the PIM sampler so that it can be used for passive remediation of polluted waters. This means designing and machining an upscaled version of the lab based version say moving from 5.5 ml to 2500 ml.

References

Abdul-wahab, S.A., Marikar, F.A., 2012. The environmental impact of gold mines : pollution by heavy metals. Cent. Eur. J. Eng. 2, 304–313.

Aguilar-Martıneza,. Palacios-Corvilloa M.A,. Greenwood R, Mills G.A. , Vranad B, Gomez.-Gomez M.M., 2008. Calibration and use of the Chemcatcher passive sampler for monitoring organotin compounds in water. Anal. Chim. Acta 618, 157–167.

Akcil A, Koldas. S, 2006. Acid Mine Drainage (AMD): Causes , treatment and case studies. J. Clean. Prod. 14, 1139–1145.

Allan I.J., Knutsson, J., Guigues N., Mills, G.A., Fouillac, A., 2008. Chemcatcher and DGT passive sampling devices for regulatory monitoring of trace metals in surface water. J. Environ. Monit. 10, 821–829.

Allan J.I., Knutsson J., Guigues N., Mills, G., Fouillac, A.M., Richard, G., 2007. Evaluation of the Chemcatcher and DGT passive samplers for monitoring metals with highly fluctuating water concentrations. J. Environ. Monit. 9, 672–681.

Almeida M.I.G.S., Cattrall R.W., Kolev, S.D., 2017. Polymer inclusion membranes (PIMs) in chemical analysis - A review. Anal. Chim. Acta 987, 1–14.

Almeida M.I.G.S., Cleopas C., Pettigrove J.V., Cattrall, R.W., Kolev, S.D., 2014. Development of a passive sampler for Zinc (II) in urban pond waters using a polymer inclusion membrane. Environ. Pollut. 193, 233–239

Almeida, M.I.G.S., Cattrall, R.W., Kolev, S.D., 2012. Recent trends in extraction and transport of metal ions using polymer inclusion membranes (PIMs). J. Memb. Sci. 415–416, 9–23.

Almeida, M.I.G.S., Silva, A.M.L., Coleman, R.A., Pettigrove, V.J., Cattrall, R.W., Kolev, S.D., 2016. Development of a passive sampler based on a polymer inclusion membrane for total ammonia monitoring in freshwaters. Anal. Bioanal. Chem. 408, 3213–3222.

Amico, E.D., Mazzocchi, M., Cavalca, L., Allievi, L., 2008. Assessment of bacterial community structure in a long-term copper-polluted ex-vineyard soil. Microbiol. Res. 163, 671–683.

Arous, O., Amara, M., Kerdjoudj, H., 2010. Selective Transport of Metal Ions Using Polymer Inclusion Membranes Containing Crown Ethers and Cryptands. Arab. J. Sci. Eng. 35, 79–93.

Aslibekian O., 2003. environmetal risk assesment of metals contamination of soils and plants in the vicinity of a lead-zinc mine Korea. enviromental geochem 25, 247–266.

Baczynska Monika, Magdalena. Regel-Rosocka, Marek Nowicki, M.W., 2015. Effect of the structure of polymer inclusion membranes on Zn (II) transport from chloride aqueous solutions. J. Appl. Polym. Sci. Appl. 42319, 1–11.

Baytak, S., Turker, R.A., 2009. Determination of chromium, cadmium and manganese in water and fish samples after preconcentration using penicillium digitatum immobilized on pumice stone. Clean 4–5, 314–318.

Benosmane. N, Boutemeur. B, Hamdi, B, 2018- Removal of phenol from aqueous solution using polymer inclusion membrane based on mixture of CTA and CA, Applied Water Science, 8, 1-6

Benosmanea Nadjib, Safouane M. Hamdib, Maamar Hamdia, B.B., 2009. Selective transport ofmetal ions across polymer inclusion membranes (PIMs) containing calix[4]resorcinarenes. Sep. Purif. Technol. 65, 211–219.

Bringas, E., Iba, R., Ortiz, I., Rom, M.F.S., 2010. Liquid membrane technology : fundamentals and review of its applications. J Chem Technol Biotechnol 85, 2–10.

Brown R.H, R.P Harvey, C.J Purnell, Saunders K., 1984. A Diffusive Sampler Evaluation Protocol. Am. Ind. Hyg. Assoc. J. 45, 67–75.

Camden-Smith, B., Pretorius, P., Camden-Smith, P., Tutu, H., 2015. Chemical transformations of metals leaching from gold tailings, in: Agreeing on Solutions for More Sustainable Mine Water Management-Proceedings of the 10th ICARD and IMWA Annual Conference, Santiago, Chile.

Casadellà, A., Schaetzle, O., Nijmeijer, K., Loos, K., 2016. Polymer inclusion membranes (PIM) for the recovery of potassium in the presence of competitive cations. Polymers (Basel). 8, 1–14. Cempel, M., Nikel, G., 2006. Nickel : A Review of Its Sources and Environmental Toxicology 15, 375–382.

Cempel M, Nikel G. 2006 Nickel: A Review of Its Sources and Environmental Toxicology Polish J. of Environ. Stud. Vol. 15, No. 3, 375-382.

Chimuka Luke, Cukrowska Ewa, Jönsson Jan Åke, 2004, Why liquid membrane extraction is an attractive alternative in sample preparation Pure Appl. Chem., Vol. 76, No. 4, pp. 707–722.

Cho, Y., Cattrall, R.W., Kolev, S.D., 2018. A novel polymer inclusion membrane based method for continuous clean-up of thiocyanate from gold mine tailings water. J. Hazard. Mater. 341, 297–303.

Collins, R.N., Kinsela, A.S., 2010. Chemosphere The aqueous phase speciation and chemistry of cobalt in terrestrial environments. Chemosphere 79, 763–771.

Collins, R.N., Kinsela, A.S., 2010. The aqueous phase speciation and chemistry of cobalt in terrestrial environments. Chemosphere 79, 763–771.

Concas, A., Ardau, C., Cristini, A., Zuddas, P., Cao, G., 2006. Mobility of heavy metals from tailings to stream waters in a mining activity contaminated site. Chemosphere 63, 244–253.

Croft, C.F., Almeida, M.I.G.S., Cattrall, R.W., Kolev, S.D., 2018. Separation of lanthanum (III), gadolinium (III) and ytterbium (III) from sulfuric acid solutions by using a polymer inclusion membrane. J. Memb. Sci. 545, 259–265.

Dabrin, A., Ghestem, J., Uher, E., Gonzalez, J., Allan, I.J., Schintu, M., 2016. Metal measurement in aquatic environments by passive sampling methods : Lessons learning from an in situ intercomparison exercise. Environ. Pollut. 208, 299–308.

Davison W.,.Zang., H 1994. In situ speciation measurements of trace components in natural waters using thin-film gels. Nature 367, 546–548.

Davison, W., Zhang, H., 2012. Progress in understanding the use of diffusive gradients in thin films (DGT) – back to basics. Environ. Chem. 9, 1–13.

Donkor A. K,. Bonzongo J. J, Nartey V. K,. Adotey D.K., 2005. An Heavy Metals in Sediments of the Gold Mining Impacted Pra River Basin, Ghana,West Africa. Soil Sediment Contam. 14, 479–2005.

Duruibe, J.O., Ogwuegbu, M.O.C., Egwurugwu, J.N., 2007. Heavy metal pollution and human biotoxic effects. Int. J. Phys. Sci. 2, 112–118.

Edwards, K.J., Bond, P.L., Gihring, T.M., Banfield, J.F., 2000. An Archaeal Iron-Oxidizing Extreme Acidophile Important in Acid Mine Drainage. Science (80-.). 287, 1796–1800.

Eljaddi, T., Lebrun, L., Hlaibi, M., 2017. Review on mechanism of facilitated transport on liquid membranes. J. Membr. Sci. Res. 3, 199–208.

Elumalai, Vetrimurugan B. and E.L, 2017. Human Exposure Risk Assessment Due to Heavy Metals in Groundwater by Pollution Index and Multivariate Statistical Methods : A Case Study from. Water 9, 234.

España J S, 2014. The Behavior of Iron and Aluminum in Acid Mine Drainage : The Behavior of Iron and Aluminum in Acid Mine Drainage : Speciation , Mineralogy , and. Thermodyn. Solubility Environ. 137–150.

Fashola, M.O., Ngole-jeme, V.M., Babalola, O.O., 2016. Heavy Metal Pollution from Gold Mines : Environmental Effects and Bacterial Strategies for Resistance. Int. J. Environ. Res. Public Health 13, 1047.

Fayiga, A.O., 2005. Arsenic uptake by two hyperraaccumulator ferns from four arsenic contamination soils. Water. Air. Soil Pollut. 168, 71–89.

Franco-Hernandez, 2010. heavy metals concentrations in plants growing on mine tailng in central Mexico. Bioresour. Technol. 101, 3864–3869.

Fu Fenglian, Q.W., 2011. Removal of heavy metal ions from wastewaters: A review. J. Environ. Manage. 92, 407–418.

Gajda, B., 2012. The application of polymer inclusive membranes for removal of heavy metal ions from waste solutions. J. Achiev. Mater. Manuf. Eng. 55, 673–678.

Garcia-Rodríguez, A., Fontàs, C., Matamoros, V., Almeida, M.I.G.S., Cattrall, R.W., Kolev, S.D., 2016. Development of a polymer inclusion membrane-based

passive sampler for monitoring of sulfamethoxazole in natural waters. Minimizing the effect of the flow pattern of the aquatic system. Microchem. J. 124, 175–180.

Garcia-Rodríguez, A., Matamoros, V., Kolev, S.D., Fontàs, C., 2015. Development of a polymer inclusion membrane (PIM) for the preconcentration of antibiotics in environmental water samples. J. Memb. Sci. 492, 32–39.

Garcia-Rodríguez, A., Matamoros, V., Kolev, S.D., Fontàs, C., 2015. Development of a polymer inclusion membrane (PIM) for the preconcentration of antibiotics in environmental water samples. J. Memb. Sci. 492, 32–39.

Gega, J., Otrembska, P., 2014. Separation of Ni (II) and Cd (II) Ions with Supported Liquid Membranes (SLM) using D2EHPA as a Carrier Separation of Ni (II) and Cd (II) Ions with Supported Liquid Membranes (SLM) using D2EHPA as a Carrier. Sep. Sci. Technol. 49, 1756–1760.

Getaneh W, 2002. Metal contamination of the environment by placer and primary gold minning in ADOLA region of southern ETHOPIA. Environ. Geol. 50, 339–352.

Ghazanfari, D., Bastani, D., Mousavi, S.A., 2017. Journal of Water Process Engineering Preparation and characterization of poly (vinyl chloride) (PVC) based membrane for wastewater treatment. J. Water Process Eng. 16, 98–107.

Gherasim, C.-V., Cristea, M., Griogoras, C.-V., Bourceanu, G., 2011. New polymer inclusion membrane. Preparation and characterization. Dig. J. Nanomater. Biostructures 6, 1499–1508.

Gherasim, C.V.I. Cristea, M., Grigoras, C.V., Bourceanu, G., 2011. New Polymer Inclusion Membrane, Preparation and Characterization. Dig. J. Nanomater. Biostructures 6, 1499–1508.

Gorecki Tadeusz, J.N., 2002. Passive sampling. Trends Anal. Chem. 21, 276–291.

Grande, J.A., Zouiten, C., Valente, T., Destrigneville, C., Pokrovsky, O.S., 2018. Are Cu isotopes a useful tool to trace metal sources and processes in acid mine drainage (AMD) context? Chemosphere 193, 1071–1079.

Guell R., Anticó, E., Kolev, S.D., Benavente, J., Salvadó, V., Fontàs, C., 2011. Development and characterization of polymer inclusion membranes for the separation and speciation of inorganic As species. J. Membr. Sci. j 383, 88–95.

Gunatilake, S.K., 2015. Methods of Removing Heavy Metals from Industrial Wastewater. J. Multidiscip. Eng. Sci. Stud. 1, 12–18.

Gupta V. K.,. Nayak A,.Agarwal S., 2015. Bioadsorbents for remediation of heavy metals : Current status and their future prospects. Environ. Eng. Res 20, 1–18.

Javed, M., Usmani, N., 2013. Assessment of heavy metal (Cu , Ni , Fe , Co , Mn , Cr, Zn) pollution in effluent dominated rivulet water and their effect on glycogen metabolism and histology of Mastacembelus armatus. Spring Plus 2, 1–13.

Javed, M., Usmani, N., 2013. Assessment of heavy metal (Cu , Ni , Fe , Co , Mn , Cr, Zn) pollution in effluent dominated rivulet water and their effect on glycogen metabolism and histology of Mastacembelus armatus. Spring Plus 2, 1–13.

Kagaya, S., Ryokan, Y., Cattrall, R.W., Kolev, S.D., 2012. Stability studies of poly(vinyl chloride)-based polymer inclusion membranes containing Aliquat 336 as a carrier. Sep. Purif. Technol. 101, 69–75.

Kavitha, N., Palanivelu, K., 2012. Recovery of copper(II) through polymer inclusion membrane with di (2-ethylhexyl) phosphoric acid as carrier from e-waste. J. Memb. Sci. 415–416, 663–669.

Kaya, A., Alpoguz, H.K., Yilmaz, A., 2013. Application of Cr(VI) Transport through the Polymer Inclusion Membrane with a New Synthesized Calix[4]arene Derivative. Eng. Chem. Res 54, 5428−5436.

Kebiche-senhadji, O., Mansouri, L., Tingry, S., Seta, P., Benamor, M., 2008. Facilitated Cd (II) transport across CTA polymer inclusion membrane using anion (Aliquat 336) and cation (D2EHPA) metal carriers. J. Memb. Sci. 310, 438–445.

Khalid, A., Ibrahim, A., Al-Hamouz, O.C.S., Laoui, T., Benamor, A., Atieh, M.A., 2017. Fabrication of polysulfone nanocomposite membranes with silver-doped carbon nanotubes and their antifouling performance. J. Appl. Polym. Sci. 134.

Kiswandono, A.A., Siswanta, D., Aprilita, N.H., Santosa, S.J., Hayashita, T., 2013. Extending the life time of polymer inclusion membrane containing copoly(eugenol-DVB) as carrier for phenol transport. Indones. J. Chem. 13, 254–261.

Kocherginsky, N.M., Yang, Q., Seelam, L., 2016. Recent advances in supported liquid membrane technology. Sep. Purif. Technol. 53, 171–177.

Kolev, S.D., Baba, Y., Cattrall, R.W., Tasaki, T., Pereira, N., Perera, J.M., Stevens, G.W., 2009. Solid phase extraction of zinc(II) using a PVC-based polymer inclusion membrane with di(2-ethylhexyl)phosphoric acid (D2EHPA) as the carrier. Talanta 78, 795–799.

Kolev, S.D., John, A.M.S., Cattrall, R.W., 2013. Mathematical modeling of the extraction of uranium (VI) into a polymer inclusion membrane composed of PVC and di- (2-ethylhexyl) phosphoric acid. J. Memb. Sci. 425–426, 169–175.

Konczyk, J., Kozlowski, C., Walkowiak, W., 2010. Removal of chromium(III) from acidic aqueous solution by polymer inclusion membranes with D2EHPA and Aliquat 336. Desalination 263, 211–216.

León Loreto, León Gerardo, 2016. Kinetic Study of Copper (II) Simultaneous Extraction / Stripping from Aqueous Solutions Transport Mechanisms. Metals (Basel). 6, 2–8.

Li, W., Zhao, H., Teasdale, P.R., John, R., Zhang, S., 2002. Application of a cellulose phosphate ion exchange membrane as a binding phase in the diffusive

gradients in thin films technique for measurement of trace metals. Anal. Chim. Acta 464, 331–339.

Li, Y., Wang, D., Hsien, T., Chan, K., Lai, J., 2017. Polymer Inclusion Membranes with Strip Dispersion. water 9, 399.

Ling, Y.Y, Bukhari, F., Suah, M., 2017. Extraction of malachite green from wastewater by using polymer inclusion membrane. Biochem. Pharmacol. 5, 785–794.

Luptakova, A., Balintova, M., Jencarova, J., Macingova, E.V.A., Prascakova, M., 2010. Metals Recovery From Acid Mine Drainage. Nov. Biotechnol. 10–1, 23–32.

Macomber, L., Hausinger, R.P., Macomber, L., 2011. Mechanisms of nickel toxicity in microorganisms w. metallomics 3, 1153–1162.

Mahanty, B., Mohapatra, P.K., Raut, D.R., Das, D.K., Behere, P.G., Afzal, M., Verboom, W., 2016. Polymer Inclusion Membrane Containing a Tripodal Diglycolamide Ligand: Actinide Ion Uptake and Transport Studies. Ind. Eng. Chem. Res. 55, 2202–2209.

Masaaki Sugiura, M.K.& S.U., 1987. Effect of Plasticizer on Carrier-Mediated Transport of Zinc Ion through Cellulose Triacetate Membranes. Sep. Sci. Technol. 22, 2263–2268.

Matshusa, K., Ogola, J., Klaus, M., 2012. Dispersion of Metals at Louis Moore Gold Tailings Dam, Limpopo Province, South Africa. Int. Mine Water Assoc. Conference, 334A–334E.

Meng, X., Wang, C., Zhou, P., Xin, X., Wang, L., 2017. Transport and selectivity of indium through polymer inclusion membrane in hydrochloric acid medium. Front. Environ. Sci. Eng 11.

Mengistu, H., Roeyset, O., Tessema, A., Abiye, T.A., Demlie, M.B., 2012. Diffusive gradient in thin-films (DGT) as risk assessment and management tools in the central witwatersrand goldfield, South Africa. Water SA 38, 15–22.

Miege, C., Nicolas, M., Allan, I., Dulio, V., Foppes, S., Tiixier, C., Vermeirssen, E., Brant, J., Toole, S.O., Lardy-fontan, S., Ghestem, J., Gonzalez, J., Coquery, M., Vrana, B., 2015. Position paper on passive sampling techniques for the monitoring of contaminants in the aquatic environment – Achievements to date and perspectives. Trends Environ. Anal. Chem. 8, 20–26.

Minello, M.C.S., Paçó, A.L., Martines, M.A.U., Santos, A. Dos, Padilha, P.M., Castro, G.R., Clara, M., Paçó, A.L., Martines, M.A.U., Santos, A. Dos, Padilha, P.M., Sediment, G.R.C., Martines, M.A.U., 2009. Toxic/hazardous substances and environmental engineering sediment grain size distribution and heavy metals determination in a dam on the Paraná river at Ilha Solteira, Brazil. J. Environ. Sci. Heal. 44, 861–865.

Minina Elena, 2015, PASSIVE SAMPLING TECHNOLOGIES: Current State and Future Challenges Environmental

Mocq, J., Hare, L., 2018. Influence of acid mine drainage , and its remediation , on lakewater quality and Benthic invertebrate communities. Water Air Soil Pollut. 229, 1–15.

Modoi, O., Roba, C., Török, Z., Ozunu, A., 2014. Environmental risks due to heavy metal pollution of water resulted from mining wastes in NW Romania. Environ. Eng. Manag. J. 13, 2325–2336.

Mohapatra, P.K., Lakshmi, D.S., Mohan, D., Manchanda, V.K., 2006. Uranium pertraction across a PTFE flatsheet membrane containing Aliquat 336 as the carrier. Sep. Purif. Technol. 51, 24–30.

Mostazo G., Vera R. , Fontàs C, Anticó E, 2017. Polymer inclusion membranes as a new tool for Zn speciation: influence of the membrane composition in diffusional fluxes. 15th Int. Conf. Environ. Sci. Technol. 2–4.

Mutlu, E., Demir, T., Yanik, T., Sutan, N.A., 2017. Determination of environmentally relevant water quality determination of environmentally relevant water quality parameters in Serefiye dam - Turkey. Fresenius Environ. Bull. 25, 5812–5818.

Namieśnik, J., Zabiegała, B., Kot-Wasik, A., Partyka, M., Wasik, A., 2005. Passive sampling and/or extraction techniques in environmental analysis: A review. Anal. Bioanal. Chem. 381, 279–301.

Nazir, R., Khan, M., Masab, M., Rehman, H.U.R., Rauf, N.U.R., 2015. Accumulation of heavy metals (Ni, Cu, Cd, Cr, Pb, Zn, Fe) in the soil , water and plants and analysis of physico-chemical parameters of soil and water collected from Tanda dam kohat. J. Pharm. Sci. Res. 7, 89–97.

Nghiem, L.D., Mornane, P., Potter, I.D., Perera, J.M., Cattrall, R.W., Kolev, S.D., 2006. Extraction and transport of metal ions and small organic compounds using polymer inclusion membranes (PIMs). J. Memb. Sci. 281, 7–41.

Nyoni, H., Chimuka, L., Vrana, B., Cukrowska, E., 2011. Membrane assisted passive sampler for triazine compounds in water bodies — Characterization of environmental conditions and field performance. Anal. Chim. Acta 694, 75–82.

Nyoni, H., Chimuka, L., Vrana, B., Cukrowska, E., Tutu, H., 2010. Optimisation of the membrane-assisted passive sampler and its comparison with solid phase extraction technique. Water SA 36, 501–508.

O'Rourke, M., Cattrall, R.W., Kolev, S.D., Potter, I.D., 2009. The extraction and transport of organic molecules using polymer inclusion membranes. Solvent Extr. Res. Dev., Jpn. 16, 1–12.

Ocampo, A.L., Aguilar, J.C., Rodríguez de San Miguel, E., Monroy, M., Roquero, P., de Gyves, J., 2009. Novel proton-conducting polymer inclusion membranes. J. Memb. Sci. 326, 382–387.

Pawel R., Rajewski J.,.Gierycz P., 2015. Advantages and disadvantages of SLM and PIM systems used for Chromium(III) separation from aqueous solutions. Pol. J. Environ. Stud. 24, 1283–1290.

Pesavento, M., Alberti, G., Biesuz, R., 2009. Analytica Chimica Acta Analytical methods for determination of free metal ion concentration , labile species fraction and metal complexation capacity of environmental waters : A review. Anal. Chim. Acta J. 631, 129–141.

Prashanth, L., Kattapagari, K.K., Chitturi, R.T., 2015. A review on role of essential trace elements in health and disease. J. Dr. NTR Univ. Heal. Sci. 4, 75–85.

Radzyminska-lenarcik, E., Ulewicz, M., 2015. The use of the steric effect of the carrier molecule in the polymer inclusion membranes for the separation of cobalt II), nickel (II), copper (II), and zinc II) ions. Polish J. Chem. Technol. 17, 1–6.

Rajewski J P., 2016. Abexperimental analysis of the transport mechanism of the Chromium (III) ions in the polymer inclusion memebrane system stract. Maint. Probl. 108, 105–118.

Ranjard, L., Echairi, A., Nowak, V., Lejon, D.P.H., Nouai, R., 2006. Field and microcosm experiments to evaluate the effects of agricultural Cu treatment on the density and genetic structure of microbial communities in two different soils. Fed. Eur. Microbiol. Soc. 58, 303–315.

Resina, M., Macan, J., Gyves, J. De, Munoz, M., 2006. Zn (II), Cd (II) and Cu (II) separation through organic – inorganic Hybrid Membranes containing di- (2-ethylhexyl) phosphoric acid or di- (2-ethylhexyl) dithiophosphoric acid as a carrier. J. of Membrane Sci. 268, 57–64.

Roebbert, Y., Rabe, K., Lazarov, M., Schuth, S., Schippers, A., Dold, B., Weyer, S., 2018. Fractionation of Fe and Cu isotopes in acid mine tailings : Modi fi cation and application of a sequential extraction method. Chem. Geol. 493, 67–79.

Salima, A., Ounissa, K., Lynda, M., Mohamed, B., 2012. Cationic dye (MB) removal using polymer inclusion membrane (PIMs). Procedia Eng. 33 33, 38–46.

Santisteban, M., Grande, J.A., de la Torre, M.L., Valente, T., Perez-Ostale, E., Garcia-Parez, M., 2015. Study of the transit and attenuation of pollutants in a water reservoir receiving acid mine drainage in the Iberian Pyrite Belt (SW Spain). Water Supply 16, 128–134.

Sgarlata, C., Arena, G., Longo, E., Zhang, D., Yang, Y., Bartsch, R.A., 2008. Heavy metal separation with polymer inclusion membranes. J. Memb. Sci. 323, 444–451.

Shahira, N., Zulkefeli, W., Weng, S.K., Syazana, N., Halim, A., 2018. Removal of Heavy Metals by Polymer Inclusion Membranes. Curr. Pollut. Rep. 4, 84–92.

Shokri J, Ardejani B, D, Ramazi, F H., 2016. Environmental geochemistry and acid mine drainage evaluation of an abandoned coal waste pile at the Alborz-Sharghi coal washing plant, NE Iran. Nat. Resour. Res. 25, 347–363.

Sim, S.F., Ling, T.Y., Nyanti, L., Gerunsin, N., Wong, Y.E., Kho, L.P., 2016. Assessment of heavy metals in water, sediment, and fishes of a large tropical hydroelectric dam in Sarawak, Malaysia. J. Chem. 1–10.

Simate, G.S., Ndlovu, S., 2014. Acid mine drainage: Challenges and opportunities. J. Environ. Chem. Eng. 2, 1785–1803.

Singh, R.K., Dhadke, P.M., 2002. Extraction and separation studies of zinc (II) and copper (II) with D2EHPA and PC-88A from perchlorate media 67, 41–51.

Song, J., Huang, T., Qiu, H., Niu, X., Li, X., Yingming Xie, T.H., 2018. A critical review on membrane extraction with improved stability : Potential application for recycling metals from city mine. Desalination 440, 18–38.

Šraja O L, Almeida M. I G.S., Bassetta C,. McKelviea I D,.Kolev S.D., 2018. Talanta Gas-di ff usion-based passive sampler for ammonia monitoring in marine waters. Talanta 181, 52–56.

St John, A.M., Cattrall, R.W., Kolev, S.D., 2012. Transport and separation of uranium(VI) by a polymer inclusion membrane based on di-(2-ethylhexyl) phosphoric acid. J. Memb. Sci. 409–410, 242–250.

Stern, B.R., 2010. Essentiality and Toxicity in Copper Health Risk Assessment : Overview , Update and Regulatory Considerations. J. Toxicol. Environ. Health 73, 114–127.

Syazana, N., Abdul, B., Whitten, P.G., 2016. Characteristics and cadmium extraction performance of PVC / Aliquat 336 electrospun fibres in comparison with polymer inclusion membranes. Aust. Inst. Innov. Mater. 51, 1515–1522.

Turner, G.S.C., Mills, G.A., Teasdale, P.R., Burnett, J.L., Amos, S., Fones, G.R., 2012. Analytica Chimica Acta Evaluation of DGT techniques for measuring inorganic uranium species in natural waters : Interferences , deployment time and speciation. Anal. Chim. Acta 739, 37–46.

Turull, M., Elias, G., Fontàs, C., Díez, S., 2016. Exploring new DGT samplers containing a polymer inclusion membrane for mercury monitoring. Environ. Sci. Pollut. Res. 24, 10919–10928.

Tutu, H., Cukrowska, E.M., Dohnal, V., Havel, J., 2005. Application of artificial neural networks for classification of uranium distribution in the Central Rand goldfield , South Africa. Environ. Model. Assess. 10, 143–152.

Valente, T., Grande, J.A., Ceron, J.C., de la Torre, M.L., Santisteban, M., Borrego, J., Fernandez, P., Sanchez-Rodas, D., 2016. Spatial distribution of major and trace elements in a mining dam : sources and relationships among elements of environmental concern. Environ. Earth Sci. 75, 1–11.

Van de Voorde, I., Latruwe, K., Pinoy, L., Courtijn, E., Verpoort, F., 2007. Complexation behaviour of iron(III) with Aloxime 800, D2EHPA, CYANEX 272, CYANEX 302 and CYANEX 301. Solvent Extr. Ion Exch. 25, 1–25.

Vázquez, M.I., Romero, V., Fontàs, C., Anticó, E., Benavente, J., 2014. Polymer inclusion membranes (PIMs) with the ionic liquid (IL) Aliquat 336 as extractant: Effect of base polymer and IL concentration on their physical-chemical and elastic characteristics. J. Memb. Sci. 455, 312–319.

Vellaichamy, S., 2017. Adsorptive separation of copper , nickel , lead , zinc and cadmium from aqueous solution using MWCNTs impregnated with D2EHPA and prior to their determination by FAAS : Kinetic and equilibrium studies. Sep. Sci. Technol. 52, 644–656.

Vera, R., Fontàs, C., Galceran, J., Serra, O., Anticó, E., 2018a. Polymer inclusion membrane to access Zn speciation: Comparison with root uptake. Sci. Total Environ. 622–623, 316–324.

Vera, R., Insa, S., Fontàs, C., Anticó, E., 2018b. A new extraction phase based on a polymer inclusion membrane for the detection of chlorpyrifos , diazinon and cyprodinil in natural water samples. Talanta 185, 291–298.

Viers J, Grande J , Zouiten C, Freydier R, Masbou J, Valente T, Maria-Luisa de la Torre M L, D Christine, 2018. Are Cu isotopes a useful tool to trace metal sources and processes in acid mine drainage (AMD) context ? Chemosphere 193, 1071–1079.

Vig, K., Megharaj, M., Sethunathan, N., Naidu, R., 2003. Bioavailability and toxicity of cadmium to microorganisms and their activities in soil : a review. Adv. Environ. Res. 8, 121–135.

Vrana, B., Allan, I.J., Greenwood, R., Mills, G.A., Dominiak, E., Svensson, K., Knutsson, J., Morrison, G., 2005. Passive sampling techniques for monitoring pollutants in water. Trends Anal. Chem. 24, 845–868.

Witt, K., Radzyminska-lenarcik, E., Kosciuszko, A., 2018. The Influence of the Morphology and Mechanical Properties of Polymer Inclusion Membranes (PIMs) on Zinc Ion Separation from Aqueous Solutions. Polymers (Basel). 10, 134.

Yildiz, Y., Manzak, A., Aydin, B., Tutkun, O., 2014. Preparation and application of polymer inclusion membranes (PIMs) including Alamine 336 for the extraction of metals from an aqueous solution. Mater. Tehnol. 48, 791–796.

Yousefi, S., Doulati, F., Mansour, A., 2015. The speciation of cobalt and nickel at mine waste dump using improved correlation analysis : a case study of Sarcheshmeh copper mine. Environ. Dev. Sustain. 17, 1065–1084.

Zabiegała Bożena, Kot-Wasik Agata, Urbanowicz Magdalena, Namieśnik Jacek , Passive sampling as a tool for obtaining reliable analytical information in environmental quality monitoring2010 Anal Bioanal Chem 39, 273–296.

Zabiegała, B., Kot-Wasik, A., Urbanowicz, M., Namieśnik, J., 2010. Passive sampling as a tool for obtaining reliable analytical information in environmental quality monitoring. Anal. Bioanal. Chem. 396, 273–296.

Zaheri, P., Ghassabzadeh, H., 2017. Preparation of polymer inclusion membrane including mixture of D2EHPA and Cyanex272 for the extraction of Eu from nitrate media. Chem. Pap. 71, 1623–1631.

Zaheri, P., Ghassabzadeh, H., Abolghasemi, H., Maraghe, M.G., Mohammadi, T., 2017. Facilitated Transport of Europium through Supported Liquid Membrane using Cyanex272 as Carrier and Mass Transfer Modelling. 524 Can. J. Chem. Eng. 95, 524–534.

Zawierucha Iwona, Kozlowski Cezary, Malina Grzegorz, 2016 Immobilized materials for removal of toxic metal ions from surface/groundwaters and aqueous waste streamsEnviron. Sci.: Processes Impacts, 18, 429–444.

Zhang, H., Davison, W., 1995. Performance Characteristics of Diffusion Gradients in Thin Films for the in Situ Measurement of Trace Metals in Aqueous Solution. Anal. Chem 67, 3391–3400.

Zhu, L.L., Guo, L., Zhang, Z.J., Chen, J., Zhang, S.M., 2012. The preparation of supported ionic liquids (SILs) and their application in rare metals separation. Sci. China Chem. 55, 1479–1487.

Zioui, D., Arous, O., Mameri, N., Kerdjoudj, H., Sebastian, M.S., Vilas, J.L., Nunes-pereira, J., Lanceros-méndez, S., 2017. Membranes based on polymer miscibility for selective transport and separation of metallic ions. J. Hazard. Mater. 336, 188–194.